BELL CREEK TEST SITE – PREINJECTION GEOCHEMICAL REPORT

Plains CO_2 Reduction (PCOR) Partnership Phase III
Task 4 – Deliverable D33
Task 4 – Milestone M12

Prepared for:

Andrea T. McNemar

National Energy Technology Laboratory
U.S. Department of Energy
3610 Collins Ferry Road
PO Box 880
Morgantown, WV 26507-0880

DOE Cooperative Agreement No. DE-FC26-05NT42592

Prepared by:

Bethany A. Kurz
Loreal V. Heebink
Kurt E. Eylands
Steven A. Smith
John A. Hamling
Ryan J. Klapperich
Jeffrey S. Thompson
Daniel J. Stepan
Barry W. Botnen
Hui Pu
Charles D. Gorecki
Edward N. Steadman
John A. Harju

Energy & Environmental Research Center
University of North Dakota
15 North 23rd Street, Stop 9018
Grand Forks, ND 58202-9018

July 2013

2016-EERC-03-08

Approved

EERC DISCLAIMER

ACKNOWLEDGMENT

This material is based upon work supported by the DOE NETL under Award Number DE-FC26-05NT42592.

DOE DISCLAIMER

NDIC DISCLAIMER

(B) Assumes any liabilities with respect to the use of, or for damages resulting from the use of, any information, apparatus, method, or process disclosed in this report.

Reference herein to any specific commercial product, process, or service by trade name, trademark, manufacturer, or otherwise does not necessarily constitute or imply its endorsement, recommendation, or favoring by the NDIC. The views and opinions of authors expressed herein do not necessarily state or reflect those of the NDIC.

TABLE OF CONTENTS

LIST OF FIGURES

LIST OF TABLES

Plains CO_2 Reduction (PCOR) Partnership
Energy & Environmental Research Center (EERC)

BELL CREEK TEST SITE – PREINJECTION GEOCHEMICAL REPORT

EXECUTIVE SUMMARY

The Plains CO_2 Reduction (PCOR) Partnership, led by the Energy & Environmental Research Center (EERC), is working with Denbury Onshore LLC (Denbury) to determine the effect of a large-scale injection of carbon dioxide (CO_2) into a deep clastic reservoir for the purpose of simultaneous CO_2 enhanced oil recovery (EOR) and monitor incidental CO_2 storage at the Bell Creek oil field, which is operated by Denbury Onshore, LLC. A technical team that includes Denbury, the EERC, and others is conducting a variety of activities to determine the baseline characteristics of the Muddy and overlying formations in the Bell Creek Field area, which will facilitate assessment of various migration pathways, guide monitoring strategies, and aid in the determination of the ultimate fate of injected CO_2.

The Bell Creek demonstration storage project provides a unique opportunity to conduct a detailed mineralogical and geochemical evaluation from the laboratory scale to the field scale for a complex, large-scale (>1 million tons per year) CO_2 EOR operation and monitor incidental CO_2 storage in an active oil field. To facilitate these activities, several laboratory, field, and modeling efforts are being conducted that will collectively be used to better understand the existing geochemistry of the reservoir, overlying seals, shallow subsurface, and surface at the Bell Creek site. Ultimately, the laboratory and field monitoring data will be used to refine geologic, geochemical, and CO_2 fate and transport models to gain a better understanding of reservoir response to CO_2 injection, to better predict the long-term incidental CO_2 storage capacity of the reservoir from hydrodynamic and mineralogic trapping mechanisms, and to assess the long-term integrity of the overlying cap rocks. The data will also feed into shallow subsurface geochemical modeling and assessment efforts to better understand the possible effect that CO_2 may have if it were to reach the surface or shallow groundwater in the unlikely event of out-of-zone migration.

Specific efforts summarized in this report include the following:

- Analysis of rock samples within the CO_2 injection zone (Muddy Formation) as well as on the sealing formations (Niobrara and Mowry Formations) to determine their petrographic, petrophysical, and mineralogical characteristics.
- Reservoir fluid sampling and analysis to characterize the formation water chemistry and to better understand the hydrocarbon composition of the reservoir.
- Surface water, groundwater, and shallow vadose zone soil gas sampling and analysis to establish baseline characteristics of surface and shallow subsurface environments prior to CO_2 injection.

- Preliminary review of existing literature to identify potential mineralogical effects of CO_2 injection within the Bell Creek reservoir and cap rock and also within the overlying groundwater zones in the unlikely event of out-of-zone migration.
- Laboratory-based CO_2 exposure testing of rock and water samples from the lowest groundwater zone (Hell Creek Formation) overlying the Bell Creek reservoir to better understand the possible effects of out-of-zone CO_2 migration to the shallow subsurface.

The key findings of this effort include the following:

- Of the three formations analyzed (Niobrara, Mowry, and Muddy Formations), there is very little variation in the mineral assemblages identified.
- Based on petrographic analysis of the Niobrara and Mowry shales, these formations should act as viable seals, preventing vertical migration of CO_2 and formation fluids. Based on point-counting techniques, the Niobrara and Mowry Formations exhibited very low (<1%) porosity.
- Petrographic analysis of the samples within the Muddy sandstone zones revealed varying degrees of clay lining and pore fill in almost all of the samples, with some samples only displaying a partial lining and others containing nearly filled pore space. As would be expected, zones within the Muddy Formation that contained a higher clay content, such as the Coastal Plain unit and the transition zones between the various sand benches, exhibited reduced permeability and porosity. No swelling clays were identified.
- Crude oil analysis from three wells and subsequent pressure, volume, and temperature modeling using Computer Modelling Group Ltd.'s WinProp™ were used to model PVT properties. This work reinforces the need for good crude oil composition analyses representative of those in the reservoir.
- Seasonal variations in surface and groundwater chemistry and in CO_2 concentrations from soil gas sampling were detected from baseline monitoring efforts and illustrate the need for long-term monitoring to adequately differentiate between natural variations versus injected CO_2-induced effects.
- Based on existing literature and the mineralogical content of the Bell Creek reservoir, geochemical changes to the rock and formation fluids are likely, but probably minor. Additional laboratory- and modeling-based work will be conducted in this arena to determine the magnitude and kinetics of potential geochemical reactions and their implications on injectivity.
- The results of the Hell Creek CO_2 exposure testing were consistent with existing literature and suggest that compositional changes in groundwater chemistry offer an opportunity for monitoring the potential out-of-zone migration of CO_2 into the groundwater zone overlying the Bell Creek Field.

The EERC's efforts to understand the potential geochemical changes that may occur in the field as a result of CO_2 injection are ongoing. Specific reactions unique to the Bell Creek reservoir and their implications on reservoir porosity, permeability, and CO_2 storage capacity will be evaluated through additional literature review, laboratory-based CO_2 exposure testing, and geochemical modeling.

Plains CO_2 Reduction (PCOR) Partnership
Energy & Environmental Research Center (EERC)

BELL CREEK TEST SITE – PREINJECTION GEOCHEMICAL REPORT

INTRODUCTION

The Plains CO_2 Reduction (PCOR) Partnership, led by the Energy & Environmental Research Center (EERC), is working with Denbury Onshore LLC (Denbury) to determine the effect of a large-scale injection of carbon dioxide (CO_2) into a deep clastic reservoir for the purpose of simultaneous CO_2 enhanced oil recovery (EOR) and to monitor incidental CO_2 storage at the Bell Creek oil field, which is operated by Denbury Onshore, LLC. A technical team that includes Denbury, the EERC, and others is conducting a variety of activities to determine the baseline characteristics of the Muddy and overlying formations in the Bell Creek Field area, including predictive simulations of CO_2 injection. This will facilitate assessment of various migration pathways, guide monitoring strategies, and aid in the determination of the ultimate fate of injected CO_2. Denbury will carry out the injection and production operations, while the EERC will provide support in site characterization, modeling and simulation, and integrated risk assessment and will aid in the development of the monitoring, verification, and accounting (MVA) plan.

The Bell Creek demonstration storage project provides a unique opportunity to conduct a detailed mineralogical and geochemical evaluation from the laboratory scale to the field scale for a complex, large-scale (>1 million tons a year) CO_2 EOR operation and to monitor incidental CO_2 storage in an active oil field. To facilitate these activities, several efforts are being conducted that will collectively be used to better understand the existing geochemistry of the reservoir, overlying seals, shallow subsurface, and surface at the Bell Creek site. These characterization data will facilitate predictive modeling and laboratory-based experimentation to better understand the potential geochemical reactions between CO_2 and the rocks and fluids of each respective zone.

For multiple reasons, it is important to understand the potential geochemical reactions that may occur during CO_2-based EOR and CO_2 storage projects. To evaluate the efficacy of incidental CO_2 storage, it is important to assess the likely chemical changes in the reservoir fluids, CO_2 mineralization pathways and reaction kinetics, the near- and long-term stability of the minerals formed during injection, and the long-term fate of unmineralized CO_2 in the reservoir. From a reservoir engineering perspective, it is important to determine how potential mineral dissolution and/or precipitation may or may not affect the near- and far-wellbore environments and the long-term injectivity and mobility of CO_2 and water. Understanding the geochemical reactions and reaction kinetics that may occur in the shallow subsurface (groundwater zone) or at the surface in the unlikely event of out-of-zone migration aids in determining chemical leak indicators in overlying surface and groundwaters, thereby increasing the likelihood of early detection through monitoring efforts. Verifying the geochemical integrity of the reservoir seal is important from an

EOR, incidental storage, and monitoring perspective since, ultimately, the seals are what keep the CO_2 from migrating out of the target injection zone.

OVERVIEW

The Bell Creek oil field in southeastern Montana is a subnormally pressured reservoir with significant hydrocarbon accumulation that lies near the northeastern corner of the Powder River Basin (Figure 1). Exploration and production activities for mineral and energy resources in the area over the last 55 years have yielded a significant amount of information about the geology of southeastern Montana and the northern Powder River Basin. Over the course of decades, oil and gas production through primary and secondary recovery (waterflood and polymer flood pilot tests) have declined, resulting in implementation of a CO_2 injection-based tertiary oil recovery project for EOR, with attendant monitoring of incidental CO_2 storage. CO_2 is being delivered to the site via pipeline from the Lost Cabin Gas Plant, where it is separated from the process stream during natural gas processing. The plant is located in Fremont County, Wyoming (Figure 1). It will supply around 50 million cubic feet of CO_2 per day to the Bell Creek oil field.

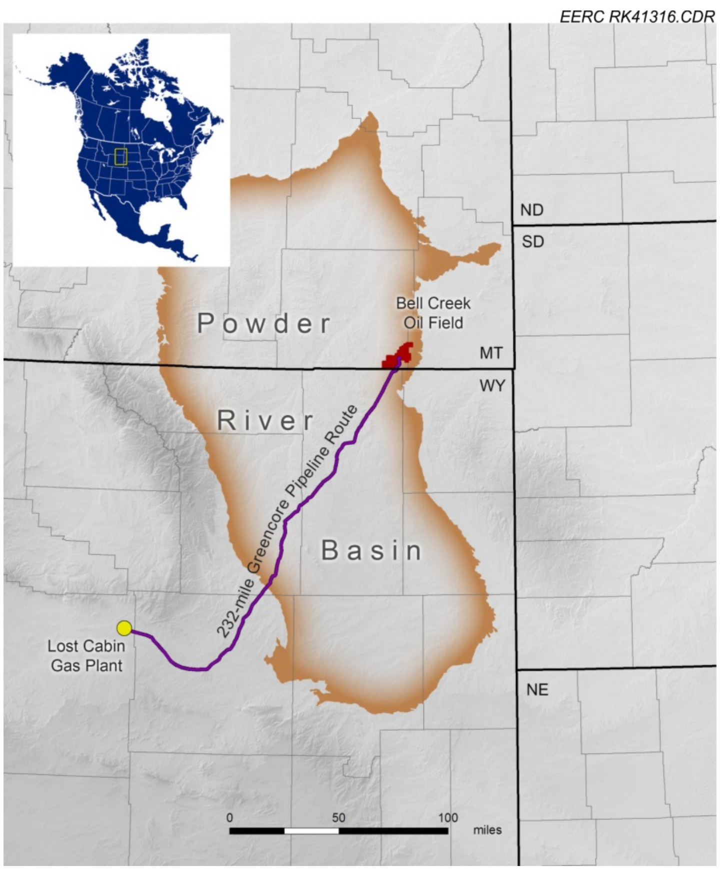

Figure 1. Map depicting the location of the Bell Creek oil field in relation to the Powder River Basin and the pipeline route to the site from the Lost Cabin Gas Plant.

The Bell Creek Field was originally separated into seven distinct operational units (A, B, C, D, E, F, and South Bell Creek Units), which in some cases are at least partially defined by the geometry of the shale-filled channels (Figure 2). The first six of these units were consolidated into the Bell Creek Consolidated (Muddy) Unit by Exxon in late 1991 when it first contemplated implementing five-spot patterns for waterflooding and a future CO_2 injection flood. In recent years, most of the oil production from Bell Creek has been from the former A, B, and D unit areas. CO_2 injection will occur in a staged approach according to nine planned CO_2 development phases, designated as Phases 1–9, across the field (Figure 3). The Bell Creek oil field will be developed sequentially in phases, with each new phase being brought online after approximately 1 year, starting with the Phase 1 area. CO_2 will be injected into the oil-bearing sandstone reservoir in the Lower Cretaceous Muddy Formation (Figure 4) at a depth of approximately 4500 feet. The overlying Upper Cretaceous Mowry Formation shale will provide the primary seal, preventing fluid migration to overlying aquifers and to the surface. The reservoir appears to be suitable for miscible flooding conditions, with an incremental oil production target of approximately 30 million barrels. The activities at the Bell Creek oil field will inject an estimated 1 million metric tons of CO_2 annually, much of which will be permanently stored at the end of the EOR project.

While the PCOR Partnership is conducting many efforts related to the Bell Creek CO_2 injection project, the focus of this interim report is to provide an update of all work that has been conducted to characterize the reservoir, overlying formations, and surface and shallow subsurface overlying the field related to mineralogy, fluid chemistry, and geochemistry. These data will ultimately be used to better understand the geochemical reactions that may occur between the injected CO_2 and the rocks and fluids of the reservoir and seal as well as between the CO_2 and the rocks and fluids of the surface and/or subsurface in the unlikely event of an out-of-zone migration. Overall, geochemistry-related activities of the Bell Creek project relevant to this evaluation include determining the 1) rock mineralogy and composition of formation fluid, 2) nature of geochemical interactions between formation and injected fluids and reservoir rock and cap rock, and 3) hydrocarbon properties. Because many of these efforts are ongoing and have not yet been integrated or evaluated with respect to their implications for CO_2 injection, this interim report will discuss each of the major efforts discretely. The key efforts that have been conducted to date include the following:

- Analyses have been conducted on rock samples within the CO_2 injection zone (Muddy Formation) as well as on the sealing formations (Niobrara and Mowry Formations) to determine the petrographic, petrophysical, and mineralogical characteristics.

- Reservoir fluids of the Bell Creek reservoir have been analyzed.

- Surface water, groundwater, and shallow-vadose-zone soil gas samples have been collected and analyzed to establish baseline characteristics of surface and shallow subsurface environments prior to CO_2 injection.

- Laboratory-based CO_2 exposure experiments have been conducted on rock and water samples from the lowest groundwater zone overlying the Bell Creek reservoir to better understand the possible effects a CO_2 leak may have in the shallow subsurface.

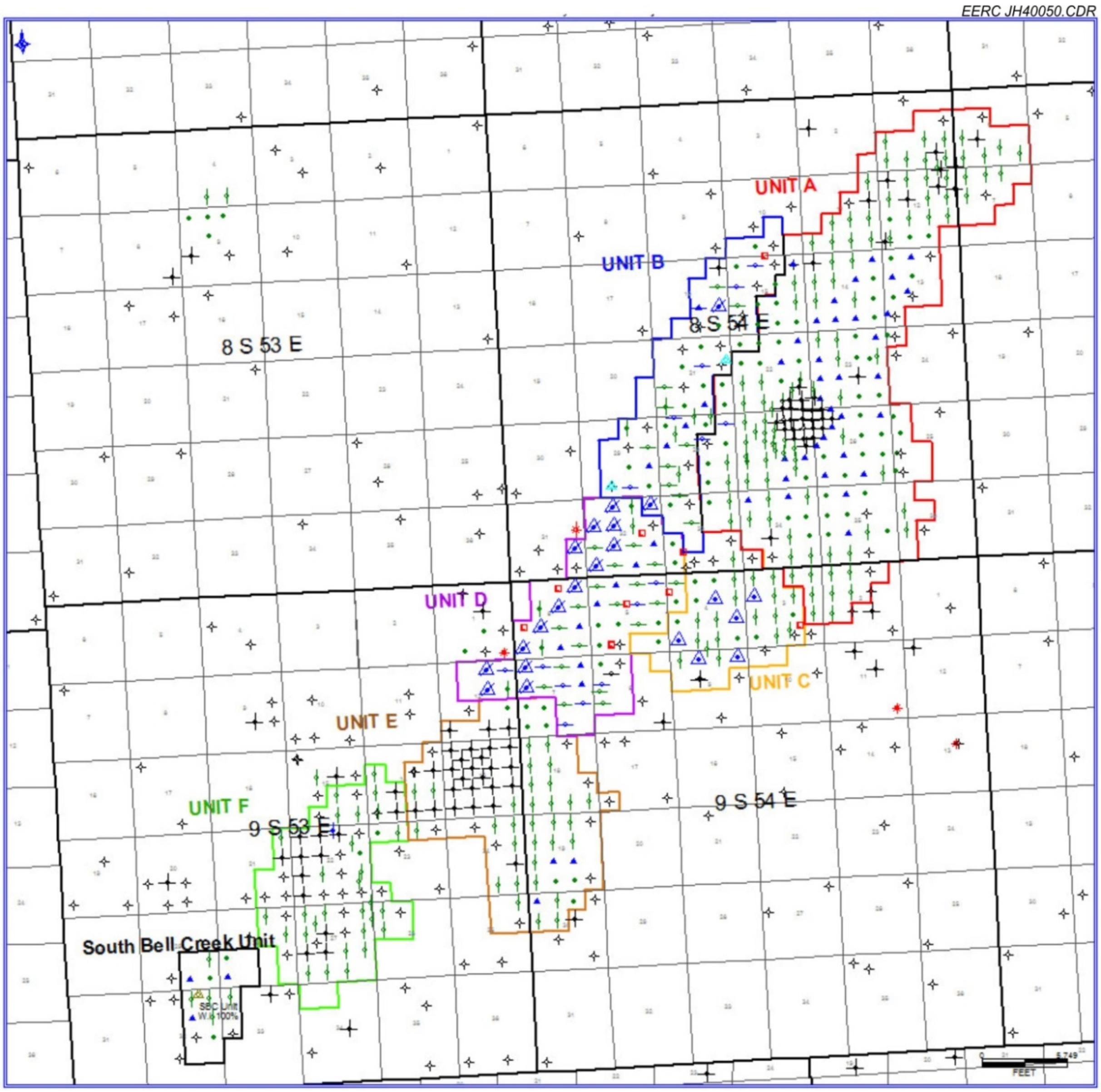

Figure 2. Map of the former Bell Creek oil field Units A, B, C, D, E, and F. The South Bell Creek Unit includes the wells that are located southwest of the F Unit (Sorensen and others, 2011).

Ultimately, the laboratory and field monitoring data will be used to refine geologic, geochemical, and CO_2 fate and transport models to gain a better understanding of reservoir response to CO_2 injection, to better predict the long-term CO_2 storage permanence through hydrodynamic and mineralogic trapping mechanisms, and to assess the long-term integrity of the overlying cap rocks. The data will also feed into shallow subsurface geochemical modeling and assessment efforts to better understand the possible effect that CO_2 may have if it were to reach the surface or a groundwater zone in the unlikely event of out-of-zone migration beyond the reservoir cap rocks.

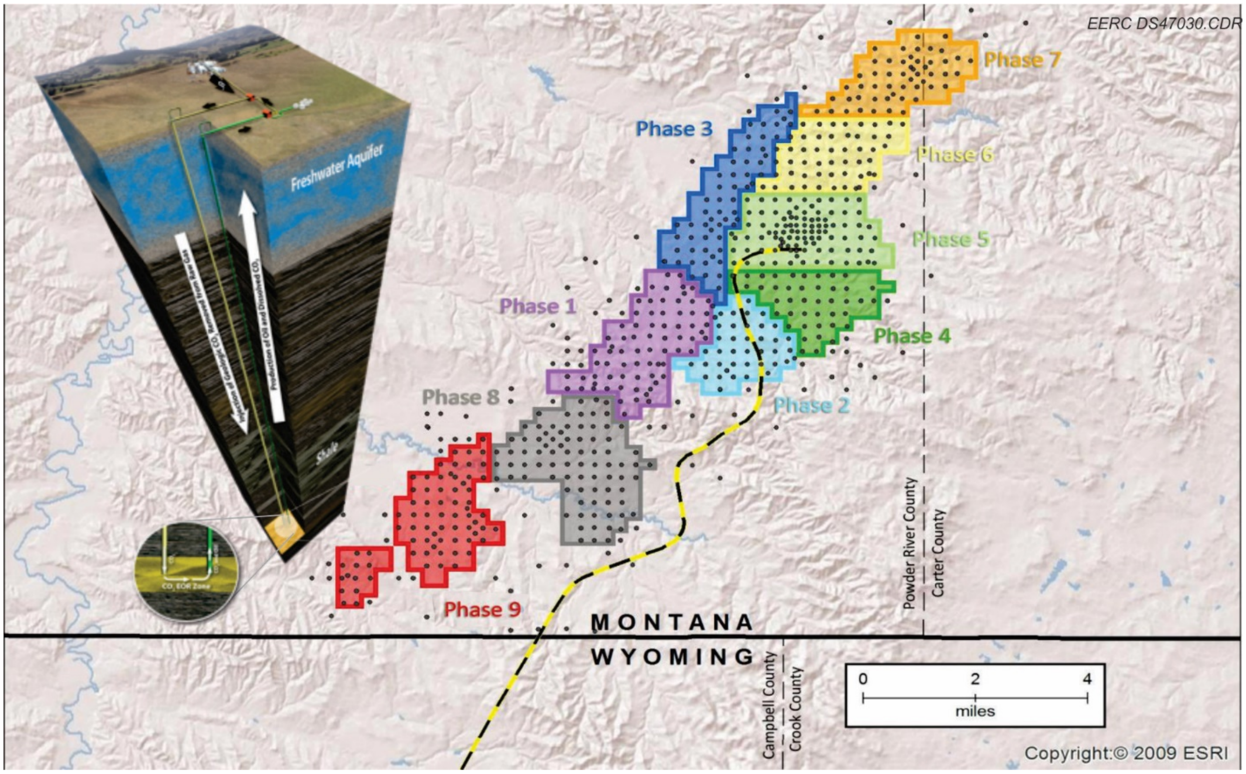

Figure 3. Bell Creek phased CO_2 EOR injection.

LOCAL GEOLOGY

The following section provides a general overview of the geology of the Bell Creek field. A more detailed geologic description is provided in the document entitled "Bell Creek Test Site – Simulation Report" (Saini and others, 2012). The Muddy Formation within the boundaries of the Bell Creek oil field are characterized by high-permeability (150–1175 mD) and high-porosity (25%–35%) sandstones deposited in a near-shore marine environment. The initial reservoir pressure was 1200 psi, which is lower than the regional hydrostatic pressure regime (2100 psi at 4500 ft). The oil field is located structurally on a shallow monocline with a 1°–2° dip to the northwest and with an axis trending southwest to northeast for a distance of approximately 20 miles.

The Muddy Formation comprises, in descending order, the Coastal Plain Member, the Bell Creek Sandstone Member, and the Rozet Member (Figure 5). The Muddy Formation is stratigraphically positioned between the thick marine shale sequences of the Skull Creek and Mowry Formations, which serve as highly effective seals for the formation.

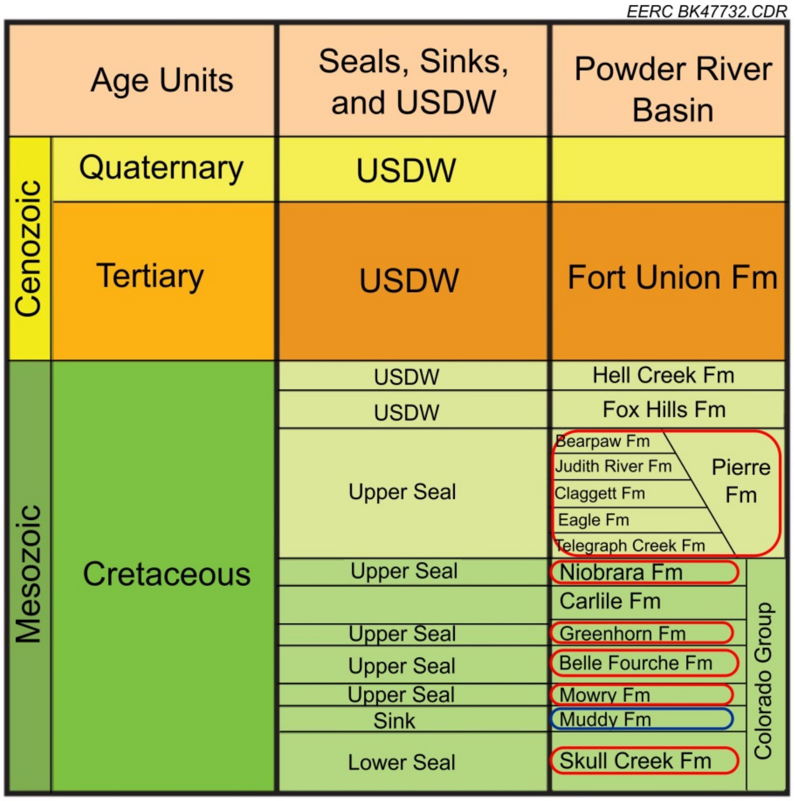

Figure 4. Late Cretaceous to Quaternary stratigraphic column of the Powder River Basin. Sealing formations are circled in red, and the primary oil-producing and sink formation is circled in blue. Formations bearing underground sources of drinking water (USDW) are also identified.

The Rozet Member directly overlies the Skull Creek shale and is marked by a thin (0.5–3-ft), hummocky cross-stratified sandstone bed, which is conformably overlain by a dark gray mudstone (Molnar and Porter, 1990). The Bell Creek Member is composed of stacked barrier bar sediments that were reworked and transported by longshore drift from these drainage systems (Molnar and Porter, 1990). The barrier bar sands of the Bell Creek Member make up the best reservoir rock within the field. These sediments intertongue with marine shales to the west–northwest and lagoonal sediments to the east–southeast, representing minor changes in sea level during deposition. This facies change updip to the east and southeast provides the trapping mechanism to allow pooling of hydrocarbons in the barrier bar sandstones. The Coastal Plain Member lies unconformably on the Bell Creek Member. It was deposited when another drop in sea level caused the incision of fluvial channels into the Bell Creek Member, some of which cut down to the Skull Creek shale. These channels, oriented mainly east–west, were filled with fluvial sandstone, floodplain shale, coal, and marginal marine deposits during the subsequent rise in sea level (Molnar and Porter, 1990). This sea level rise corresponds to the early stages of the major transgression that led to the deposition of the Mowry shale.

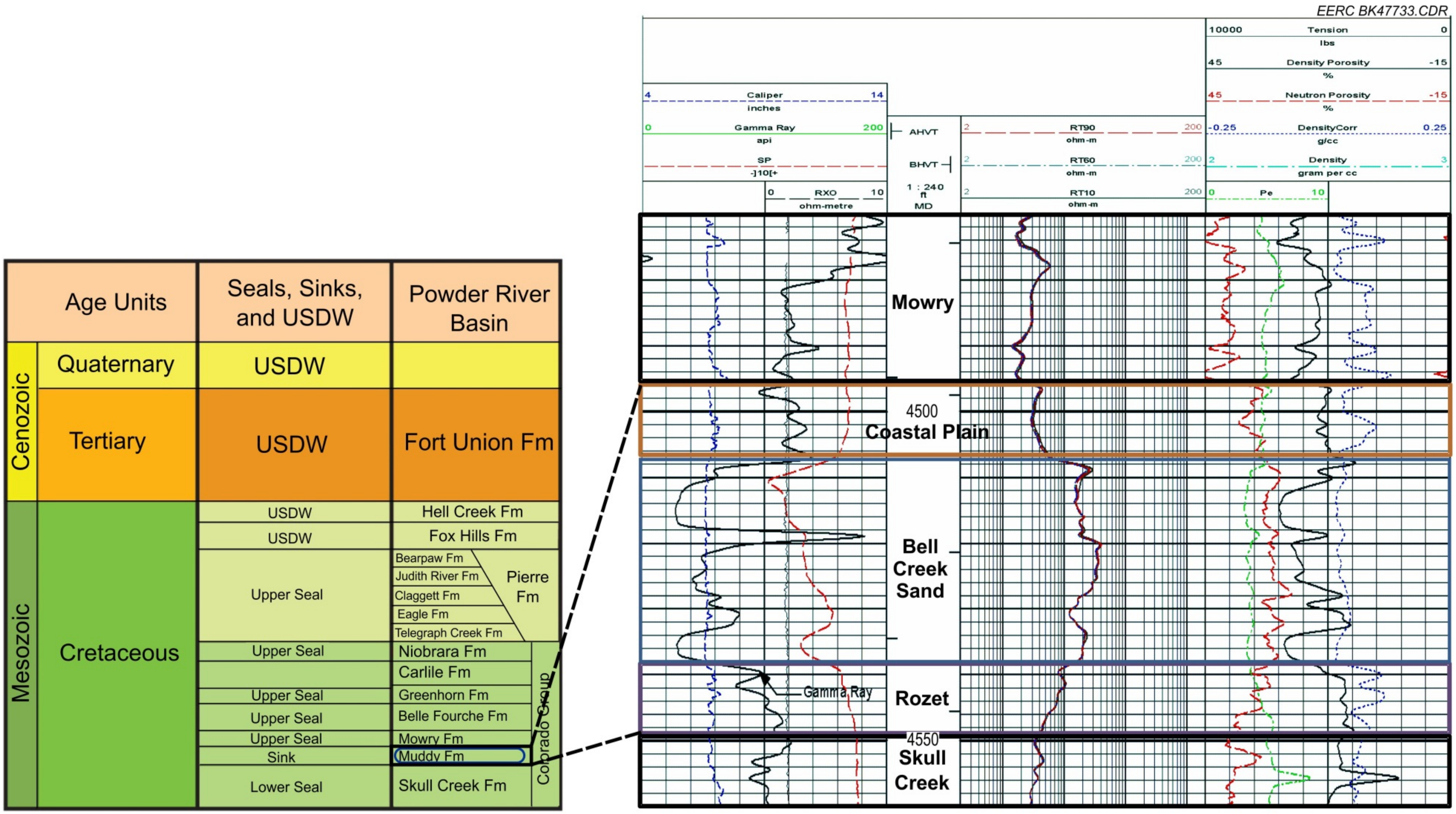

Figure 5. Stratigraphic column illustrating the nomenclature used for the Lower Cretaceous in the Bell Creek area as well as the corresponding gamma ray, resistivity, bulk density, and neutron porosity well log response for each major interval within the 05-06 OW observation well.

Directly overlying the Muddy Formation are several thousand feet of low-permeability marine shale formations, including the Mowry, Belle Fourche, Greenhorn, Niobrara, and Pierre shales, which will provide redundant layers of protection preventing upward fluid migration (Figure 4) to the USDW supplies of the groundwater zone. The USDW zones overlying the Bell Creek reservoir occur in the Cretaceous Fox Hills and Hell Creek Formations and the tertiary Fort Union Formation (Figure 4). Groundwater depths at the Bell Creek Field range from approximately 70 to 700 feet below ground surface and some 3800 to 4400 feet vertically above the reservoir rock. The Fox Hills and Hell Creek Formations were targeted for additional monitoring and/or laboratory-based CO_2 exposure experiments. The Fox Hills Formation is a Late Cretaceous marine unit of mostly medium and fine sandstone with shale interbeds deposited primarily in the northern Great Plains during the regression of the Western Interior Seaway (Cvancara, 1976; Mello, 1969). The Fox Hills Formation is overlain by the Hell Creek Formation. The Hell Creek Formation is an Upper Cretaceous fine-grained sandstone, siltstone, and carbonaceous-rich shale, mudstone, and siltstone with some lignite deposited in laterally accreting fluvial channel systems and peripheral floodplains (Berg and Davies, 1968; McGregor and Biggs, 1968).

Regional Soil Composition

The soil types and characteristics at the Bell Creek Field were compiled using soil data from the U.S. Department of Agriculture's (USDA's) Natural Resources Conservation Service (NRCS), which are available online at the Web Soil Survey Web site (http://websoilsurvey.nrcs.usda.gov, accessed June 2013). The near-surface soils typically found in the Bell Creek region consist of gently sloping to steep, shallow silt loams and fine sandy loams underlain by shale and sandstone. Upland areas have fine sandy loam subsoil underlain by broken shale. A complete soil map of the Bell Creek Field is provided in Figure 6, with details provided in Table 1. More specifically, soils in the area belong to the Elso–Remmit–Ocean Lake association.

The Elso series consists of well-drained, medium-textured, shallow soils in uplands. These soils formed from softly consolidated shale on foot slopes, narrow ridges, knobs, and tabular divides. The native vegetation consists of short grasses, and slopes range from 8% to 45%, while elevations range from 3000 to 3500 feet. Typically, the surface layer is light brownish gray silt loam about 7 inches thick. The subsoil is light brownish gray silt loam underlain by softly consolidated, interbedded silty, clayey, and sandy shale. The silt loams in the Elso series are typically nonsticky and nonplastic when wet, are strongly calcareous, and have a pH of 8.2 to 8.4.

The Remmit series consists of well-drained soils that formed in deep, fine, sandy loam material underlain by softly consolidated shale beds. The native vegetation consists of mid- and short grasses, and slopes range from 2% to 25%, while elevations range from 3000 to 4000 feet. Typically, the surface layer is grayish brown, fine, sandy loam about 12 inches thick. The subsoil is grayish brown and light olive brown, fine, sandy loam about 44 inches thick. The substratum is grayish brown silt loam that contains threads and seams of lime. The sandy loams in the Remmit series are typically nonsticky and nonplastic when wet, are noncalcareous, and have a pH of 7.3 to 9.0.

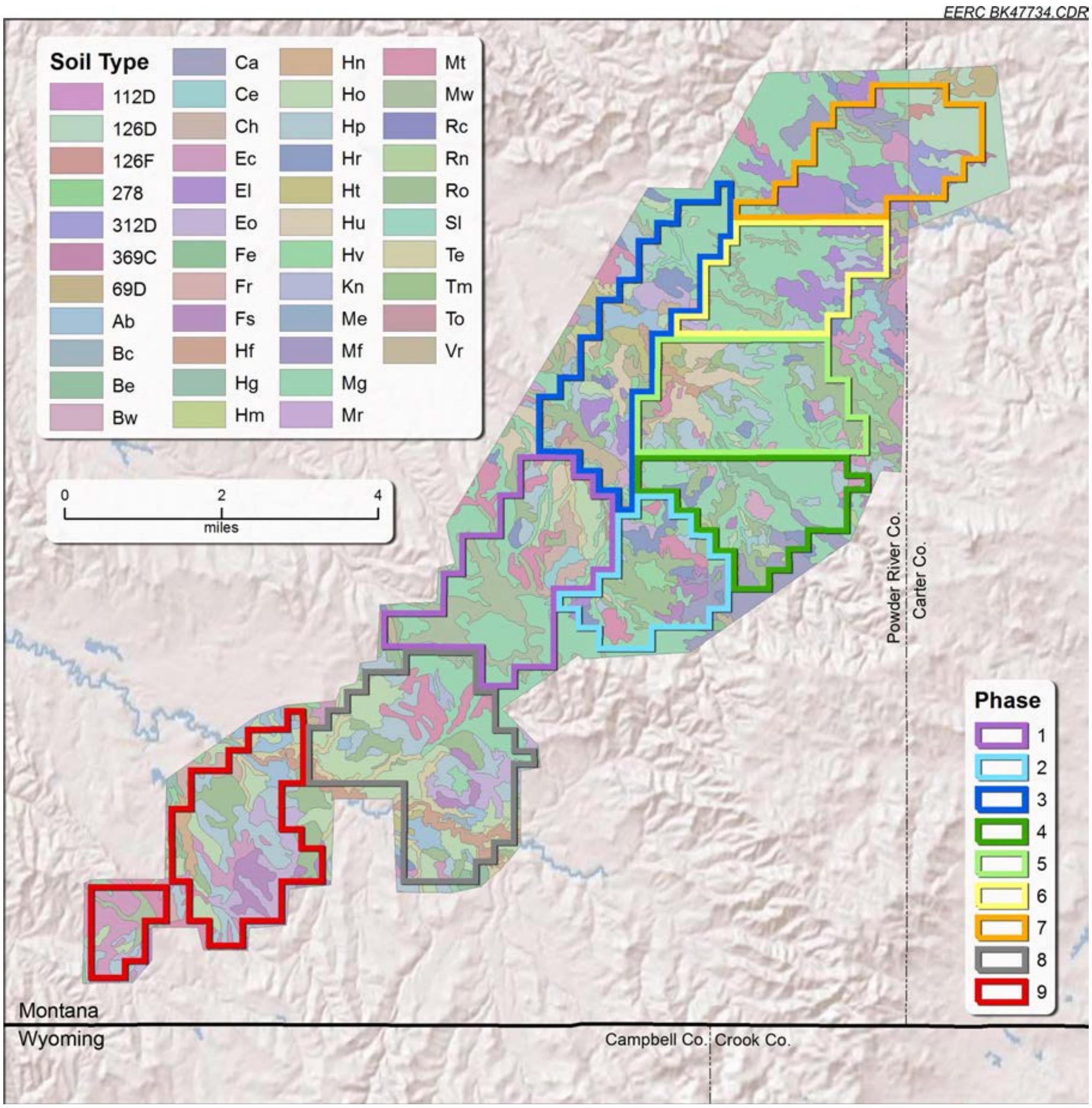

Figure 6. Soil map of Bell Creek Field (U.S. Department of Agriculture Natural Resources Conservation Service, 2013).

The Ocean Lake series consists of well-drained, fine, sandy loam soils less than 20 inches deep over softly consolidated sandstone on uplands. These soils formed under mid- and short grasses. Slopes range from 15% to 45%, and elevation ranges from 3000 to 3500 feet. Typically, the surface layer is grayish brown and light brownish gray, fine, sandy loam about 8 inches thick. The subsoil is light gray, fine sand that extends to a depth of about 15 inches. The substratum is softly consolidated sandstone that contains seams and splotches of segregated lime. The fine sandy loams in the Ocean Lake series are typically friable when moist, are nonsticky and nonplastic when wet, are noncalcareous to strongly calcareous, and have a pH of 7.4 to 7.5.

Table 1. Map Unit Symbol with Soil Name and Area[1] (U.S. Department of Agriculture Natural Resources Conservation Service, 2013)

Map Unit Symbol	Soil Name	Area, acres[1]
112D	Cabba silt loam, 8%–15% slopes	0.17
126D	Broadus–Ridge–Reeder complex, 8%–25% slopes	976.91
126F	Broadus–Ridge–Rock outcrop complex, 25%–65% slopes	47.72
278	Fairburn–Samsil–Badland complex, 10%–45% slopes	5.15
312D	Cabba–Dast complex, 8%–15% slopes	212.42
369C	Twilight–Delpoint complex, 2%–8% slopes	29.40
69D	Twilight fine sandy loam, 8%–15% slopes	141.37
Ab	Arvada–Bone complex, 0%–4% slopes	503.85
Bc	Bew silty clay, 0%–2% slopes	72.31
Be	Bew silty clay, 2%–4% slopes	167.87
Bw	Bew silty clay, 4%–8% slopes	200.19
Ca	Cabba association, 15%–50% slopes	929.10
Ce	Cushman–Elso silt loams, 4%–8% slopes	193.31
Ch	Cushman–Elso silt loams, 8%–15% slopes	339.19
Ec	Elso silt loam, 8%–15% slopes	1168.17
El	Elso silt loam, 15%–45% slopes	1326.40
Eo	Elso–Ocean Lake association, 15%–45% slopes	962.13
Fe	Farland silt loam, 4%–8% slopes	18.26
Fr	Fort Collins silt loam, 2%–4% slopes	47.35
Fs	Fort Collins silt loam, 4%–8% slopes	435.53
Hf	Haverson soils, channeled	419.17
Hg	Haverson soils, saline	61.88
Hm	Heldt silty clay loam, 4%–8% slopes	31.01
Hn	Hesper silty clay loam, 0%–2% slopes	97.41
Ho	Hesper silty clay loam, 2%–4% slopes	1934.18
Hp	Hesper silty clay loam, 4%–8% slopes	2525.37
Hr	Hesper silty clay loam, 8%–15% slopes	639.19
Ht	Hydro silty clay loam, 0%–2% slopes	326.55
Hu	Hydro silty clay loam, 2%–4% slopes	678.69
Hv	Hydro silty clay loam, 4%–8% slopes	622.35
Kn	Kyle clay, 8%–15% slopes	46.65
Me	McRae silt loam, 4%–8% slopes	16.60
Mf	Midway silty clay loam, 2%–8% slopes	16.20
Mg	Midway–Elso association, 8%–35% slopes	7536.45
Mr	Midway–Rock land association, 15%–35% slopes	14.55
Mt	Midway–Thurlow association, 8%–15% slopes	1007.20
Mw	Midway and Elso rocky soils, 35%–75% slopes	1240.75
Rc	Rapelje silt loam, 2%–8% slopes	32.81
Rn	Remmit fine sandy loam, 4%–8% slopes	81.32
Ro	Remmit–Ocean lake fine sandy loam, 8%–25% slopes	2616.15
Sl	Shale outcrop	59.74
Te	Terrace escarpments	563.90
Tm	Thurlow silty clay loam, 2%–4% slopes	31.89
To	Thurlow silty clay loam, 4%–8% slopes	26.41
Vr	Vona–Remmit fine sandy loam, 4%–8% slopes	481.27

[1] This is the area shown in Figure 6, including the areas outside the phase boundaries.

The soils making up the Elso–Remmit–Ocean Lake association are characterized as having no to very low salinity and are heavily used for rangeland, with minor agricultural use (U.S. Department of Agriculture, 1971).

The soils within the Bell Creek Field were named based on the taxonomical classification of the dominant soils. On the landscape, the soils are natural phenomena consisting of both mineral and organic components. Therefore, the map units are generalizations that cannot provide detailed geochemical properties, which can only be determined with individual sample analysis. Since this detail is only possible on a per-sample basis, the minerals found in soils can also only be generalized. A summary of the common mineral groups found in soils is provided in Table 2.

Table 2. Common Soil Minerals and Representative Chemical Formulas

Mineral Group	Formula	Comments
Silicates		
Quartz	SiO_2	Abundant in sand and silt
Feldspar	$(Na,K)AlO_2(SiO_2)_3$	Abundant in soil that is not leached extensively
Amphibole	$(Ca,Na,K)_{2.3}(Mg,Fe,Al)_5(OH)_2[(Si,Al)_4O_{11}]_2$	
Mica	$K_2Al_2O_5(Si_2O_5)_3Al_4(OH)_4$	Source of K in most temperate-zone soils
Clay Minerals		
Kaolinite	$Si_4Al_4O_{10}(OH)_8$	
Smectite, Vermiculite, Chlorite	$Mx(Si,Al)_8(Al,Fe,Mg)_4O_{20}(OH)_4$, Where M represents an interlayer cation	Abundant in clay as products of weathering, source of exchangeable cations in soil
Oxides and Hydroxides		
Gibbsite	$Al(OH)_3$	Abundant in leached soils
Goethite	$FeO(OH)$	Most abundant Fe oxide
Hematite	Fe_2O_3	Abundant in warm regions
Ferrihydrite	$Fe_{10}O_{15}\cdot 9H_2O$	Abundant in organic horizons
Birnessite	$(Na,Ca)Mn_7O_{14}\cdot 2.8H_2O$	Most abundant Mn oxide
Carbonates and Sulfates		
Calcite	$CaCO_3$	Most abundant carbonate
Gypsum	$CaSO_4\cdot 2H_2O$	Abundant in arid regions

* Table modified from Sposito, 1989.

MINERALOGY OF RESERVOIR AND OVERLYING/UNDERLYING FORMATIONS

The EERC's Applied Geology Laboratory (AGL) and Natural Materials Analytical Research Laboratory (NMARL) team conducted two assessments to date to evaluate the petrographic, petrophysical, and mineralogical variability within intervals of interest in the oil-producing zones and overlying strata of the Bell Creek reservoir. One assessment evaluated the Niobrara, Mowry, and Muddy Formations within the Bell Creek 05-06 OW monitoring well, while the other assessment focused on the Muddy Formation across 21 wells in and near the Bell Creek oil field selected from the U.S. Geological Survey (USGS) Core Research Center in Denver, Colorado. Details of these assessments can be found in the reports summarizing this work, entitled "Bell Creek 0506OW Sidewall Core Mineralogy Assessment" (Eylands and others, 2013) and "Petrophysical Assessment of USGS Core Samples for the Bell Creek Project" (Klapperich and others, 2013), respectively.

During drilling of the 05-06 OW monitoring well in December 2011, 47 sidewall core samples were acquired. Four of the samples were from the Niobrara (shale), one was from the Mowry (shale), and the remainder were from the Coastal Plain and Bell Creek Sand intervals of the Muddy Formation. The petrophysical and petrographic properties of the samples were evaluated using techniques that included the creation and analysis of thin sections, gas pycnometry, and water permeability analysis. Porosity, water permeability, and thin-section interpretation were performed on all samples with adequate sample quantity. Twelve of the 47 sidewall core samples, including one sample each from the Niobrara and Mowry Formations and ten samples from the Muddy Formation, were selected for more detailed mineralogical evaluation using x-ray diffraction (XRD), x-ray fluorescence (XRF), scanning electron microscopy (SEM), and carbon–hydrogen–nitrogen–sulfur (CHNS) analysis. Figure 7 provides a snapshot of the petrographic characteristics of the samples from this well. (Note that for this well location [05-06 OW], the Bell Creek sand unit is further divided into the Bell Creek 10, 20, and 30 units.)

In a separate characterization activity to obtain a better understanding of the geological and petrophysical properties of the Muddy Formation in and around the Bell Creek oil field, 81 core samples from 21 wells were selected from the USGS Core Research Center and analyzed by the EERC's AGL and NMARL team. Samples were selected based on a macroscale core analysis that identified lithology of interest and material competent for sampling. The samples, which consisted of core pieces and plugs, were characterized in detail for several rock properties, such as compositional mineralogy, grain size, porosity, permeability, and pore throat mineralogy.

Table 3 is an alphabetical list of the major, minor, and trace minerals found in the Muddy Formation and overlying shales through this effort. Table 4 is a summary of the major and minor mineral content listed by geologic formation. Quartz was the dominant mineral, followed by the clay minerals kaolinite and illite. Alkali and plagioclase feldspars were also found as discrete mineral grains, as was muscovite. Rutile and pyrite were minor constituents, with rutile generally found as inclusions in quartz grains and pyrite at the edges of organic compounds. Several other minor and trace minerals were found, including apatite, zircon, and monazite.

Calcite and siderite are carbonate minerals that are considered secondary minerals in these samples as they formed after deposition, primarily as cements rather than as discrete mineral grains. Pyrite is also a secondary mineral that formed after deposition but is not a cementing material. All of the other minerals are primary minerals in that they did not change after deposition.

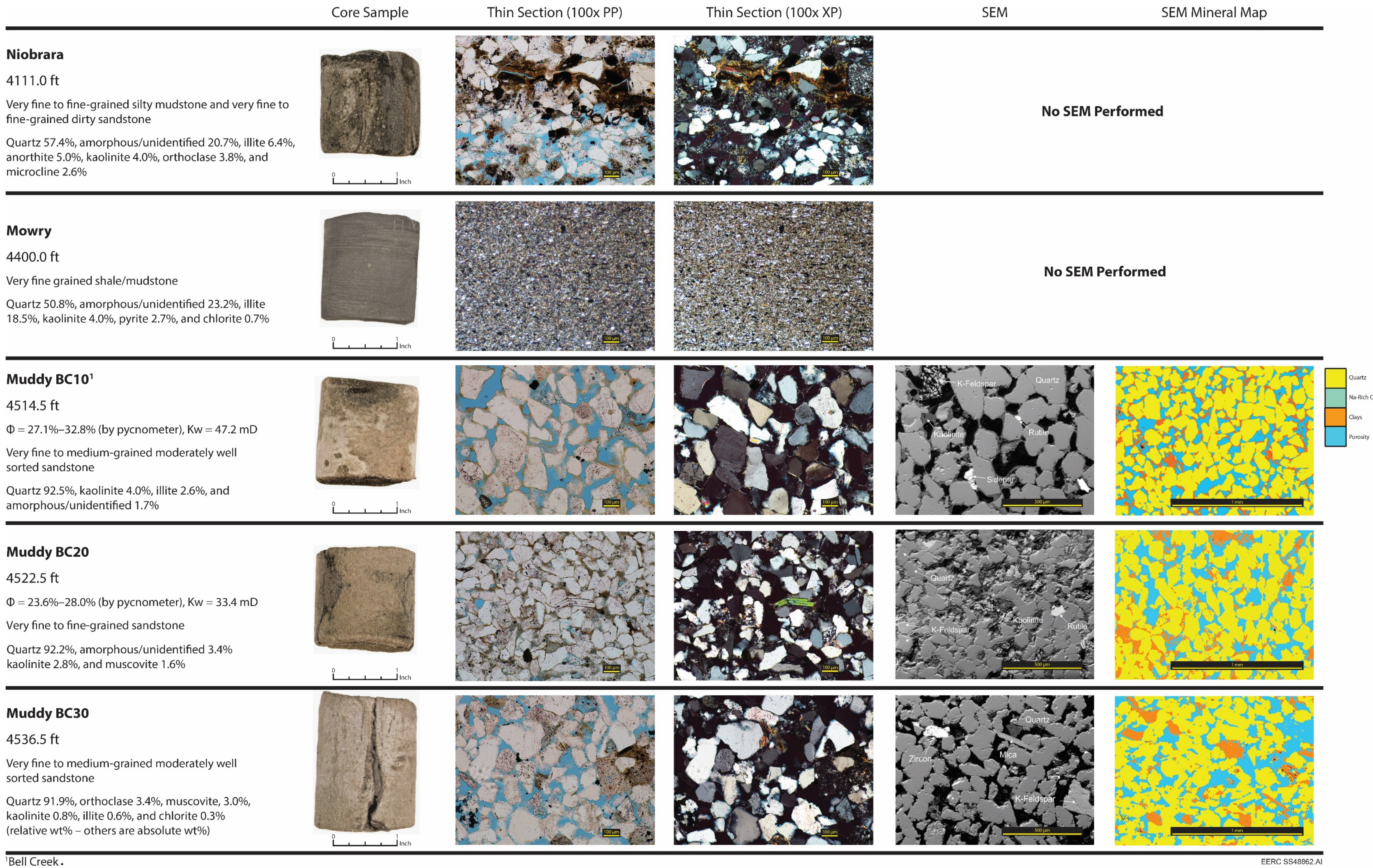

Figure 7. Representative summary of each interval tested in this evaluation, illustrating the differences in lithologic character based on thin-section and SEM analysis.

Table 3. Major, Minor, and Trace Minerals Detected in the Muddy and Adjacent Formations

Mineral Phase	Formula
Albite	$NaAlSi_3O_8$
Anorthite	$CaAl_2Si_2O_4$
Apatite	$Ca_{10}(PO_4)_6(OH,F,Cl)_2$
Calcite	$CaCO_3$
Chlorite	$(Mg,Fe)_3(Si,Al)_4O_{10}$- $(OH)_2 \cdot (Mg, Fe)_3(OH)_6$
Illite	$(K,H_3O)(Al,Mg,Fe)_2(Si,Al)_4O_{10}([OH]_2,[H_2O])$
Kaolinite	$Al_2Si_2O_6(OH)_4$
Microcline	$KAlSi_3O_8$
Monazite	$(Ce,La)PO_4$
Muscovite	$KAl_2(AlSi_3O_{10})(OH)_2$
Orthoclase	$KAlSi_3O_8$
Pyrite	FeS_2
Quartz	SiO_2
Rutile	TiO_2
Siderite	$FeCO_3$
Zircon	$ZrSiO_4$

Table 4. Summary of Major and Minor Mineral Content in the Niobrara Shale, Mowry Shale, and Muddy Formation Samples Analyzed by the EERC

Formation	Bulk Mineralogy as Determined by XRD	Additional Minor and Trace Mineral Content as Determined by Thin-Section Interpretation and/or SEM
Niobrara Shale	Quartz, anorthite, orthoclase, microcline, illite, kaolinite, calcite	Muscovite, biotite, metals
Mowry Shale	Quartz, illite, kaolinite, pyrite, chlorite	
Muddy Sandstone (Coastal Plain)	Quartz, calcite, anorthite, orthoclase, kaolinite, illite, siderite	Muscovite, metals
Muddy Sandstone (Bell Creek sand)	Quartz, kaolinite, illite, chlorite, anorthite, albite, siderite, rutile, muscovite, pyrite, calcite	Biotite, zircon, monazite

While the mineral types identified in each of the formations were similar, petrographic analysis of the Niobrara and Mowry shales demonstrated the finer-grained nature and higher clay content of these formations than in the Muddy Formation. The lithology of the Niobrara varied from a very fine to fine-grained silty mudstone with angular to subrounded quartz grains encompassed within a clay matrix, with porosity limited to horizontal and vertical fractures. The second lithology is very fine to fine-grained dirty sandstone with angular to subangular quartz cemented by clays and quartz. The Mowry lithology was very fined grained shale/mudstone, with fine-grained quartz distributed evenly throughout. Based on point-counting techniques, the Niobrara exhibited very low (<1%) to low (~10%) porosity, while the Mowry Formation was especially tight, with porosity less than 1%.

Petrographic analysis of the samples within the Muddy sandstone zones often revealed weathered feldspar (the likely source of kaolinite in the samples) as well as partial quartz grain dissolution and resulting silica overgrowths, which occurred in almost all sandstone samples. Clay lining and pore fill were also common attributes in many of the Muddy sandstones. The degree of clay lining varied substantially, with some samples only displaying a partial lining and others containing nearly filled pore space. As would be expected, the zones within the Muddy Formation that contained a higher clay content, such as the Coastal Plain unit and the transition zones between the various sand benches, generally had reduced permeability and porosity. Siderite, chlorite, and/or pyrite were also observed as either primary or secondary components of the sandstone units. Siderite occurred either as very fine-grained rhombs or irregularly shaped microcrystalline pore fill. Kaolinite was the predominant clay in nearly every sample. A low-porosity, calcite-cemented quartz sandstone unit was also identified in several of the wells.

RESERVOIR FLUID COMPOSITIONS

Characterization of the reservoir fluids is important for understanding potential geochemical interactions within the reservoir following CO_2 injection. The data obtained are important for understanding the minimum miscibility pressure (MMP) needed to most efficiently extract the oil from the reservoir and how the oil will behave during the injection process. The reservoir fluid characteristics are key components needed for modeling and simulation efforts, which will be used to predict any potential geochemical interactions between the rocks and fluids of the reservoir and overlying formations with the injected CO_2.

Formation Water Analyses and Madison Aquifer Properties

The original water chemistry of the Muddy Formation in Bell Creek has been altered slightly by secondary oil recovery, primarily flooding with water from the Cretaceous Madison Formation. Water injection was initiated in August 1970, reached a plateau in late 1973, and continues today.

The EERC analyzed samples of water used as injection water and produced water from the Bell Creek Field and characterized the samples based on a suite of analyses. Samples analyzed included:

- Preinjection water extracted from the Madison Formation via Water Supply Well No. 1, referred to as Madison produced water.
- Blended production water from a tank battery (Production Tank Battery #3), referred to as production water.
- Blended production water from Phase 1 after undergoing treatment in a “heater treater,” referred to as treated production water.

Results of the production water analyses are provided in Table 5.

Table 5. Production Water Analyses

	Madison Produced Water	Production* Water	Treated Production Water*
Alkalinity, as bicarbonate (HCO_3^-), mg/L	210	1260	1270
Alkalinity, as carbonate (CO_3^{2-}), mg/L	0	91	0
Alkalinity, as hydroxide (OH^-), mg/L	0	0	0
Alkalinity, total as $CaCO_3$, mg/L	172	1180	1040
Calcium, mg/L	207	13	61
Chloride, mg/L	64	1710	1580
Magnesium, mg/L	52	3	17
Potassium, mg/L	8	9	9
Sodium, mg/L	44	1350	1030
Sulfate, mg/L	594	5	61
Total Dissolved Solids (TDS), mg/L	962	3070	4650
pH	7.0	8.9	7.3

* Represents blended production water from all producing wells.

Reservoir Fluids

To better understand the effectiveness of tertiary oil recovery in the Bell Creek Field using CO_2, reservoir fluid samples were collected from three wells for compositional analysis and determination of MMP and pressure, volume, and temperature (PVT) properties. These data were further used to conduct PVT modeling using WinProp™, a program developed by Computer Modelling Group Ltd to identify and model the phase behavior and properties of reservoir fluids.

Initial fluid property data from across the Bell Creek Field show a range in American Petroleum Institute (API) gravity from 32.5 to 41, gas-to-oil ratios (GORs) ranging from 200 to 306 scf/bbl, and oil viscosity (at the bubble point and reservoir temperature) varying from 1.02 to 2.75 cP. A summary of these initial fluid property data is given in Table 6 (Burt and others, 1975).

The laboratory analyses of samples collected in 2009 indicated that the crude oil from two of the wells were compositionally alike, with similar concentrations of light, intermediate, and heavy components. A less detailed analysis was conducted on the third sample. In all three samples, no hydrogen sulfide was detected in the oil and the mole fraction of C7+ hydrocarbons was greater than 25%. The composition of a recombined live crude oil sample from Well 5-11, a representative sample from Phase 1, expressed in terms of the carbon number of hydrocarbon constituents, is shown in Figure 8.

Lab-measured MMP values for the oil samples, recombined to original reservoir conditions, ranged from 1165 to 3220 psia. Subsequent lab-measured MMP values for oil samples at depleted conditions (i.e., GORs of ~40 scf/stb) range from 1342 psia to 1845 psia. Miscibility is affected by reservoir fluid composition, injection gas composition, and reservoir temperature. This highlights the need for actual crude oil compositional analyses that are representative of the current oil and GOR in the reservoir.

Table 6. Original Bell Creek Field Fluid Properties (Burt and others, 1975)

Property	A	B	C	D	E	F (Ranch Creek)
API Gravity	32.5	35	35.5	37.5	40	41
Original P, psig	1190	1230	1215	1200	1200	1150
Reservoir Temp., °F	108	103	108	108	108	108
Bubble Point, psia	1190	1230	1215	1200	700	665
FVF* Orig.	1.112	1.122	–	–	1.140	1.205
GOR, scf/bbl	200	224	–	–	247	306
Viscosity at Bubble Point, cP	2.75	–	–	–	1.2	1.2

* Formation volume factor.

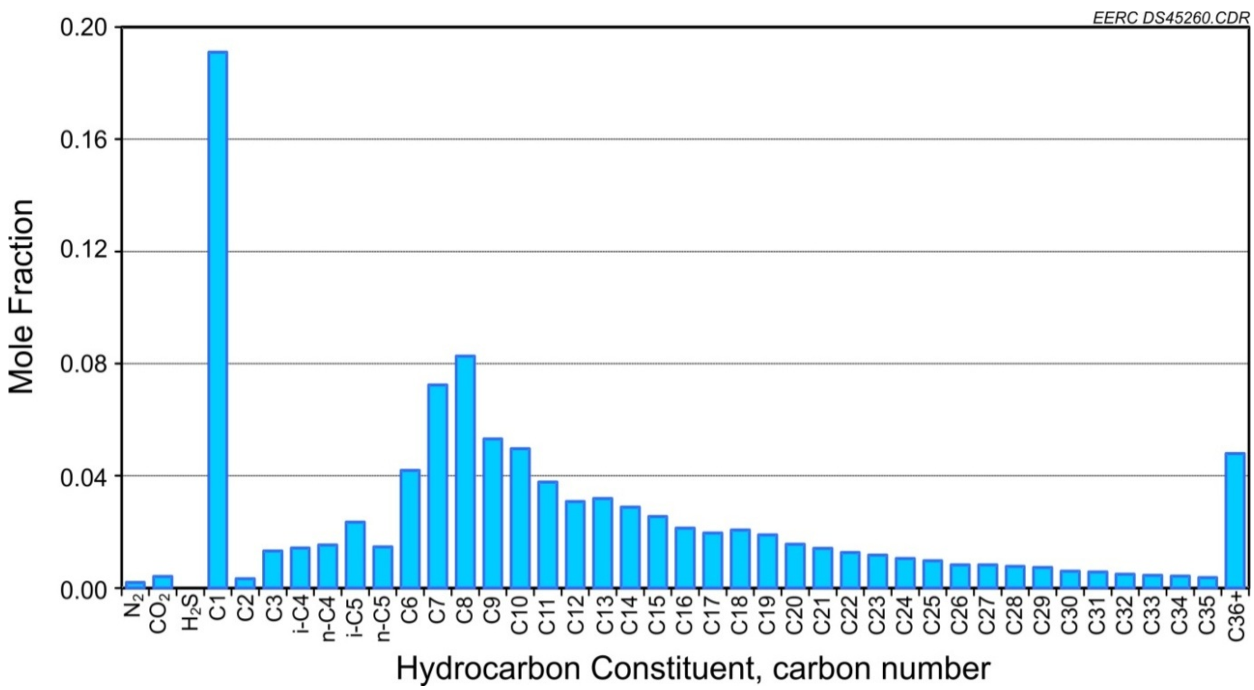

Figure 8. Composition of recombined live crude oil at original conditions (Well 5-11).

A more recent PVT modeling investigation was conducted, and the modeling results suggest that the depleted Bell Creek oil has a MMP of 1180 psia at 40 scf/bbl of GOR, which shows a significant drop from the 2970 psia at the original reservoir condition (GOR at 275 scf/bbl). Lab-measured data support a 1342-psia MMP for the same oil at depleted conditions.

SURFACE AND NEAR-SURFACE WATER AND SOIL GAS COMPOSITION

A surface and near-surface-monitoring program is in place to provide critical data that can be used to verify site security, assess variances to the injection program, and determine the fate of injected CO_2. A technical team is conducting a variety of sampling activities at the Bell Creek oil field, focused primarily in the area in which CO_2 injection will begin, to provide a detailed chemical characterization during multiple sampling events. The surface and near-surface monitoring comprises three parts: sampling of surface water features, sampling of shallow groundwater, and sampling of soil gas in the vadose zone. Two new groundwater-monitoring wells in the injection area (Phase 1) have been completed in the Fox Hills Formation, the deepest USDW, to enhance the near-surface program. Sampling these zones will provide baseline chemistry including concentrations of CO_2, which can later be used to determine if CO_2 levels found in these media during injection are because of natural occurrence (is within a probable statistical range of naturally occurring levels as determined by baseline data) or may be the result of an out-of-zone fluid migration. If CO_2 were to migrate from the deep subsurface, it could affect all of these environments or any one independently, depending on the geology and geography of the near-surface environment and the environmental conditions at that time (i.e., season of year, groundwater levels, etc.). The baseline monitoring program was completed in April 2013, and the results are summarized in the following section.

Water Composition

Water samples from nine different surface waters, seven stock wells, seven drinking water (residential) wells, and two dedicated groundwater-monitoring wells have been sampled and analyzed. Because of significant evaporation, some of the surface water sites could not be sampled during all of the sampling events. Existing well records indicated that the stock wells and residential wells were drilled and completed in the Hell Creek Formation. As stated previously, the new groundwater-monitoring wells were completed in the Fox Hills Formation. The locations of all water sources are shown in Figure 9. Detailed field and laboratory analyses were conducted on the water samples. Field analyses included pH, temperature, alkalinity, specific conductance (SC), dissolved oxygen (DO), and dissolved carbon dioxide. Laboratory analyses included major cations and anions, dissolved gases, purgeable and extractable organic compounds, hydrocarbons, metals, radionuclides, and isotopic analyses. Details of the sampling techniques and results are being compiled into a draft report entitled “Bell Creek Test Site – Baseline MVA Activities.”

A summary of the range of values obtained in the field are provided in Table 7 based on the category of water source. In general, waters in the Bell Creek Field are slightly alkaline, with pH levels typically ranging from around 7 to greater than 9. A majority of dissolved CO_2 measurements for surface waters and stock well samples were less than 20 mg/L, and in many of the samples, no CO_2 was detected.

SC levels were fairly consistent throughout the baseline sampling period for individual sampling locations, typically ranging from about 200 to 1200 μS/cm overall, depending on sampling location. One exception was the Surface Water #3 location, where SC was significantly higher and ranged from 4000 to 6000 μS/cm. Surface Water #3 is on a natural stream about 2 miles downstream of a National Pollutant Discharge Elimination System-permitted point source discharge of produced water, which has somewhat higher levels of dissolved salts, specifically sodium chloride. SC values measured during the warmer June 2012 and August 2012 sampling events were at their highest levels, likely due to surface evaporation and low-streamflow conditions.

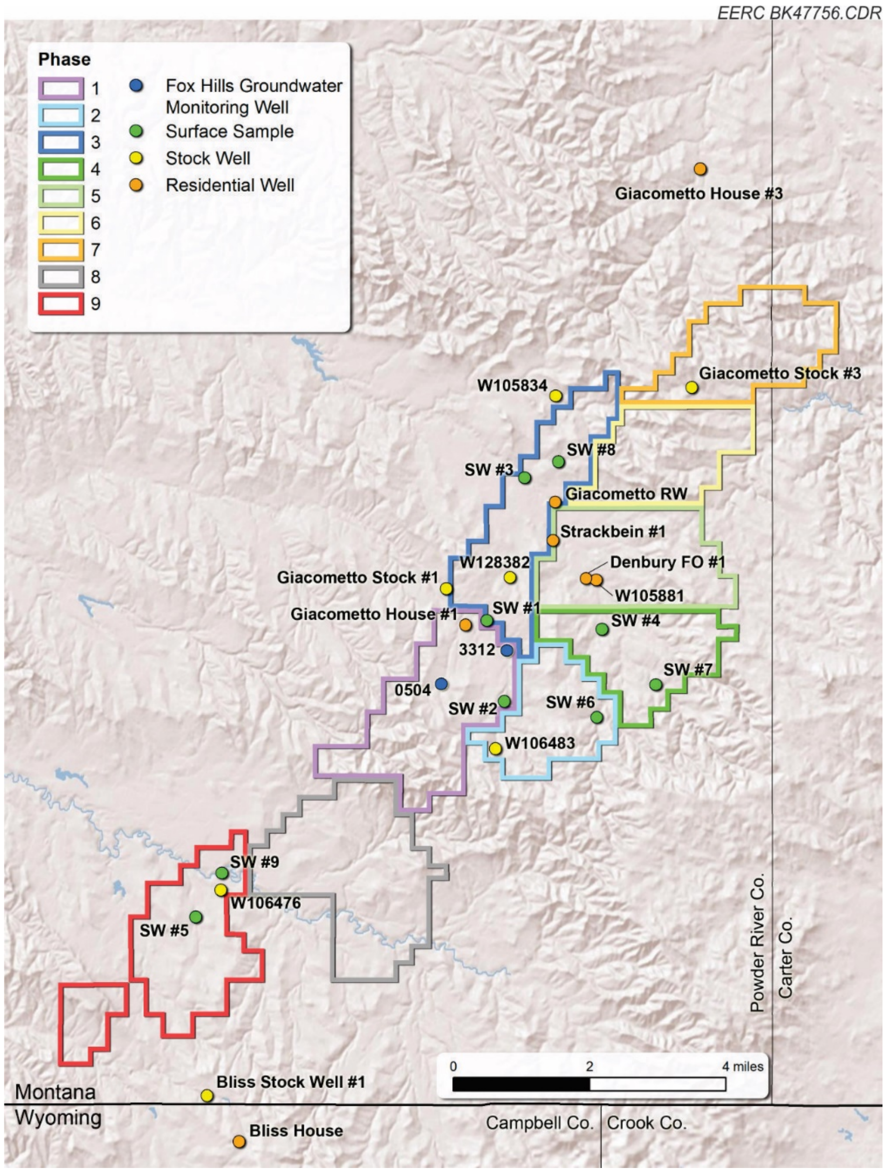

Figure 9. Bell Creek baseline surface and groundwater well location map (SW refers to Surface Water; RW stands for Rural Water; FO is Field Office).

Alkalinity was also measured in the field with values generally ranging from 110 to 400 mg/L, with confirmation analyses conducted in the laboratory. The Surface Water #3 sample showed consistently high alkalinity ≥900 mg/L as $CaCO_3$, consistent with the SC trend. The Surface Water #9 sample, a small, low-flow stream susceptible to evaporation concentration, also exhibited higher alkalinity concentrations, averaging 520 mg/L for the August and November 2012 sampling events.

Table 7. Bell Creek Area Water Quality – Range of Field Results

Parameter	Surface Waters[a]	Residential Wells	Stock Wells	Groundwater Wells[b]
pH	6.44–10.4	8.52–9.72	7.11–9.39	9.17–9.51
Water Temperature, °C	1.2–27.9	5.2–19.6	9.7–17.4	13.2–13.7
Dissolved Oxygen, mg/L	0.55–16.7	0.02–2.37	0.1–4.88	0.11–0.27
Specific Conductance, µS/cm	163–6140	391–906	448–1943	466–506
Dissolved CO_2, mg/L	ND[c]–35	ND	ND–27	ND
Alkalinity, as $CaCO_3$, mg/L	111–1190	165–336	180–405	201–273
Cl, mg/L	4–1500	3–18	2–30	ND

[a] Samples subject to evaporative losses.
[b] One data point per well.
[c] Not detected.

Select physical and organic parameter results obtained through laboratory analyses are provided as a range of values in Table 8 based on the category of water source. Dissolved methane was detected in the water samples, albeit at very low levels. A majority of the dissolved methane was at concentrations very near the method detection limit of 0.001 mg/L for measuring dissolved methane. The highest concentration of methane detected was 0.129 mg/L at one of the surface water-monitoring sites. The methane content of the various water types, especially the surface water samples, is likely a result of microbial decomposition of organic matter, a common occurrence in natural systems where organic matter is present.

The range of major anion and cation concentrations determined from all six baseline events are reported in Table 9, and grouped based on water type (surface water, residential well, or stock well). The chemical analysis of the Fox Hills groundwater-monitoring wells is listed separately in Table 10. Many of the analytes were not present at detectable levels, and all werewell below maximum contaminant levels (MCLs) established by U.S. Environmental Protection Agency

Table 8. Bell Creek Area Water Quality – Range of Select Laboratory Physical and Organic Parameter Results

Parameter	Surface Waters[a]	Residential Wells	Stock Wells	Groundwater Wells[b]
	Physical Parameters, mg/L			
Measured TDS	42–3790	134–614	66–1640	309–346
Alkalinity as $CaCO_3$	98.3–1360	180–290	181–397	201–250
Total Organic Carbon (TOC)	7.1–317	ND[c]–4.0	ND–4.2	2.4–2.7
Dissolved Organic Carbon (DOC)	6.5–252	0.6–3.6	0.7–4.5	2.2–2.9
Total Inorganic Carbon (TIC)	20.6–348	43.0–70.3	46.4–105	45.4–59.8
Dissolved Inorganic Carbon (DIC)	18.3–342	43.7–71.1	46.1–107	45.6–59.8
Methane	0.002–0.129	ND–0.006	ND–0.006	0.001–0.002

[a] Samples subject to evaporative losses.
[b] One data point per well.
[c] Not detected.

Table 9. Bell Creek Area Water Quality Range for All Six Baseline Events

Parameter	Surface Waters	Residential Wells	Stock Wells
	Anions, mg/L		
Bicarbonate	55.5–1550	155–318	203–489
Bromide	<1–13	<1	<1
Carbonate	<0.1–64	8.8–39	<0.1–25
Chloride	3.3–1910	1.10–3.98	<1–9
Fluoride	<1	<1	<1
Nitrate	–	<0.1	–
Nitrite	–	<0.1	–
Sulfate	<5–742	45–224	31–930
Sulfide	<0.05–4.30	<0.05–0.40	<0.05–1.10
	Cations, mg/L		
Barium	0.036–0.301	<0.005–0.033	<0.005–0.035
Boron	<0.2–4.3	<0.2	<0.2
Calcium	13–111	<1–25	3–255
Iron	0.006–1.470	<0.005–0.056	<0.005–0.769
Magnesium	5–80	<1–5	<1–148
Manganese	0.006–1.130	<0.005–0.145	0.017–0.224
Phosphorus	<0.1–0.6	<0.1	<0.1
Potassium	4–36	<1–2	<1–8
Silicon	<1–10	4–6	4–11
Sodium	7–1460	107–238	78–353
Strontium	0.1–3.0	<0.1–0.4	<0.1–4.3
Measured TDS, mg/L	42–3788	134–614	66–1750

(EPA) primary drinking water regulations. Table 11 lists the results of priority pollutant analyses that were conducted on groundwater samples. Almost all of the samples had nondetectable concentrations of priority pollutants, and those that were detected (copper, selenium, and zinc) were well below a MCL established by EPA.

The detailed results of the volatile organic compound (VOC) analyses were below detectable limits for the analytical technique. Semi-VOCs were well below EPA MCLs with mostly nondetects. The samples were also analyzed for additional organics, including ethane, ethene, and total petroleum hydrocarbons. None of these constituents were detected in any of the samples.

Radionuclides were analyzed for all baseline residential well samples. As shown in Table 12, baseline monitoring results indicate that all radionuclides were well below established EPA MCLs.

Select samples were submitted for additional isotropic analysis from each sampling event (each time from the same well or surface source). Both surface water and stock well samples analyzed from the Bell Creek Field show fractionation consistent with meteoric origins (Figure 10). The stock well samples in particular are very consistent between the seasonal sampling

Table 10. Bell Creek Area Monitoring Well Water Quality – Select Results for Baseline Event (April 2013)

Parameter	MW0504	MW3312
pH	9.17	9.51
Temperature, °C	13.2	13.7
SC, μS/cm	506	466
DO, mg/L	0.11	0.27
Dissolved CO_2, mg/L	ND[a]	ND
Alkalinity as $CaCO_3$, mg/L	250	201
	Anions, mg/L	
Bicarbonate	275	196
Bromide	ND	ND
Carbonate	14.6	24.5
Chloride	1.60	2.00
Fluoride	ND	ND
Nitrate	ND	ND
Nitrite	ND	ND
Sulfate	50.6	72.9
Sulfide	ND	ND
	Cations, mg/L	
Barium	0.013	0.015
Boron	ND	ND
Calcium	2.16	2.36
Iron	0.029	0.031
Magnesium	ND	ND
Manganese	0.014	0.007
Phosphorus	ND	ND
Potassium	ND	ND
Silicon	4.60	4.60
Sodium	141	124
Strontinum	ND	ND
Measured TDS, mg/L	346	309
Charge Balance Error, %	1.2	−0.8

[a] Not detected at the analytical reporting limit (see Stepan and others, 2013, for detection limits).

events. Some deviation is observed in the surface water samples, which is attributed to natural evaporation. Plots of the carbon isotopes in the water samples are also consistent with natural processes (Figure 11). The carbon istotope fractionation measured in the water samples is consistent with values expected in natural systems. Once again, the stock well samples have produced consistent values, with the greatest variation occurring in surface waters, which are more strongly influenced by various climatic factors.

Table 11. Priority Pollutant Metals (dissolved) in Residential, Stock Well, and Groundwater Well Water During Baseline Water-Sampling Events (ranges are presented where a specific constituent was detected), mg/L

Priority Pollutant Metals	Residential Wells	Stock Wells	Groundwater Wells	EPA MCL Regulation
Antimony	<0.005	<0.005	<0.005	0.006
Arsenic	<0.001	<0.001	0.011–0.013	0.01
Beryllium	<0.004	<0.004	<0.004	0.004
Cadmium	<0.002	<0.002	<0.002	0.005
Chromium	<0.005	<0.005	<0.005	0.1
Copper	<0.005–0.009	<0.005	<0.005	1.3[a]
Lead	<0.005	<0.005	<0.005	0.015[a]
Mercury	<0.0001	<0.0001	<0.0001	0.002
Nickel	<0.005	<0.005–0.016	<0.005	None
Selenium	<0.001	<0.001–0.01	<0.001	0.05
Silver	<0.005	<0.005	<0.005	0.10[b]
Thallium	<0.0005	<0.0005	<0.0005	0.0005
Zinc	<0.005–0.01	<0.005–0.568	<0.005	5[b]

[a] Regulated by a treatment technique that requires systems to control the corrosiveness of their water. If more than 10% of tap water samples exceed the action level, water systems must take additional steps. For copper, the action level is 1.3 mg/L and for lead 0.015 mg/L. The national secondary drinking water standard for copper is equal to 1.0 mg/L.

[b] Regulated only by national secondary drinking water regulations, which are nonenforceable guidelines regulating contaminants that may cause cosmetic or aesthetic effects in drinking water.

Table 12. Radionuclide Results for Residential Wells – Range of Results for All Five Baseline Sampling Events

Radionuclide	Residential Wells, pCi[1]/L	Groundwater Well, pCi/L	EPA MCL, pCi/L
Gross Alpha	<1.0–4.9	5.4	15
Gross Beta	<1.3–1.6	2.5	50
Radium 226	<0.06–0.3	0.04	5
Radium 228	<0.6–2.3	0.2	5
Radium 226 + Radium 228	<0.7–2.3	0.4	5

[1] pCi is picocurie.

The greatest changes in water chemistry were observed in surface waters, where evaporation played a major role. Groundwaters exhibited more consistent chemistry quality, but more variability for key parameters such as pH and dissolved CO_2 existed in surface waters and stock wells compared to residential wells, with stock wells showing the greatest seasonal changes. All of the wells that were monitored were drilled into the same water-bearing formation, and the reason for the differences in changing concentrations in different wells is unknown at this time.

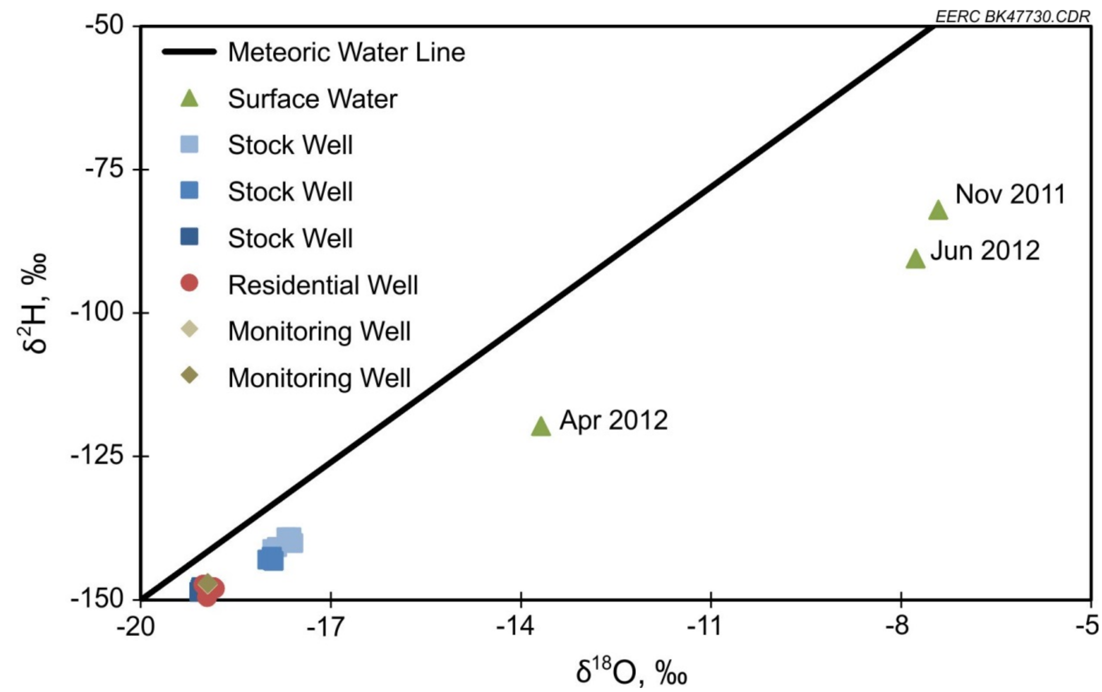

Figure 10. Isotopic values ^{2}H and ^{18}O measured in surface and groundwater samples at the Bell Creek Field area.

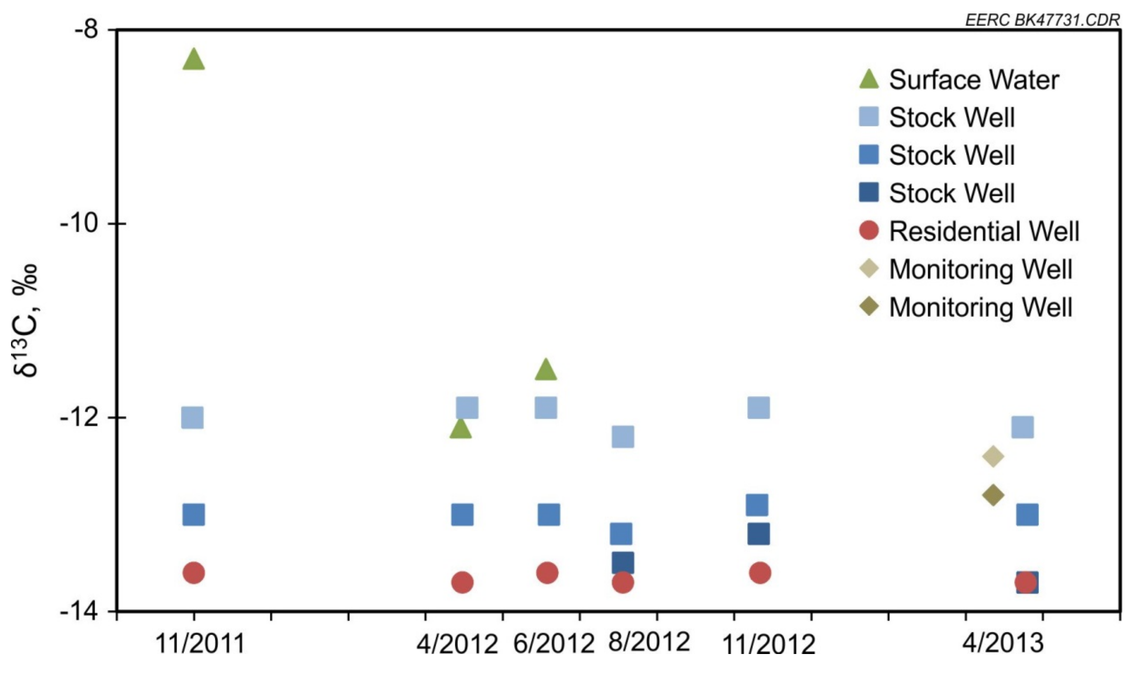

Figure 11. Distribution of ^{13}C dissolved in water samples collected during the seasonal sampling events.

In general, good-quality water exists in the Bell Creek oil field. More variability for key parameters such as pH and dissolved CO_2 exists in surface waters and stock wells compared to residential wells. Water samples were below detectable limits and/or satisfied EPA MCL regulations for petroleum hydrocarbons, VOCs, semi-VOCs, and dissolved gases such as ethane and ethene. Surface waters tend to be predominantly calcium–magnesium–sulfate chemistry, while groundwaters are sodium sulfate-dominated. Stable water isotopes indicated the values fall within the ranges expected for H and O isotopes originating from natural processes. Carbon isotopes of DIC were indicative of natural background levels resulting from dissolution of mineralized CO_2 and contained measurable levels of ^{14}C, indicating recent origin.

Soil Gas Composition

Soil gas sampling consisted of extracting representative samples of the gases present within the vadose zone, which includes naturally occurring CO_2. Soil gas-sampling sites were established at 186 locations across the Bell Creek Field, with emphasis on the Phase 1 area, and at select locations (six to eight well locations per phase unit) throughout the remainder of the field. Soil gas samples were collected at 124 active well locations as well as 52 plugged and abandoned well sites, which could provide a greater potential pathway for out-of-zone fluid migration, and ten interspaced (between active wells) locations, chosen to provide preinjection baseline data at locations not associated with wells. Figure 12 is a map of soil gas-sampling locations.

Near-surface vadose zone soil gas sampling showed normal background levels of soil gases, with higher concentrations of CO_2 observed during warmer and wetter climate conditions. Analyses indicated the presence of nitrogen, oxygen, and carbon dioxide as the only detectable soil gases (Table 13). Methane, carbon monoxide, ethane, ethylene, and hydrogen were not detected in any of the soil gas samples. Figure 13 is a plot of O_2 versus CO_2 for the near-surface soil gas-sampling sites. These results show increasing levels of CO_2 and decreasing levels of O_2 with depth, as is consistent with biological respiration of soil organic matter and not oxidation of methane.

Carbon isotope data in the soil gas showed that the soil gas carbon is consistent with natural processes. The signatures detected in the soil gas are indicative of a C3 plant-dominated environment, with some mixing of CO_2 resulting from plant decomposition and/or the presence of a smaller population of C4 plants (both of which generate less negative enrichment values).

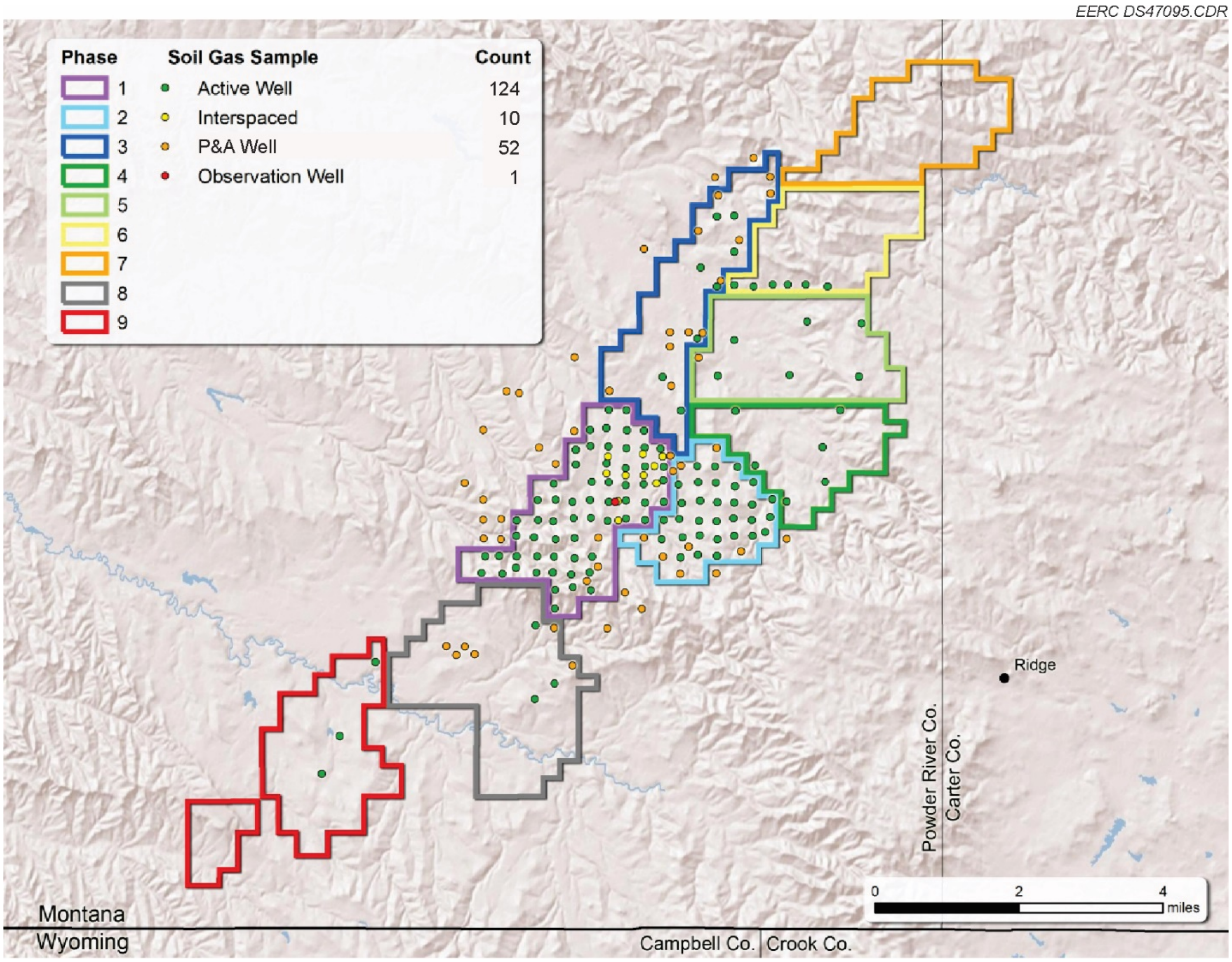

Figure 12. Bell Creek baseline soil gas-sampling locations.

Table 13. Soil Gas Sample Result Ranges, November 2011 – November 2012, %

Sample Type	CO_2	O_2	N_2
Active Well	0.04–4.15	16.0–21.6	73.6–81.5
Interspaced Location	0.03–1.74	19.4–21.4	74.8–79.8
Plugged and Abandoned Wells	0.04–2.96	18.4–21.5	75.4–81.1

In addition to the soil gas measurements at active wells, plugged and abandoned wells, and interspaced locations, ten fixed soil gas profile stations (SGPSs) were installed in the Phase 1 area of the Bell Creek site in October 2012 to provide an understanding of how the concentrations of soil gases vary with depth. Nine of the ten SGPSs were installed near existing active wells, and the other SGPS was installed near EERC Monitoring Well 05-06 OW. Each SGPS consisted of a shallow polyvinyl chloride (PVC) well with nested tubing individually screened at depths of 3.5, 9.0, and 14 feet below the ground surface. Locations of the fixed SGPSs are shown in Figure 14.

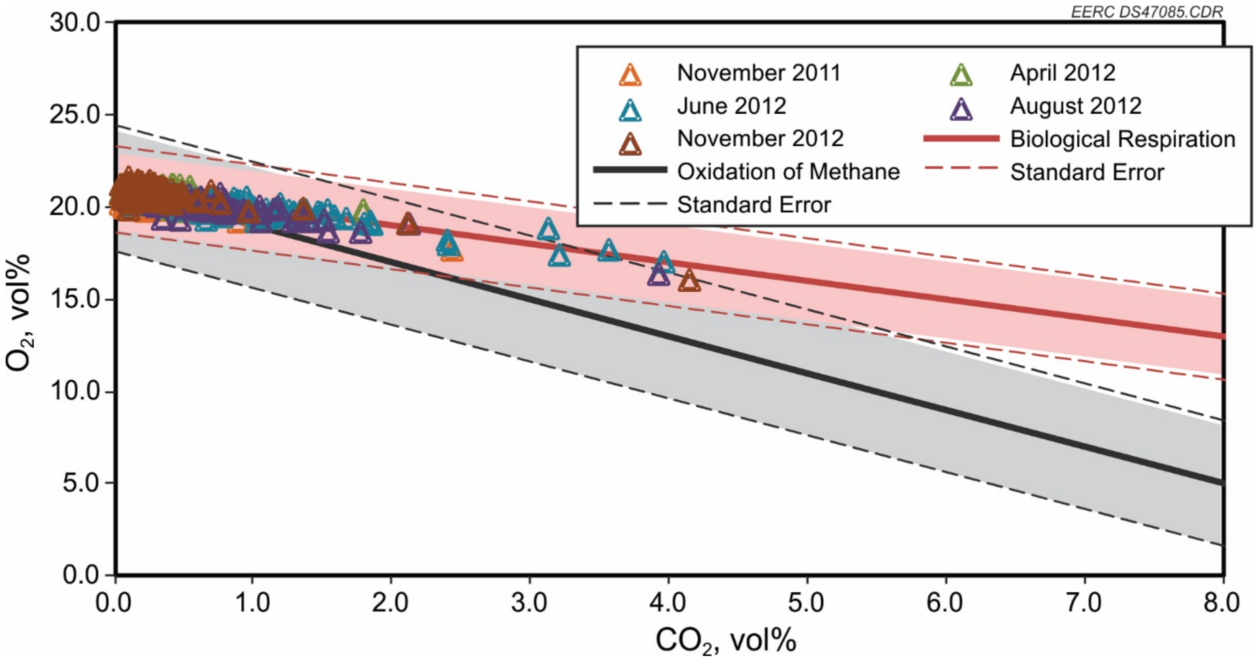

Figure 13. Bell Creek baseline O_2 versus CO_2 at active well sites – Agilent Micro Quad 490 GC. Samples collected from November 2011 to November 2012.

Figure 15 is a plot of O_2 versus CO_2 for the individual depths at all ten SGPS locations. The increasing levels of CO_2 and decreasing levels of O_2 with depth suggest that the near-surface soils tend to undergo normal biological respiration. The O_2-to-CO_2 ratios near Monitoring Well 05-06 OW were not indicative of biological respiration and were more consistent with methane oxidation; however, no methane was detected in any of the wells. Because these observations were based on a limited data set, it is difficult to make any conclusions at this time. It is also unclear how surface disturbances (such as drilling pad construction and leveling) associated with drilling activities may or may not have disrupted the natural environment. Data will continue to be collected to provide additional insight with respect to this well.

SHALLOW CO_2 EXPOSURE LABORATORY EXPERIMENTS

As part of ongoing Bell Creek geochemistry efforts, the EERC conducted a laboratory geochemical evaluation complementary to the MVA activities to determine the potential and unlikely effect of out-of-zone migration of CO_2 into the freshwater aquifers overlying the Bell Creek reservoir. Increased CO_2 concentrations in the groundwater zone could lead to enhanced and varied chemical modifications that could increase mineral weathering, change the geochemistry of the water sediment equilibrium, change the water quality, and/or potentially release trace metals into the groundwater system. Monitoring of shallow groundwater wells before, during, and after injection of CO_2 in a deep repository could be an effective way to identify out-of-zone CO_2. A key goal of this study was to increase the likelihood of an early leak detection (if present) by identifying potential indicator species in the groundwater zones overlying the Bell Creek reservoir in the unlikely event of out-of-zone CO_2 migration.

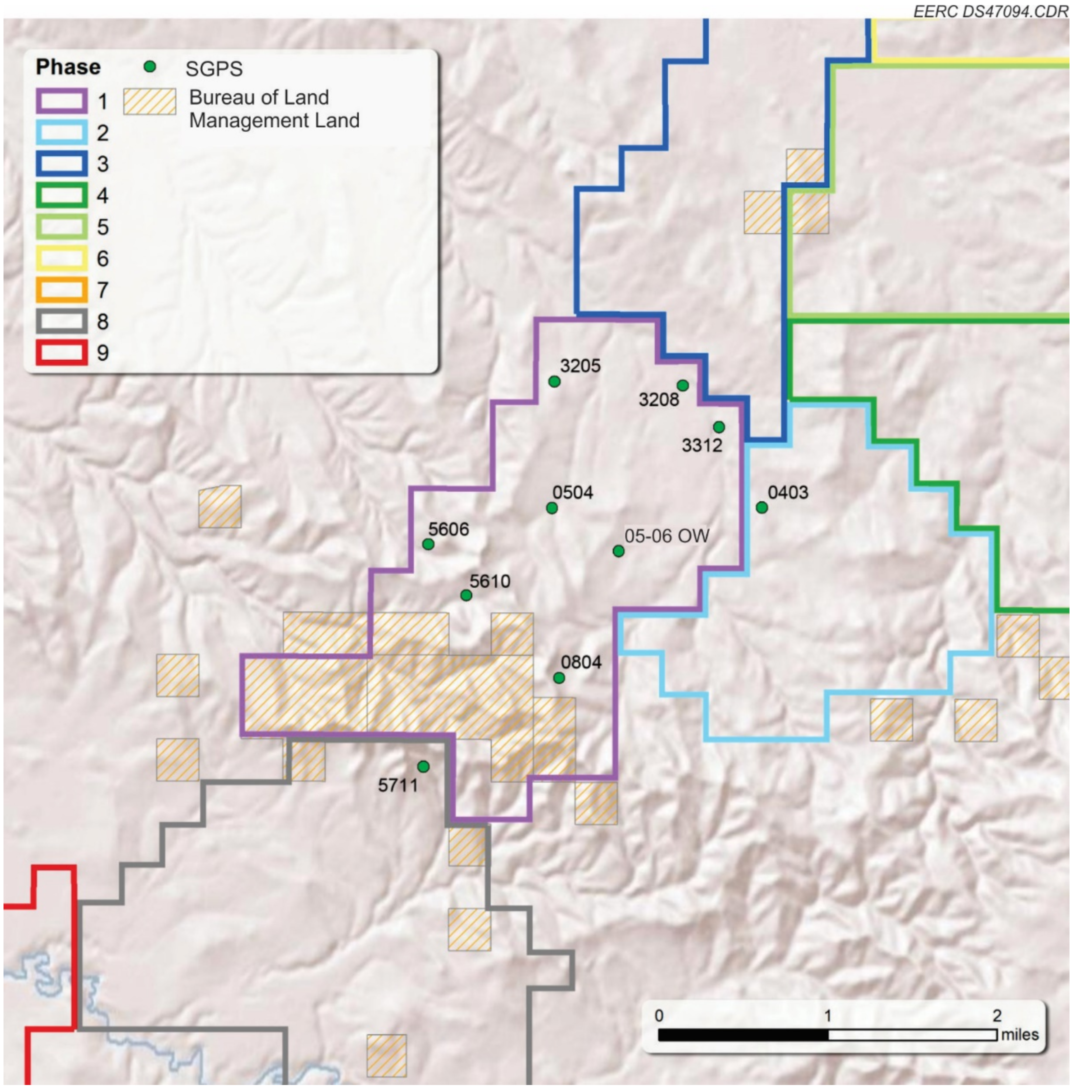

Figure 14. SGPSs located within and around the Phase 1 area, installed near existing active wells.

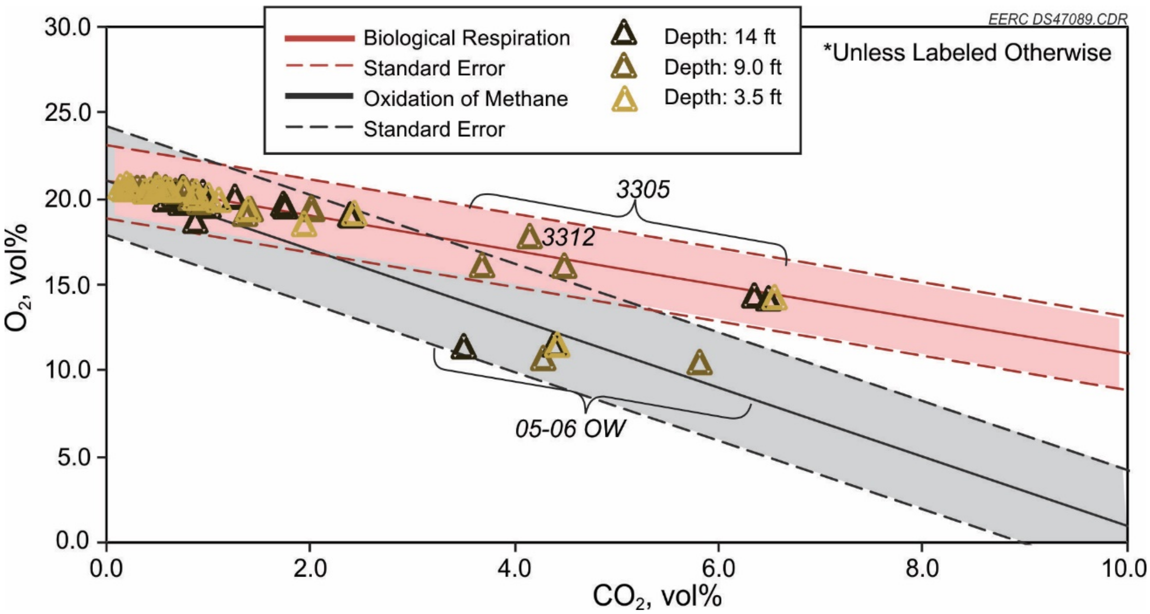

Figure 15. Bell Creek baseline O_2 versus CO_2 at SGPS sites – Agilent Micro Quad 490 GC. Samples collected in October and November 2012.

Laboratory experiments were designed to expose drill cuttings from the Bell Creek 05-06 OW monitoring well and groundwater collected during field sampling activities from the Hell Creek Formation to CO_2 at corresponding in situ temperatures and pressures. The results of the batch experiment testing provided information and semiquantitative data on potential mineralogical dissolution and/or precipitation reactions in the formation rock following exposure to CO_2. In addition, the comparison of baseline groundwater concentrations to exposed groundwater concentrations provided data about potential mineral-phase dissolution and other groundwater chemistry changes caused by exposure to CO_2. A variety of analytical techniques were used to obtain mineralogical and chemical data for the formation samples and groundwater prior to and following CO_2 exposure. These geochemical data can provide valuable insight regarding the potential impact and identification of elevated CO_2 exposure of the groundwater zone.

Rock cuttings from the Hell Creek Formation were collected in December 2011 by EERC personnel during the drilling of the 05-06 OW monitoring well as part of MVA activities in the Bell Creek oil field. Six samples of the drill cuttings were selected from various depths spanning the Hell Creek formation for use in the CO_2 exposure experiments. As shown in Figure 16, the samples ranged in composition from clayey sandstone to a varied mixture of shale and sandstone. The XRD results from the six samples show the dominance of quartz with minor amounts of plagioclase feldspars and clays, illite and kaolinite (Table 14). In addition, some of the samples, HC120-150 and HC300-330, show significant carbonates, calcite, and dolomite.

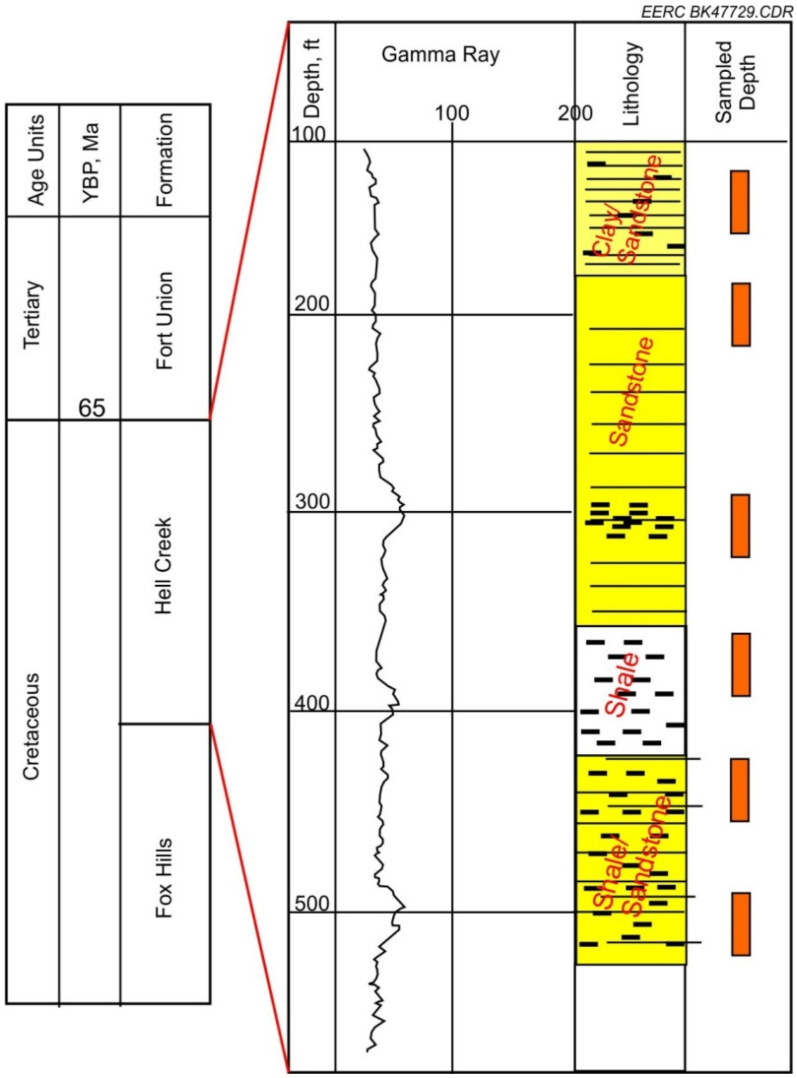

Figure 16. Stratigraphy of the Hell Creek Formation showing cutting depths and lithology (YBP refers to "years before present").

Table 14. Mineralogical Content of the Hell Creek Formation Samples as Determined by XRD

Report Sample ID	XRD Phase	wt%	Crystal Density, g/cm^3
HC120-150	Amorphous/Unknown	10.6	
	Dolomite	4.0	2.86
	Albite	4.5	2.62
	Quartz	44.6	2.65
	Kaolinite	5.2	2.55
	Illite	12.5	2.81
	Anorthite	10.6	2.76
	Calcite	8.0	2.74
HC180-210	Amorphous/Unknown	1.4	
	Quartz	63.0	2.65
	Kaolinite	1.8	2.54
	Illite	9.9	2.80
	Anorthite	23.9	2.76
HC300-330	Amorphous/Unknown	4.2	
	Dolomite	7.3	2.86
	Albite	3.6	2.63
	Quartz	45.9	2.65
	Kaolinite	3.5	2.54
	Illite	12.0	2.80
	Anorthite	12.6	2.75
	Calcite	10.9	2.73
HC360-390	Amorphous/Unknown	7.3	
	Dolomite	3.3	2.85
	Quartz	48.9	2.65
	Kaolinite	5.5	2.54
	Illite	15.9	2.80
	Anorthite	16.9	2.75
	Calcite	2.2	2.76
HC420-450	Amorphous/Unknown	9.4	
	Albite	22.7	2.62
	Quartz	54.5	2.65
	Kaolinite	1.4	2.57
	Illite	9.7	2.77
	Pyrite	2.3	5.02
HC480-520	Amorphous/Unknown	6.2	
	Albite	21.2	2.62
	Quartz	54.2	2.65
	Kaolinite	5.0	2.57
	Illite	11.1	2.77
	Anorthite	2.3	2.75

Three water wells located within the Bell Creek Field and screened in the Hell Creek Formation were used to provide the groundwater for these experiments. As shown in Figure 17, the specific wells were the Giacometto House #3, the Bliss Stock Well #1, and the W106476 stock well. Water samples from these wells were collected by the EERC monitoring team in April 2012 and stored under refrigeration at the EERC.

To conduct the CO_2 exposure tests, each of the three groundwater samples was combined with drill cuttings from two different depths. The drill cuttings were matched with the corresponding groundwater from a similar depth ranging from 120 to 520 feet below ground surface. In addition to the six rock-cutting samples, three other samples were included for CO_2 exposure in the reactor for quality assurance/quality control purposes. Magnesium silicate (Mg_2SiO_4) powder (American Chemical Society-grade) was used as a standard to test the

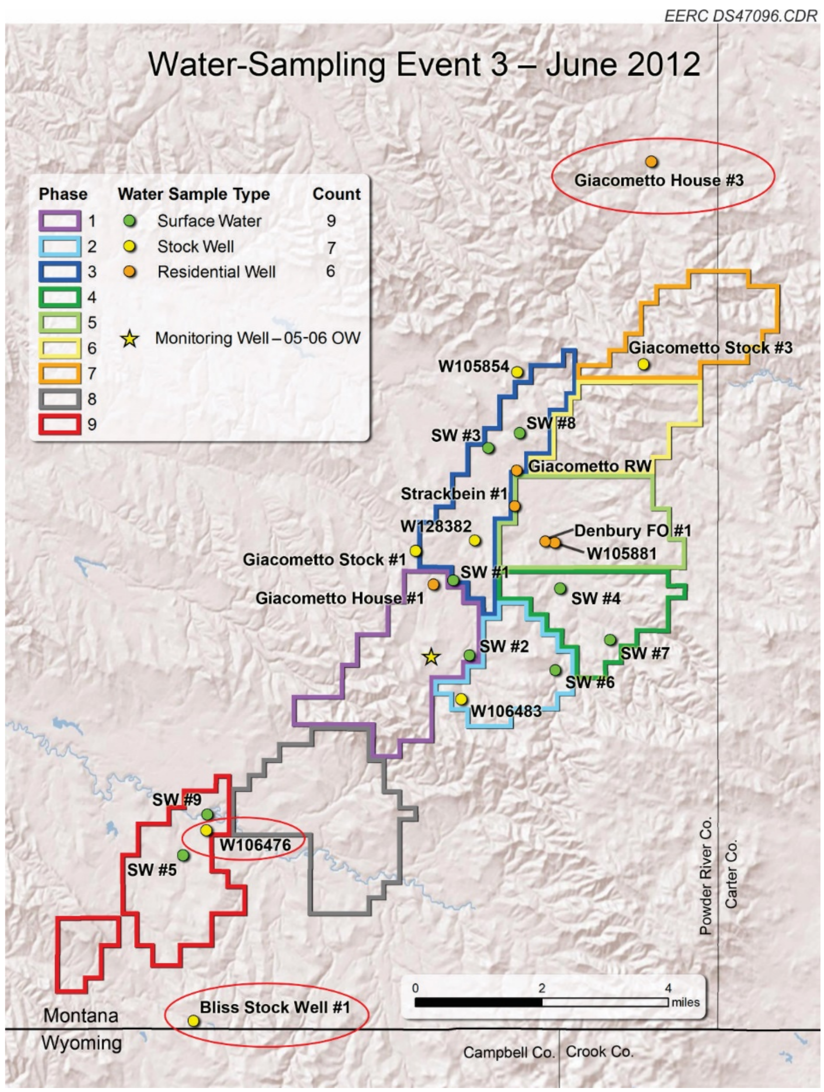

Figure 17. Bell Creek oil field showing the location of various wells, including those that were used in this study, highlighted.

reactivity of CO_2 and was exposed with one groundwater sample. The two other samples were a groundwater blank and nanopure deionized water blank, each reacted without any solids (i.e., cuttings). Table 15 summarizes the combination of solid and liquid samples used in the CO_2 exposure tests.

Approximately 4 g of material for each drill-cutting sample was placed in a 15-mL glass vial along with 12 mL of the corresponding groundwater. The samples were then placed on racks inside a high-pressure stainless steel vessel connected to a commercial-grade CO_2 gas supply cylinder (Figure 18). The reactor vessel and its contents were purged with CO_2 initially and continuously connected to maintain CO_2 pressure for the duration of the experiment. Since there is little difference in the solubility of CO_2 at the estimated pressures and temperatures associated with the sample and groundwater depths herein, the tests were run at 200 psi and 25°C. A 30-day exposure time was conservatively selected for the batch reaction tests based on evaluation of control samples (magnesium silicate, calcite, dolomite, and other minerals) which indicated that a complete carbonation reaction was achieved after approximately 2 weeks. Following the exposure to CO_2 at temperature and pressure, the groundwater and solids were separated before analysis.

Geochemical analyses of the groundwater were performed on the groundwater samples before and after exposure to CO_2. Groundwater analyses included anions, cations, trace metals, pH, TDS, TIC, and TOC. The three groundwater samples had similar composition, primarily comprising sodium bicarbonate and sodium sulfate. Analyses were performed on the formation rock samples before and after exposure to CO_2 to identify bulk mineralogy via XRD, bulk chemistry via XRF, and detailed phase mapping via SEM.

Table 15. Solid and Liquid Combination Sample Identification

Sample ID	Lithology	Depth, ft.	Mass, g	Groundwater Source
05-06 OW–HC120-150	Clay/sandstone	120–150	4.06	Giacometto House #3
05-06 OW–HC180-210	Sandstone	180–210	4.05	Giacometto House #3
05-06 OW–HC300-330	Sandstone/clay	300–330	3.12	Bliss Stock Well #1
05-06 OW–HC360-390	Sandstone/clay/shale	360–390	3.34	Bliss Stock Well #1
05-06 OW–HC420-450	Sandstone/shale	420–450	3.14	W106476
05-06 OW–HC480-520	Sandstone	480–520	3.09	W106476
Mg_2SiO_4–Std[1]	NA[2]	NA	4.01	W106476
W106476–Blk[3]	NA	NA	NA	W106476
DI[4] Water–Blk	NA	NA	NA	NA

[1] Standard.
[2] Not applicable.
[3] Blank.
[4] Deionized.

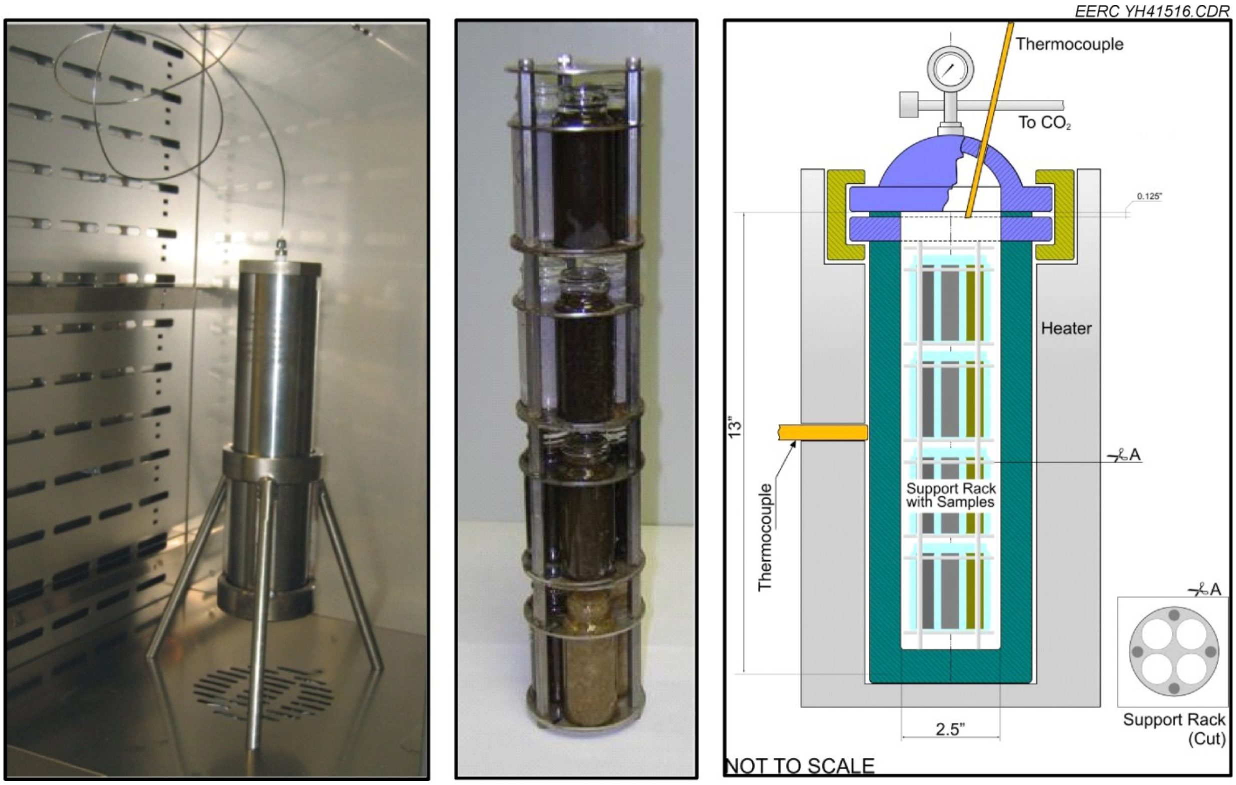

Figure 18. CO_2 batch reactor.

The results of the batch tests were fairly consistent in terms of water chemistry changes pre- and post-CO_2 exposure (Tables 16–18). A decrease in pH was observed in all samples, along with a corresponding increase in bicarbonate alkalinity. Calcium, magnesium, potassium, chloride, and sulfate increased in all groundwater samples following exposure to CO_2. In all but the two most shallow samples from the formation (05-06 OW–HC120-150 and 05-06 OW–HC180-210), there were also significant increases in silicon, manganese, and strontium. As a result of minerals dissolving into the groundwater, the TDS levels also increased with exposure to CO_2. The exposure appeared to have very little measurable effect on the bulk chemistry and mineralogy of the solids, which is not unexpected given the sensitivity of the water analyses when compared to XRD and XRF. However, the water chemistry changes observed by this study are consistent with the various dissolution reactions between CO_2 and calcite, dolomite, plagioclase, illite, and kaolinite described in the literature (Raistrick and others (2009); Wigand and others (2008); Alemu and others (2011); Carroll and others, 2011).

Implications for Groundwater Monitoring

The results of the CO_2 exposure experiments suggest that compositional changes in groundwater chemistry offer an opportunity for monitoring potential, but unlikely, vertical migration of CO_2 into the groundwater zone overlying the Bell Creek Field. A decrease in groundwater pH might be used to detect CO_2 presence, particularly if it is accompanied by a corresponding increase in TDS. Monitoring of groundwater pH and TDS (through measuring

Table 16. Water Analysis Results for HC120-150 and HC180-210 with Giacometto House #3 Groundwater

Sample ID:	Giacometto House #3 Preexposure Groundwater	05-06 OW–HC120-150 Postexposure Liquid	05-06 OW–HC180-210 Postexposure Liquid
pH	9.39	7.62	7.75
Sodium, mg/L	179	193	192
Potassium, mg/L	<1	25	7.8
Calcium, mg/L	1.88	325	237
Magnesium, mg/L	<1	123	55.3
Iron, mg/L	<0.005	0.14	0.48
Sulfate, mg/L	118	167	167
Phosphorous, mg/L	<0.1	<1	<1
Chloride, mg/L	1.8	8.0	4.7
Alkalinity, as Bicarbonate (HCO_3^-), mg/L	299	927	706
Alkalinity, as Carbonate (CO_3^{2-}), mg/L	21.7	0	0
Alkalinity, total as $CaCO_3$, mg/L	282	760	579
Total Inorganic Carbon, mg/L	63.6	585	409
Total Dissolved Solids at 180°C, mg/L	442	1140	770
Silicon, mg/L	4.21	12	17
Aluminum, mg/L	<0.05	<0.5	<0.5
Manganese, mg/L	0.00839	2.51	2.87
Strontium, mg/L	<0.1	5.34	2.67

SC) is an easy and relatively robust way to monitor potential changes in groundwater chemistry that could be indicative of a vertical CO_2 migration.

However, extreme caution must be exercised when interpreting changes in groundwater composition. Baseline data in certain wells showed a significant seasonal variation in pH. While the reason for these changes is unknown, they can be misinterpreted as a potential vertical CO_2 migration. The pH observed during the CO_2–rock exposure tests was compared to the range of values observed during baseline data collection for the groundwater-sampling locations. In certain cases, where pH appears to be seasonably stable or even slightly variable, the difference in groundwater pH after exposure to CO_2 was readily discernible. However, where significant variation in seasonal pH exists, the relative difference in groundwater pH after exposure is less apparent.

TDS in groundwater, as measured by SC, might be a better indicator of a potential vertical CO_2 migration. When compared to the field data, the differences in SC are much more distinct than pH and, in general, the baseline seasonal variation in groundwater SC was relatively small compared to pH.

Table 17. Water Analysis Results for HC300-300 and HC360-390 with Bliss Stock Well #1 Groundwater

Sample ID:	Bliss Stock Well #1 Preexposure Groundwater	05-06 OW– HC300-330 Postexposure Liquid	05-06 OW– HC360-390 Postexposure Liquid
pH	9.04	7.47	7.58
Sodium, mg/L	207	207	210
Potassium, mg/L	1.54	8.7	17
Calcium, mg/L	13.1	604	408
Magnesium, mg/L	2.73	59.6	113
Iron, mg/L	0.058	3.32	0.009
Sulfate, mg/L	279	368	347
Phosphorous, mg/L	<0.1	<1	<1
Chloride, mg/L	3.26	6.0	6.4
Alkalinity, as Bicarbonate (HCO_3^-), mg/L	217	1820	881
Alkalinity, as Carbonate (CO_3^{2-}), mg/L	8.2	0	0
Alkalinity, total as $CaCO_3$, mg/L	192	1490	722
Total Inorganic Carbon, mg/L	44.7	648	585
Total Dissolved Solids at 180°C, mg/L	592	1980	1340
Silicon, mg/L	5.17	12	12
Aluminum, mg/L	<0.05	<0.5	<0.5
Manganese, mg/L	0.0459	2.91	1.40
Strontium, mg/L	0.32	4.21	5.71

The magnitude of change, either a decrease in pH or an increase in SC, however, will vary depending on the amount of CO_2 present and the duration of contact. The EERC is developing a test plan to determine the utility of using changes in groundwater pH and SC as a tool to detect and quantify a vertical migration of CO_2.

CURRENT AND FUTURE WORK

Current and future work related to the geochemical characterization of the Bell Creek Field includes additional mineralogical and petrophysical characterization of the reservoir and cap rock, continued surface, subsurface, and deep groundwater baseline characterization and monitoring, and geochemical modeling and predictive simulation. The goal of these activities is to more effectively monitor, verify, and account for the location and mobility of injected CO_2 at Bell Creek.

Additional Mineralogical Characterization of Bell Creek Area Formations

Reservoir characterization efforts will continue as core samples from two newly redrilled wells within the Bell Creek oil field will be analyzed by the EERC. Additional petrographic thin-section interpretations will assist in determining additional, more detailed mineralogical and

Table 18. Water Analysis Results for HC420-450 and HC480-520 with W106476 Groundwater

Sample ID:	W106476 Preexposure Groundwater	05-06 OW– HC420-450 Postexposure Liquid	05-06 OW– HC480-520 Postexposure Liquid
pH	9.29	8.06	7.44
Sodium, mg/L	308	313	323
Potassium, mg/L	1.03	5.0	5.0
Calcium, mg/L	4.04	184	379
Magnesium, mg/L	<1	31.5	31.5
Iron, mg/L	0.083	6.62	6.62
Sulfate, mg/L	353	349	346
Phosphorous, mg/L	<0.1	<1	<1
Chloride, mg/L	2.25	4.6	8.2
Alkalinity, as Bicarbonate (HCO_3^-), mg/L	343	1010	1930
Alkalinity, as Carbonate (CO_3^{2-}), mg/L	21.6	0	0
Alkalinity, total as $CaCO_3$, mg/L	317	828	1580
Total Inorganic Carbon, mg/L	74.2	514	570
Total Dissolved Solids at 180°C, mg/L	822	1380	1880
Silicon, mg/L	4.25	15	15
Aluminum, mg/L	<0.05	<0.5	<0.5
Manganese, mg/L	0.0209	4.38	4.38
Strontium, mg/L	0.10	1.62	2.92

petrophysical evaluations to be performed. Ultimately, the characterization work will be used to assess the implications of fluid flow and geochemical stability within the reservoir during the CO_2 flood, both qualitatively and through geologic and geochemical modeling.

Reservoir CO_2 Exposure Experiments

Additional geochemical modeling and laboratory CO_2 exposure tests are planned to evaluate the efficacy of monitoring changes in groundwater chemistry as an indicator of a potential vertical CO_2 migration. The aqueous geochemical modeling simulations will be evaluated using the PHREEQC model, which will be used to predict a range of anticipated geochemistry changes based on chemical equilibrium established in response to varying levels of CO_2 exposure. Modeling data will be used to predict the potential geochemical changes that may occur based on the different amounts and rates of CO_2 in the freshwater zones. These models will then be used to help design the monitoring parameters needed to detect changes in the groundwater chemistry that may be indicative of a vertical migration event and serve as a trigger for further, more detailed investigation of the anomaly. Data input to the model includes formation temperature and pressure, percentages of minerals present in the formation, effective porosity, major cations and anions in the groundwater, pH, and water density. Samples of Fox Hills groundwater, collected and chemically characterized as part of the MVA program, will provide the necessary chemistry input data. XRD and XRF analyses will need to be conducted on drill cuttings to provide the necessary mineralogical model input data. Formation pressure and water density will be calculated, and effective porosity will be estimated based on available data in the literature.

The laboratory testing will provide insight into key chemical constituents in Fox Hills groundwater that have the best potential for use as indicator parameters. Based on previous CO_2 exposure studies using Hell Creek Formation groundwater, pH and/or specific conductance measurements should provide data sufficient to detect a potential vertical CO_2 migration. Since the groundwater in the Fox Hills appears to be of a higher quality (based on preliminary field data) than that of the Hell Creek, different levels of change in response to CO_2 exposure are anticipated.

Key goals of the laboratory testing are to determine the magnitude of change in groundwater chemistry in response to CO_2 exposure and the rate at which those changes occur under different levels (concentrations) of CO_2. Data from the exposure experiments will provide necessary information, such as expected changes in pH, water chemistry, and rock mineralogy that can be used to characterize a CO_2 leak into the Fox Hills Formation.

Geochemical Modeling

The goal of this activity is to model the interaction between the injected CO_2, the reservoir fluids, and the rocks to determine 1) the potential amount of CO_2 that may be incidentally stored through mineral precipitation and 2) the effects of mineral precipitation on permeability and injectivity. As stated throughout this interim report, the laboratory and field monitoring data will be used to refine geologic, geochemical, and CO_2 fate and transport models to gain a better understanding of reservoir behavior upon CO_2 injection, to better predict the long-term incidental CO_2 storage of the reservoir from hydrodynamic and mineralogic trapping mechanisms and to assess the long-term integrity of the overlying cap rocks.

Reaction-type modeling will use the results from the batch CO_2 exposure experiments to determine potential reactions based on the composition of the rock and water using the parameters of the experiments. Near-wellbore modeling will further incorporate laboratory evaluations with field observations to model and simulate potential geochemical changes around individual injection wells. The data will also feed into shallow subsurface geochemical modeling and assessment efforts to better understand the possible effect that CO_2 may have if it were to reach the surface or a groundwater zone in the unlikely event of an out-of-zone migration beyond the reservoir cap rocks.

Monitoring Activities Related to Geochemistry

Detailed sampling and analysis of surface water and groundwater at the same locations established during baseline monitoring, plus the Fox Hills monitoring wells, will be conducted by the EERC at least once annually in the fall. The EERC will also continue to monitor soil gas at the ten soil gas-profiling stations on a monthly basis. In addition, detailed sampling and analysis of soil gas samples collected at all 186 locations established during the baseline MVA activities will be conducted at least annually. This sampling event will be conducted in the fall to coincide with the lowest observed levels of soil gas CO_2 and the timing of the detailed groundwater-sampling events. The EERC will also collect samples of CO_2 from the Lost Cabin Gas Plant to determine isotopic signature and to verify chemical composition prior to injection. It is recommended that all the above monitoring activities continue throughout the lifetime of the active EOR Bell Creek incidental CO_2 storage-monitoring project.

CONCLUSIONS

The Bell Creek demonstration project provides a unique opportunity to conduct a detailed mineralogical and geochemical evaluation of a complex, large-scale CO_2 EOR operation and to monitor incidental CO_2 storage associated with EOR activities in an active oil field. The ultimate goal of the geochemistry evaluation is the integration of current and future mineralogical characterization efforts, laboratory-based CO_2 exposure experiments, fieldwide monitoring activities, and multi-scale geochemical modeling efforts to provide a comprehensive understanding of potential geochemical reactions that could take place in all areas of the field. Understanding the potential geochemical reactions between CO_2 and the rocks and fluids of the reservoir, overlying seals, shallow subsurface, and surface at the Bell Creek site is important to:

- Anticipate potential mineral dissolution and/or precipitation reactions that may affect CO_2 injectivity.

- Estimate the long-term incidental storage of CO_2 through hydrodynamic and mineralogical trapping mechanisms to aid in verification and accounting efforts.

- Verify the integrity of the overlying cap rock.

- Predict chemical changes in the groundwater and/or surface waters that can be used as indicator species for monitoring efforts in the unlikely event of out-of-zone migration.

Ultimately, this assessment will help accomplish the primary objectives of the Bell Creek demonstration project, which are to demonstrate that 1) incidental CO_2 storage can be safely and permanently achieved on a commercial scale in conjunction with a commercial EOR operation; 2) oil-bearing sandstone formations are viable sinks for CO_2; 3) MVA methods can be established to effectively monitor incidental CO_2 storage during a commercial EOR project; and 4) the lessons learned and best practices employed will provide the data, information, and knowledge needed to develop similar MVA plans for CO_2 storage projects across the region. A thorough understanding of the geochemistry of the Bell Creek oil field and its surrounding area is critical to achieve these objectives.

REFERENCES

Alemu, B.L., Aagaard, P., Munz, I.A., and Skurtveit, E., 2011, Caprock interaction with CO_2—a laboratory study of reactivity of shale with supercritical CO_2 and brine: Applied Geochemistry, v. 26, p. 1975–1989.

Bachu, S., Gunter, W.D., and Perkins, E.H., 1994, Aquifer disposal of CO_2—hydrodynamic and mineral trapping: Energy Conversion and Management, v. 35, no. 4, p. 269–279. www.sciencedirect.com/science/article/pii/0196890494900604.

Berg, R.R., and Davies, D.A., 1968, Origin of Lower Cretaceous Muddy Sandstone at Bell Creek Field, Montana: American Association of Petroleum Geologists Bulletin, v. 52, no. 10, p. 1888–1898.

Burt, R.A., Haddenhorst, F.A., and Hartford, J.C., 1975, Performance and operations review of the major multi-reservoir, Bell Creek Field, Montana: SPE 5330, SPE Rocky Mountain Regional Meeting.

Carroll, S.A., NcNab, W.W., and Torres, S.C., 2011, Experimental study of cement–sandstone/shale–brine–CO_2 interactions: Geochemical Transactions, v. 12. Located at www.geochemicaltransactions.com/content/12/1/9 (accessed May 2013).

Cvancara, A.M., 1976, Geology of the Fox Hills Formation (Late Cretaceous) in the Williston Basin of North Dakota, with reference to Uranium Potential, North Dakota Geological Survey, Report of Investigation No. 55, 24 p.

Eylands, K.E., Kurz, B.A., Hamling, J.A., Heebink, L.V., Smith, S.A., LaBonte, J.L., Mibeck, B.A.F., Kleven, P.L., Klapperich, R.J., Braunberger, J.R., and Gorecki, C.D., 2013, Bell Creek 0506OW sidewall core mineralogy assessment, April 2013.

Fischer, S., Zemke, K., Liebscher, A., Wandrey, M., and CO_2SINK Group., 2011, Petrophysical and petrochemical effects of long-term CO_2-exposure experiments on brine-saturated reservoir sandstone: Energy Procedia, v. 4, p. 4487–4494.

Gunter, W.D., Bachu, S., and Benson, S.M., 2004, The role of hydrogeological and geochemical trapping in sedimentary basins for secure geological storage for carbon dioxide, *In* Baines, S.J., and Worden, R.H. eds., Geological storage of carbon dioxide: London, United Kingdom, Geological Society, Special Publication 233, p. 129–145.

Kaszuba, J.P., and Janecky, D.R., 2009, Geochemical impacts of sequestering carbon dioxide in brine formations, *In* McPherson, B.J., and Sundquist, E.T. eds., Carbon sequestration and its role in the global carbon cycle: Geophysical Monograph Series, v. 183, p. 239–248. www.agu.org/books/gm/v183/.

Klapperich, R.J., Shah, J., LaBonte, J.L., Lindeman, C.D., Mibeck, B.A.F., Eylands, K.E., Huffman, B.W., Bremer, J.M., Bailey, T.P., Heebink, L.V., and Smith, S.A., Kleven, 2013, Petrophysical assessment of USGS core samples for the Bell Creek project.

Li, L., Peters, C.A., and Celia, M.A., 2005, Upscaling geochemical reaction rates using pore-scale network modeling: Advances in Water Resources, v. 29, no. 9, p. 1351–1370.

McGregor, A.A., and Biggs C.A., 1968, Bell Creek Field, Montana—A rich stratigraphic trap: The American Association of Petroleum Geologists Bulletin, October, vol. 52, no. 10, p. 1869–1887.

Mello, J.F., 1969, Foraminifera and stratigraphy of the upper part of the Pierre Shale and lower part of the Fox Hills Sandstone (Cretaceous), north-central South Dakota: U.S. Geological Survey Prof. Paper 611, 121 p.

Molnar, P.S., and Porter, M.L., 1990, Geologic reservoir study of the Bell Creek Field, Carter and Powder River Counties, Montana: Exxon USA proprietary report, Midland, Texas, 127 p.

Pauwels, H., Gausa, I., Nindre, Y.M., Pearce, J., and Czernichowski-Lauriol, I., 2007, Chemistry of fluids from a natural analogue for a geological CO_2 storage site (Montmiral, France)—lessons for CO_2–water–rock interaction assessment and monitoring: Applied Geochemistry, v. 22, no. 12, p. 2817–2833.

Raistrick, M., Hutcheon, I., Shevalier, M., Nightingale, M., Johnson, G., Taylor, S., Mayer, B., Durocher, K., Perkins, E., and Gunter, B., 2009, Carbon dioxide–water–silicate mineral reactions enhance CO_2 storage—evidence from produced fluid measurements and geochemical modeling at the IEA Weyburn-Midale Project: Energy Procedia, v. 1, no. 1, p. 3149–3155.

Saini, D., Braunberger, J.R., Pu, H., Bailey, T.P., Ge, J., Crotty, C.M., Liu, G., Hamling, J.A., Gorecki, G., Steadman, E.N., and Harju, J.A., 2012, Bell Creek test site – simulation report: Plains CO_2 Reduction (PCOR) Partnership Phase III, Task 9 – Deliverable D66, August 2012.

Sayegh, S.G., Krause, F.F., Girard, M., and DeBree, C., 1990, Rock/fluid interactions of carbonated brines in a sandstone reservoir—Pembina Cardium, Alberta, Canada: SPE Formation Evaluation, v. 5, no. 4, p. 399–405.

Sorensen, J.A., Smith, S.A., Gorecki, C.D., Steadman, E.N., Harju, J.A., 2011, Bell Creek test site – geological characterization experimental design package: Plains CO_2 Reduction (PCOR) Partnership Phase III, Task 4 – Deliverable D31, Task 4 – Milestone 28, January 2011.

Sposito, G., 1989, The chemistry of soils: New York, NY: Oxford University Press.

Stepan, D.J., Kalenze, N.S., Leroux, K.M., Klapperich, R.J., Botnen, B.W., Hamling, J.A., Gorecki, G.D., Steadman, E.N., and Harju, J.A., 2013, Bell Creek Test Site – Baseline MVA Activities, March.

U.S. Department of Agriculture Natural Resources Conservation Service, 2013, Web soil survey: http://websoilsurvey.nrcs.usda.gov (accessed June 2013).

U.S. Department of Agriculture Soil Conservation Service and Forest Service, 1971, Soil survey Powder River area Montana: June.

Wandrey, M., Fischer, S., Zemke, K., Liebscher, A., Scherf, A.K., Vieth-Hillebrand, A., Zettlitzer, M., and Würdemann, H., 2011, Monitoring petrophysical, mineralogical, geochemical and microbiological effects of CO_2 exposure—results of long-term experiments under in situ conditions: Energy Procedia, v. 4, p. 3644–3650.

Wellman, P.T., Grigg, R.P., McPherson, B.J., Svec, R.K., and Lichtner, P.C., 2003, Evaluation of CO_2–brine–reservoir rock interaction with laboratory flow tests and reactive transport modeling: SPE International Symposium on Oilfield Chemistry, Houston, Texas, February 5–7, 2003, Paper SPE 80228.

Wigand, M., Carey, J.W., Schütt, H., Spangenberg, E., and Erzinger, J., 2008, Geochemical effects of CO_2 sequestration in sandstones under simulated in situ conditions of deep saline aquifers: Applied Geochemistry, v. 23, p. 2735–2745.

APPENDIX A

DATA SHEETS

	Applied Geology Laboratory		
	Niobrara Formation	Well Name: 05-06 OW	ID: S-00982
	American Petroleum Institute (API) No.: 25075224310000	Lithology: Shale	Depth: 2937.00'

SAMPLE PHOTOGRAPH

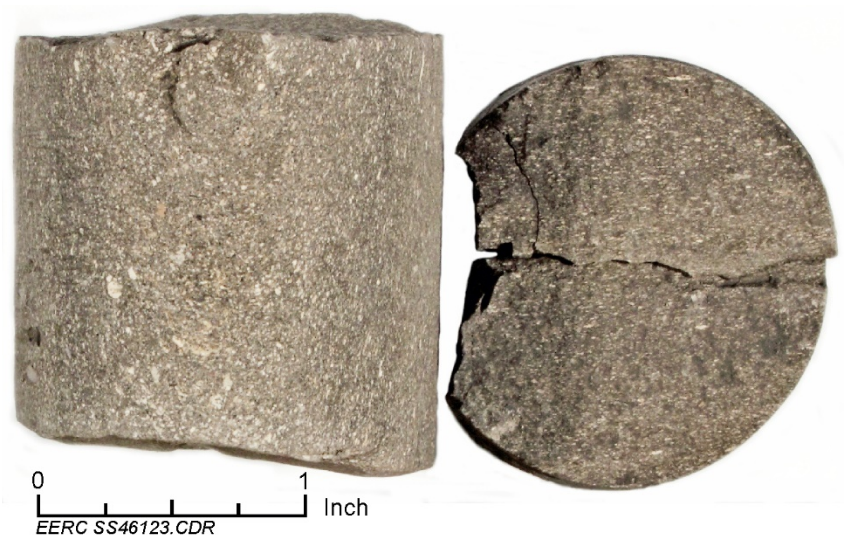

PHYSICAL PROPERTIES

Porosity

Pycnometer Effective Porosity Average (range), vol%	Pycnometer Effective Porosity by MetaRock Laboratories, vol%	Thin-Section Point Count Porosity, % occurrence	Thin-Section Image Segmentation Pore Space, area%
36.4 (35.0–37.7)	27.8	NT*	0.26

* NT indicates that the sample was not tested.

Density

Bulk Volume, cm^3	Skeletal Density, g/cm^3
32.3	2.64

Residual Fluid Saturations

Residual Oil Saturation, %	Residual Water Saturation, %
0	38.3

Permeability

Permeability to Water, mD	Permeability to Air, mD
0.09	Pending

PHOTOMICROGRAPHS

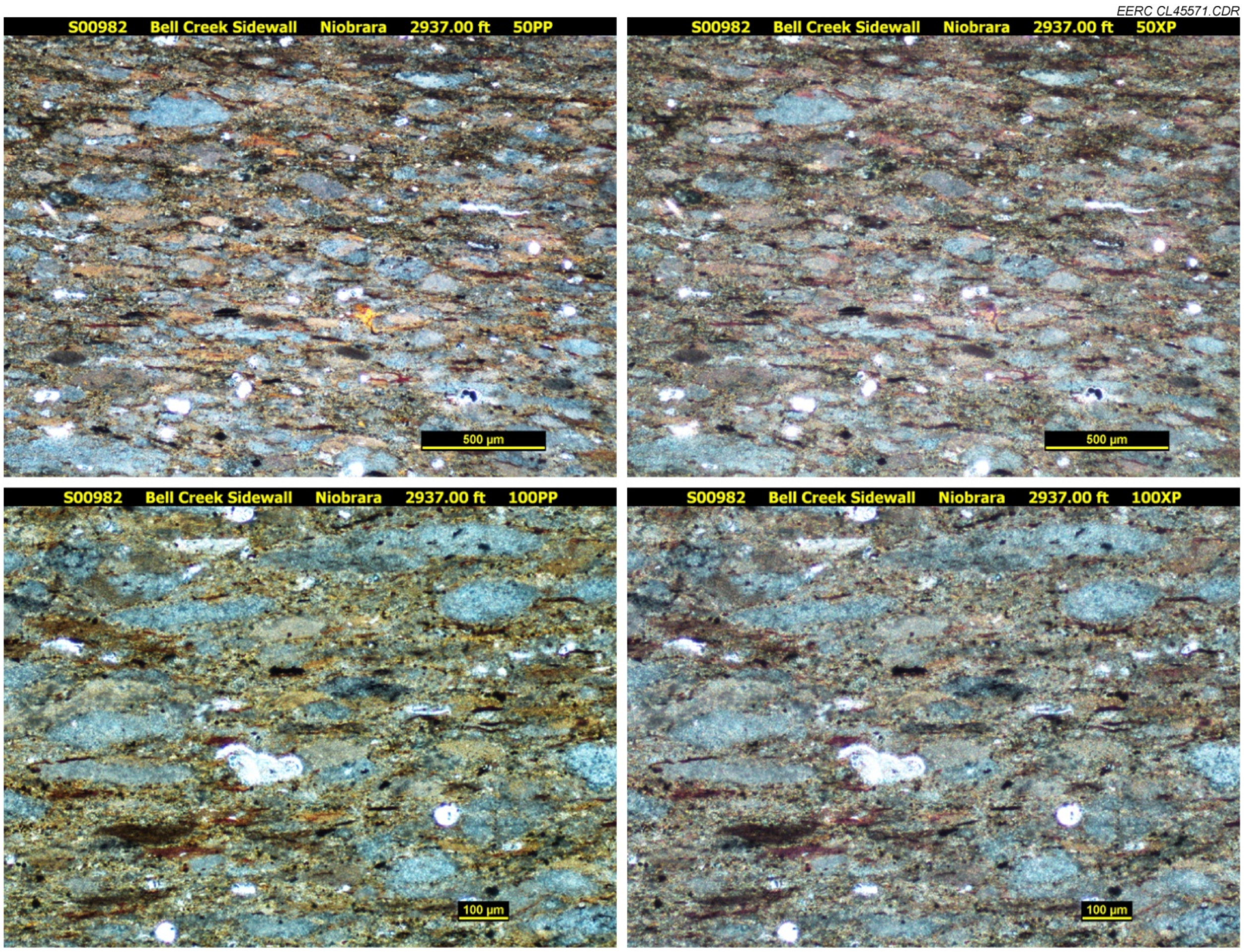

The sample collected from 2937.00 ft is organic-rich carbonaceous shale. Multiple horizontal and occasional vertical fractures of varying aperture reside in the sample. Most fractures are partially filled with clays and/or organics. Organics are also dispersed as lenses and in a globular fashion. Porosity resides in partially filled fractures and within compacted carbonate concretions. Many carbonate shell fragments are seen throughout the sample.

THIN-SECTION PORE ANALYSIS BY DIGITAL IMAGE SEGMENTATION

Depth: 2937.00 ft; W = 28.66 mm; H = 16.91 mm

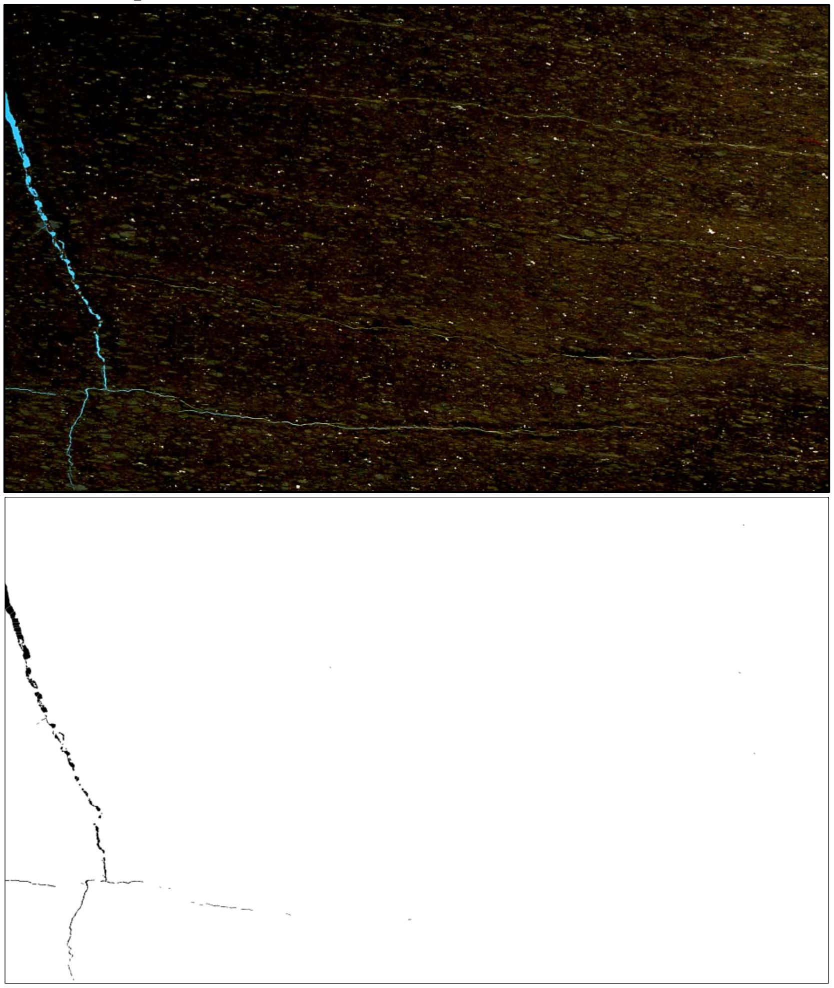

Pore Space, area%	Mean Pore Area, µm^2	Pore Area Range, µm^2	Mean Pore Perimeter, µm	Pore Perimeter Range, µm
0.3*	5579	420–74,877	307	77–1421

* The pore space consists primarily of fractures.

This page intentionally left blank.

SAMPLE PHOTOGRAPH

PHYSICAL PROPERTIES

Porosity

Pycnometer Effective Porosity Average (range), vol%	Pycnometer Effective Porosity by MetaRock Laboratories, vol%	Thin-Section Point Count Porosity, % occurrence	Thin-Section Image Segmentation Pore Space, area%
25.3 (24.0–26.8)	NT	NT	0.14

Density

Bulk Volume, cm^3	Skeletal Density, g/cm^3
34.9	2.58

Residual Fluid Saturations

Residual Oil Saturation, %	Residual Water Saturation, %
0	53.1

Permeability

Permeability to Water, mD	Permeability to Air, mD
0.11	Pending

PHOTOMICROGRAPHS

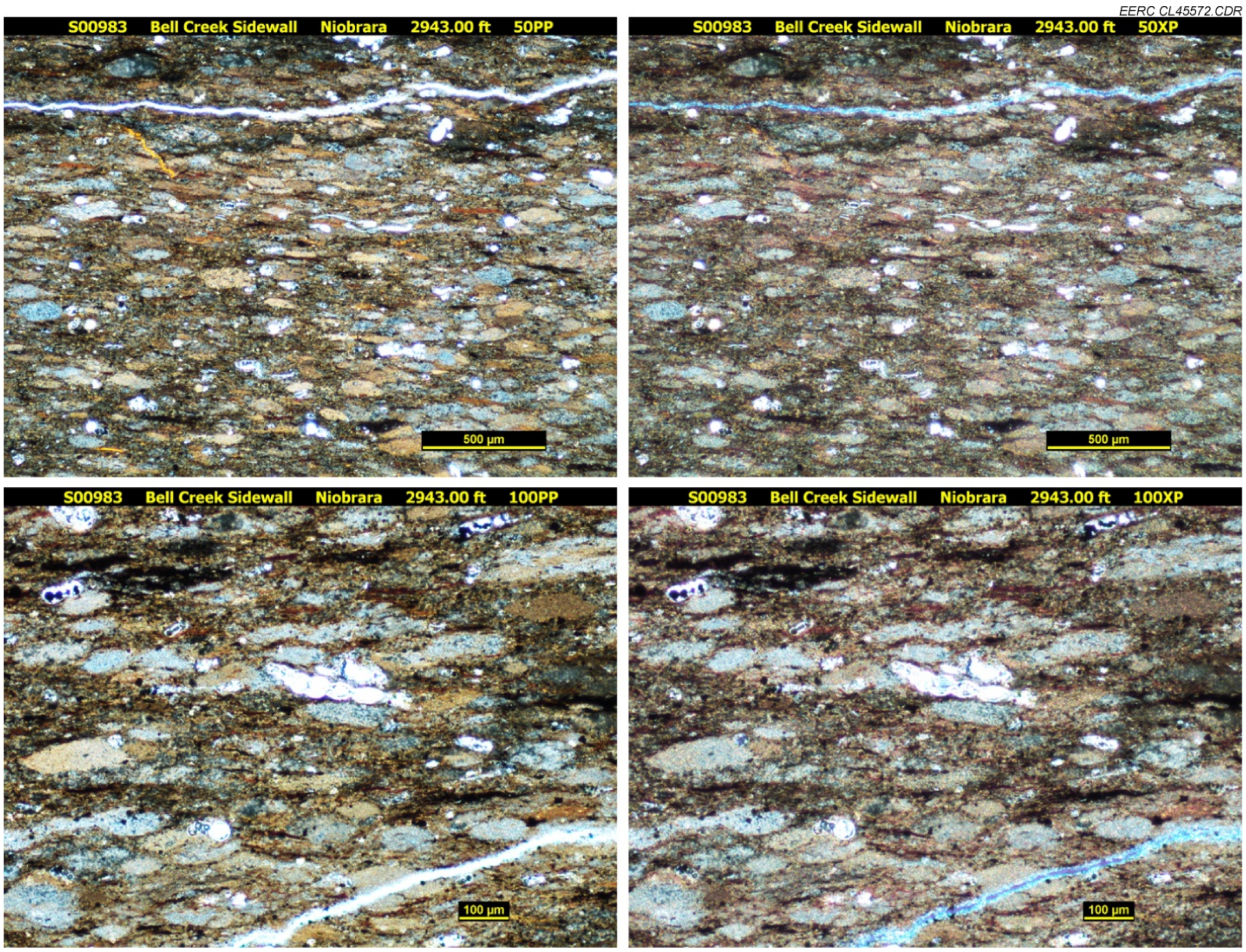

The sample collected from 2943.00 ft is very similar to the sample from 2937.00 ft. It is organic-rich carbonaceous shale having multiple horizontal and occasional vertical fractures of varying aperture within the sample. Most fractures are partially filled with clays and or organics. Organics are also dispersed as lenses and in a globular fashion. Porosity resides in partially filled fractures and within compacted carbonate concretions. Many carbonate shell fragments are seen throughout the sample.

THIN-SECTION PORE ANALYSIS BY DIGITAL IMAGE SEGMENTATION

Depth: 2943.00 ft; W = 19.49 mm; H = 10.60 mm

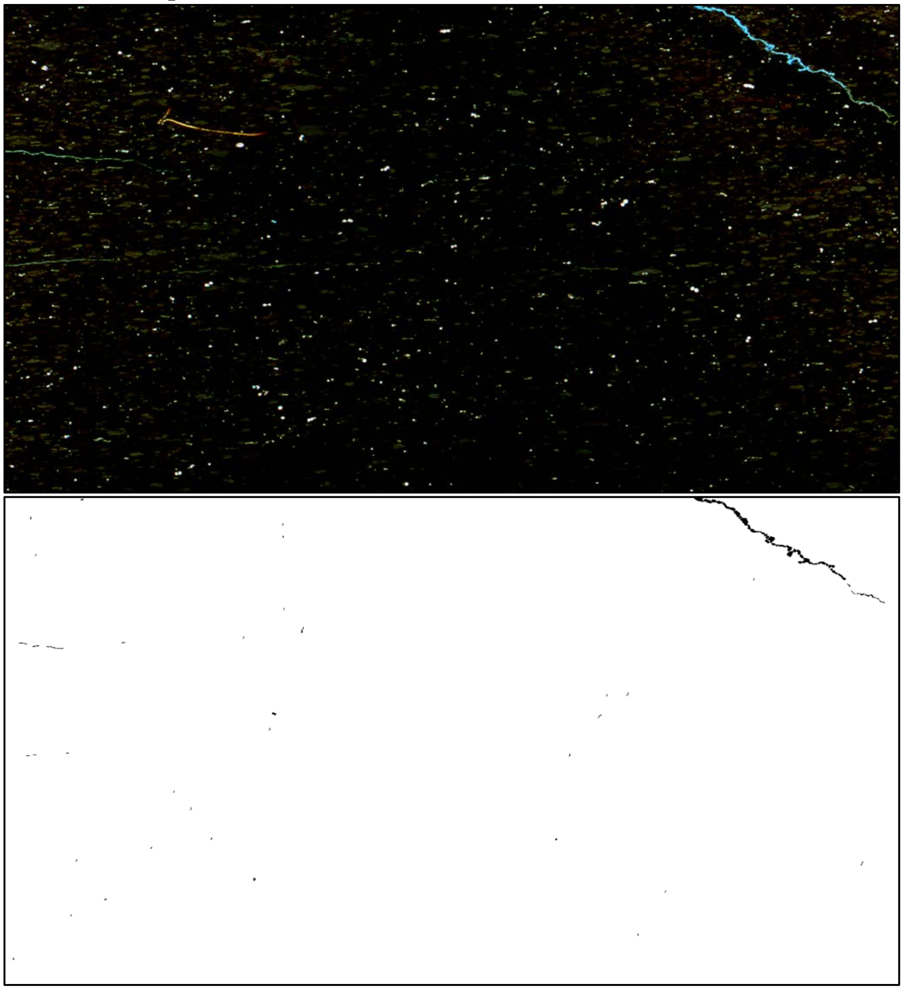

Pore Space, area%	Mean Pore Area, μm^2	Pore Area Range, μm^2	Mean Pore Perimeter, μm	Pore Perimeter Range, μm
0.1*	2654	476–14,729	216	96–642

* The pore space consists primarily of fractures.

This page intentionally left blank.

SAMPLE PHOTOGRAPH

PHYSICAL PROPERTIES

Porosity

Pycnometer Effective Porosity Average (range), vol%	Pycnometer Effective Porosity by MetaRock Laboratories, vol%	Thin-Section Point Count Porosity, % occurrence	Thin-Section Image Segmentation Pore Space, area%
N/A*	N/A	NT	6.5

* N/A indicates that the sample is too friable and/or lacked the structural integrity for a specific test.

Density

Bulk Volume, cm^3	Skeletal Density, g/cm^3
N/A	N/A

Residual Fluid Saturations

Residual Oil Saturation, %	Residual Water Saturation, %
N/A	N/A

Permeability

Permeability to Water, mD	Permeability to Air, mD
N/A	N/A

PHOTOMICROGRAPHS

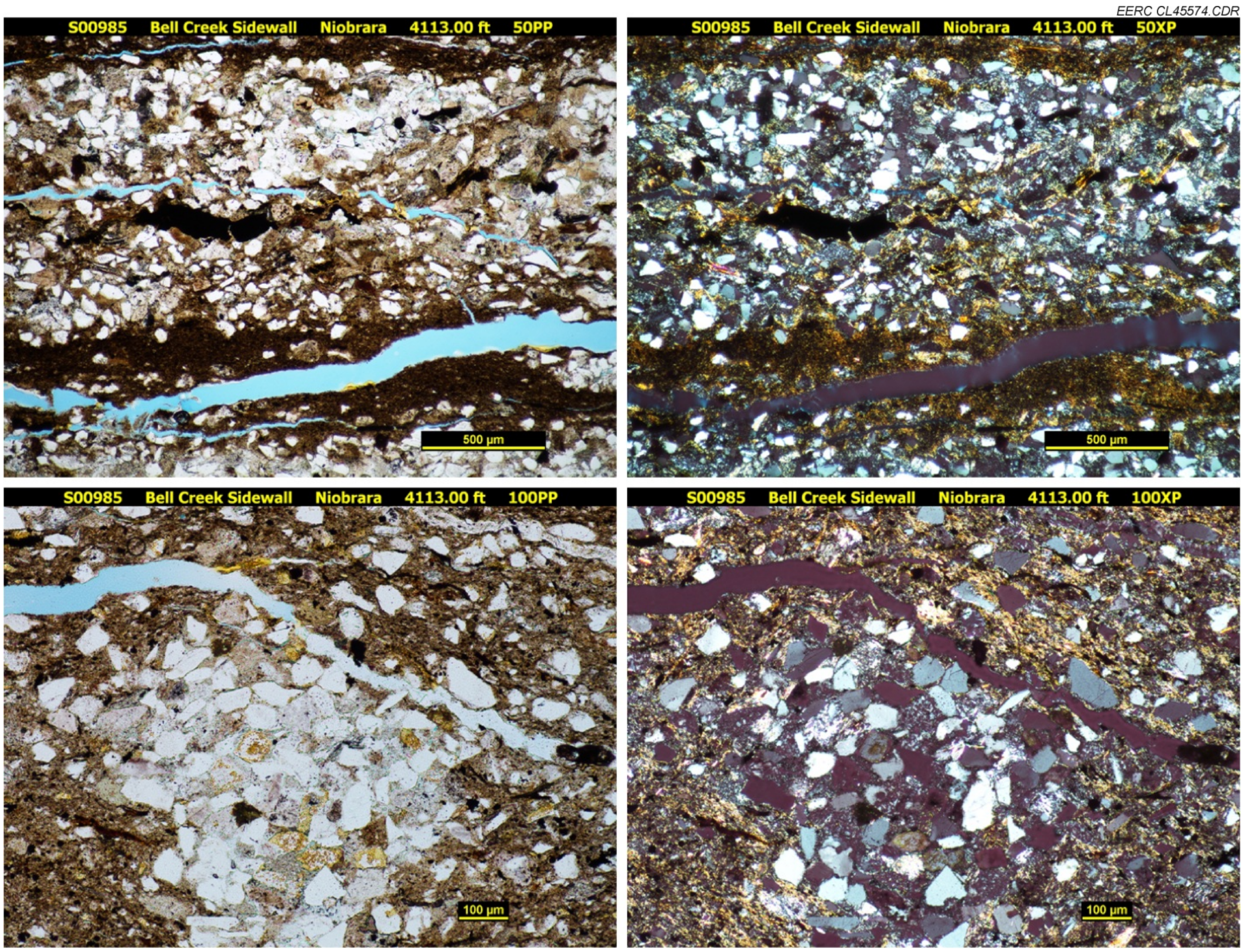

The sample collected from 4113.00 ft is very fine grained silty mudstone. Monocrystalline quartz is angular to subangular, encompassed within a matrix of clays, organics, and silica. Porosity is the result of horizontal and vertical fractures, as well as cement dissolution. Some of the observed fractures are likely the result of the sampling process. Trace levels of metal, siderite, feldspars, and muscovite are observed. A small amount of compaction is detected, and no evidence of fossils is observed.

THIN-SECTION PORE ANALYSIS BY DIGITAL IMAGE SEGMENTATION

Depth: 4113.00 ft; W = 23.26 mm; H = 18.92 mm

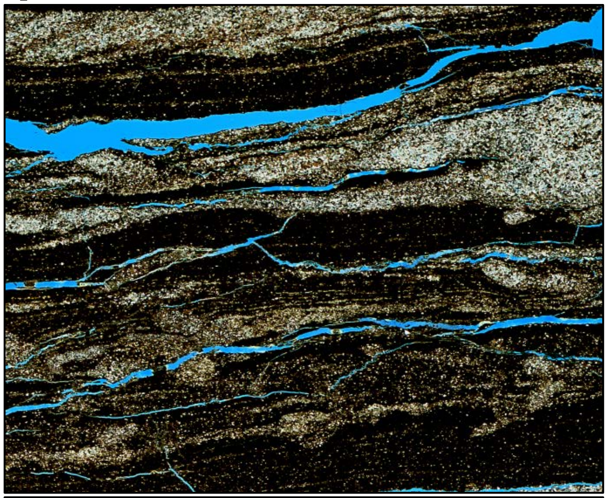

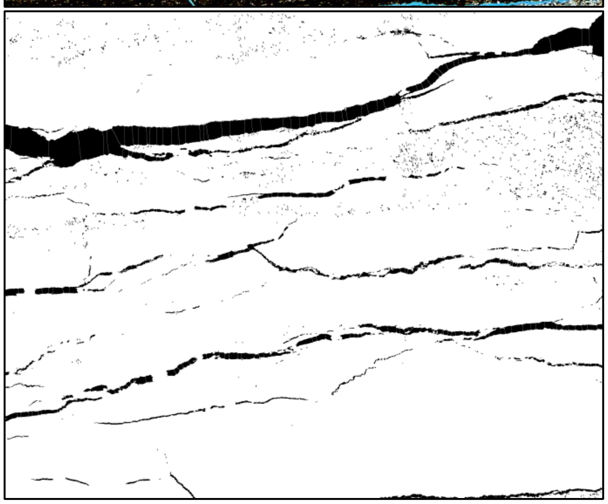

Pore Space, area%	Mean Pore Area, μm^2	Pore Area Range, μm^2	Mean Pore Perimeter, µm	Pore Perimeter Range, µm
6.5*	9173	168–1,140,540	300	48–5460

* The pore space consists of a) pores: 0.5 area% and b) fractures: 6.0 area%. Some of the observed fractures are likely the result of the sampling process.

This page intentionally left blank.

SAMPLE PHOTOGRAPH

PHYSICAL PROPERTIES

Porosity

Pycnometer Effective Porosity Average (range), vol%	Pycnometer Effective Porosity by MetaRock Laboratories, vol%	Thin-Section Point Count Porosity, % occurrence	Thin-Section Image Segmentation Pore Space, area%
N/A	N/A	NT	3.5

Density

Bulk Volume, cm^3	Skeletal Density, g/cm^3
N/A	N/A

Residual Fluid Saturations

Residual Oil Saturation, %	Residual Water Saturation, %
N/A	N/A

Permeability

Permeability to Water, mD	Permeability to Air, mD
N/A	N/A

PHOTOMICROGRAPHS

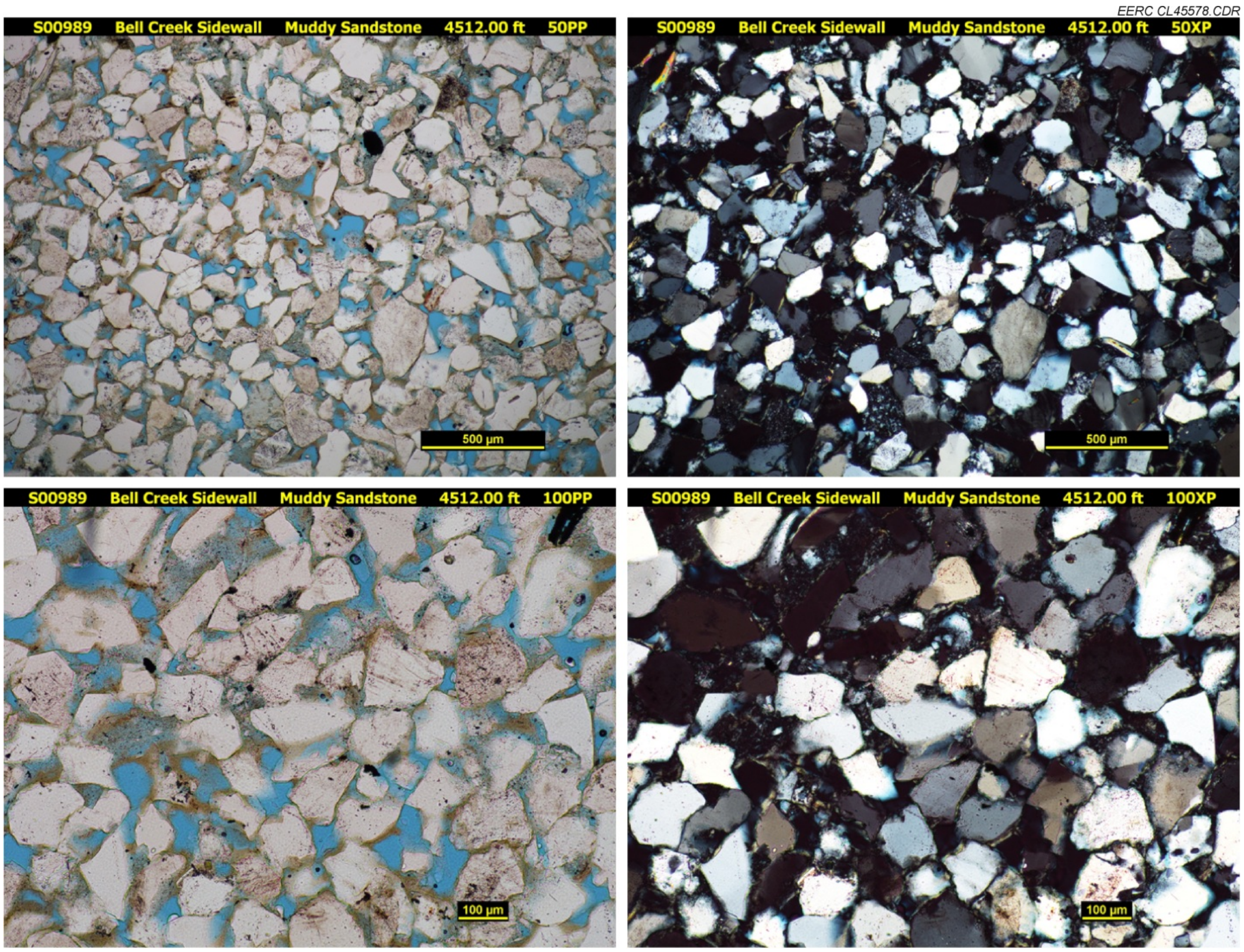

The sample collected at a depth of 4512.00 ft displays fine-grained, moderately well sorted sandstone. The quartz is angular to subrounded and is grain-supported, displaying both monocrystalline and polycrystalline grains. Trace levels of overgrowths are observed. The cementing agents are clays. Porosity exists as intergranular and as the result of cement and grain dissolution. Secondary components are metals, muscovite, rutile, feldspars, and organics. No fractures or fossilization are detected.

THIN-SECTION PORE ANALYSIS BY DIGITAL IMAGE SEGMENTATION

Depth: 4512.00 ft; W = 27.75 mm; H = 20.21 mm

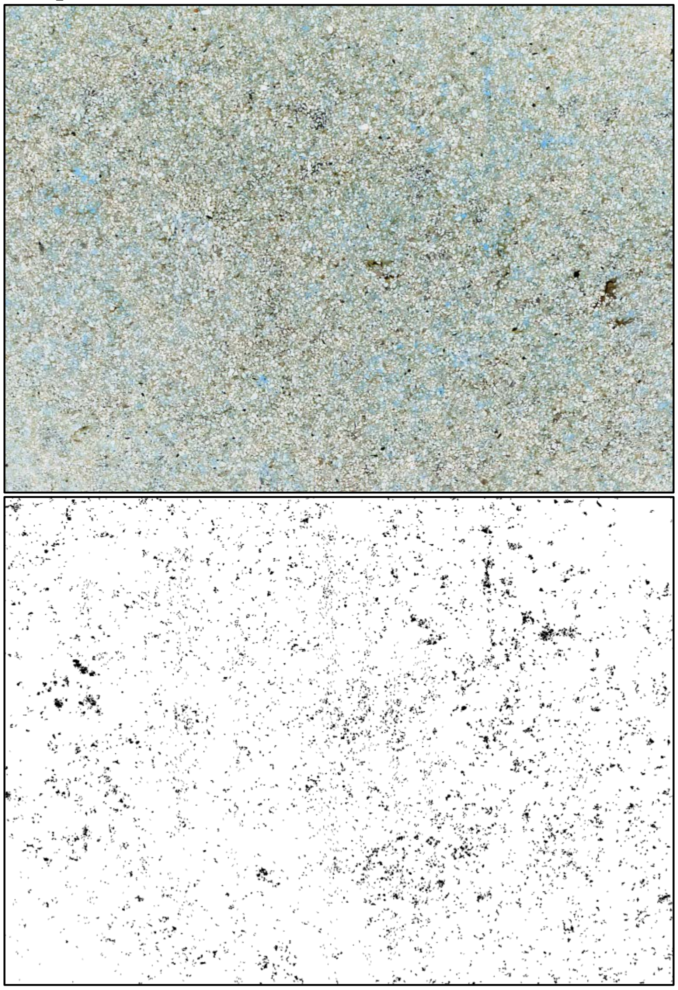

Pore Space, area%	Mean Pore Area, µm^2	Pore Area Range, µm^2	Mean Pore Perimeter, µm	Pore Perimeter Range, µm
3.5	2135	140–37,046	190	45–1081

This page intentionally left blank.

SAMPLE PHOTOGRAPH

PHYSICAL PROPERTIES

Porosity

Pycnometer Effective Porosity Average (range), vol%	Pycnometer Effective Porosity by MetaRock Laboratories, vol%	Thin-Section Point Count Porosity, % occurrence	Thin-Section Image Segmentation Pore Space, area%
N/A	N/A	NT	20.0

Density

Bulk Volume, cm^3	Skeletal Density, g/cm^3
N/A	N/A

Residual Fluid Saturations

Residual Oil Saturation, %	Residual Water Saturation, %
N/A	N/A

Permeability

Permeability to Water, mD	Permeability to Air, mD
N/A	N/A

PHOTOMICROGRAPHS

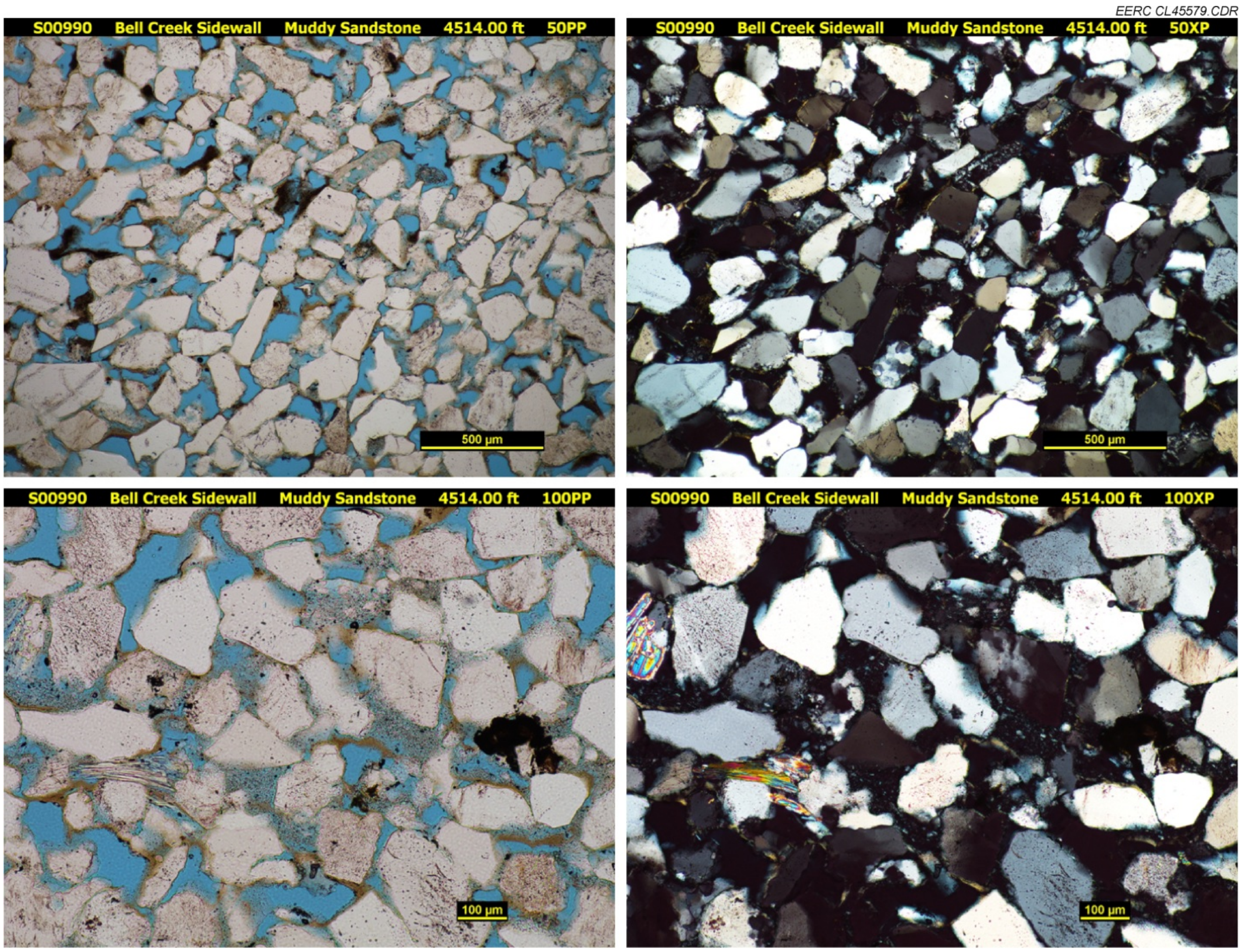

The sample collected at the 4514.00-ft depth is similar to the sample from the 4512.00-ft depth and comprises fine-grained, moderately well sorted sandstone. Quartz grains are angular to subrounded and display monocrystalline and polycrystalline properties. The cementing agents are clays. Porosity exists as intergranular and as the result of cement and grain dissolution, which is more extensive than the previous sample. Secondary components are metals, muscovite, rutile, and organics. No fractures or fossilization are detected.

THIN-SECTION PORE ANALYSIS BY DIGITAL IMAGE SEGMENTATION

Depth: 4514.00 ft; W = 19.44 mm; H = 17.72 mm

Pore Space, area%	Mean Pore Area, µm^2	Pore Area Range, µm^2	Mean Pore Perimeter, µm	Pore Perimeter Range, µm
20.0	3407	56–46,343	253	26–1286

This page intentionally left blank.

SAMPLE PHOTOGRAPH

PHYSICAL PROPERTIES

Porosity

Pycnometer Effective Porosity Average (range), vol%	Pycnometer Effective Porosity by MetaRock Laboratories, vol%	Thin-Section Point Count Porosity, % occurrence	Thin-Section Image Segmentation Pore Space, area%
28.4 (24.9–31.2)	NT	NT	N/A

Density

Bulk Volume, cm^3	Skeletal Density, g/cm^3
30.5	2.65

Residual Fluid Saturations

Residual Oil Saturation, %	Residual Water Saturation, %
12.7	45.1

Permeability

Permeability to Water, mD	Permeability to Air, mD
50	Pending

No Thin Section Created

In order to retain the longest possible plug for other analyses, very little was removed during the facing process. Therefore, the sample did not provide enough material for thin-section creation.

SAMPLE PHOTOGRAPH

PHYSICAL PROPERTIES

Porosity

Pycnometer Effective Porosity Average (range), vol%	Pycnometer Effective Porosity by MetaRock Laboratories, vol%	Thin-Section Point Count Porosity, % occurrence	Thin-Section Image Segmentation Pore Space, area%
N/A	N/A	NT	23.4

Density

Bulk Volume, cm^3	Skeletal Density, g/cm^3
N/A	N/A

Residual Fluid Saturations

Residual Oil Saturation, %	Residual Water Saturation, %
N/A	N/A

Permeability

Permeability to Water, mD	Permeability to Air, mD
N/A	N/A

PHOTOMICROGRAPHS

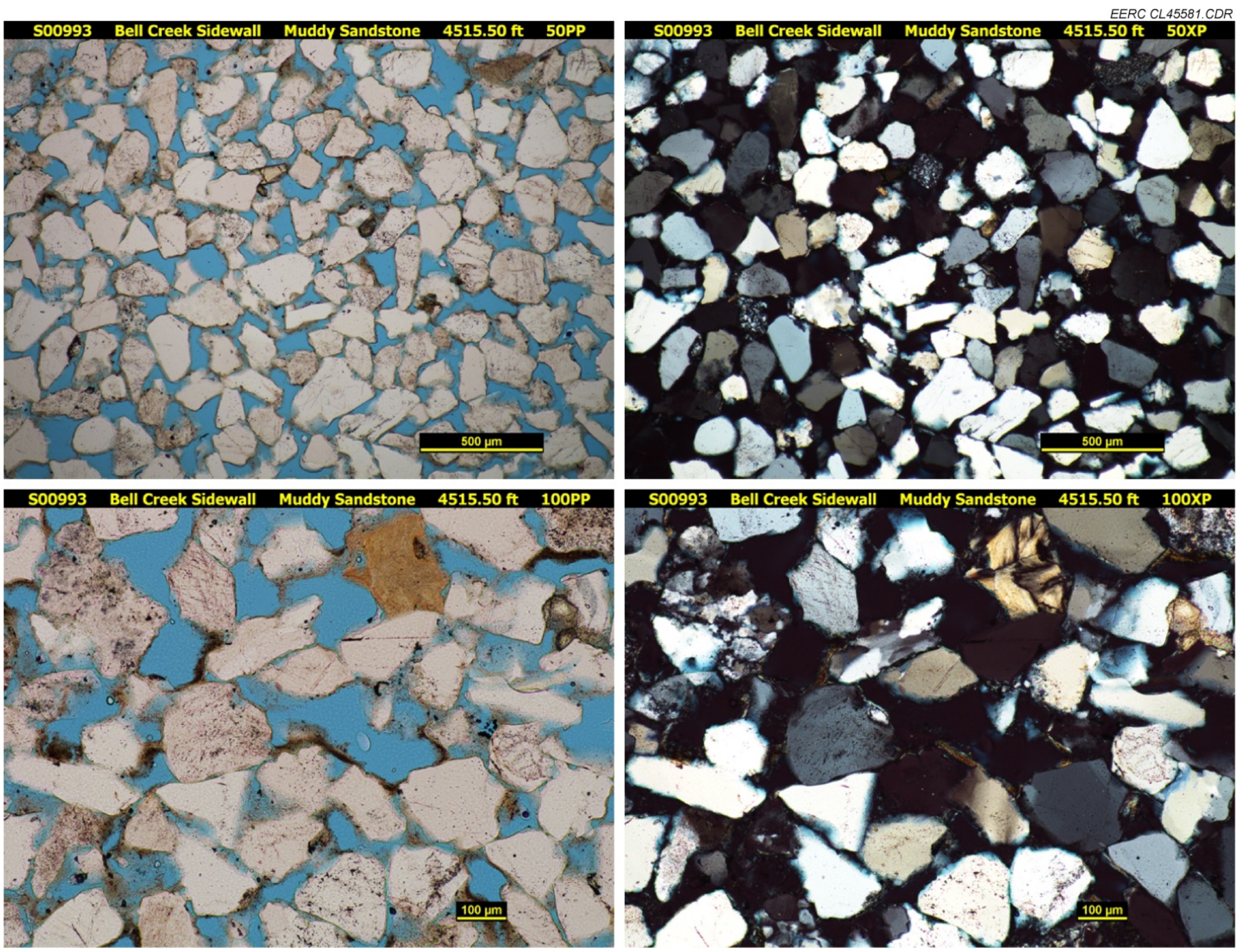

The sample collected at the 4515.50-ft depth is clean, fine-grained, moderately well sorted sandstone. Quartz grains are angular to subrounded, displaying monocrystalline and few polycrystalline grains. Trace levels of feldspars, rutile, clays, and metals are present. Porosity exists as intergranular and as the result of cement and (feldspar) grain dissolution. No fractures, fossilization, or quartz overgrowth are detected.

THIN-SECTION PORE ANALYSIS BY DIGITAL IMAGE SEGMENTATION

Depth: 4515.00 ft; W = 28.23 mm; H = 9.46 mm

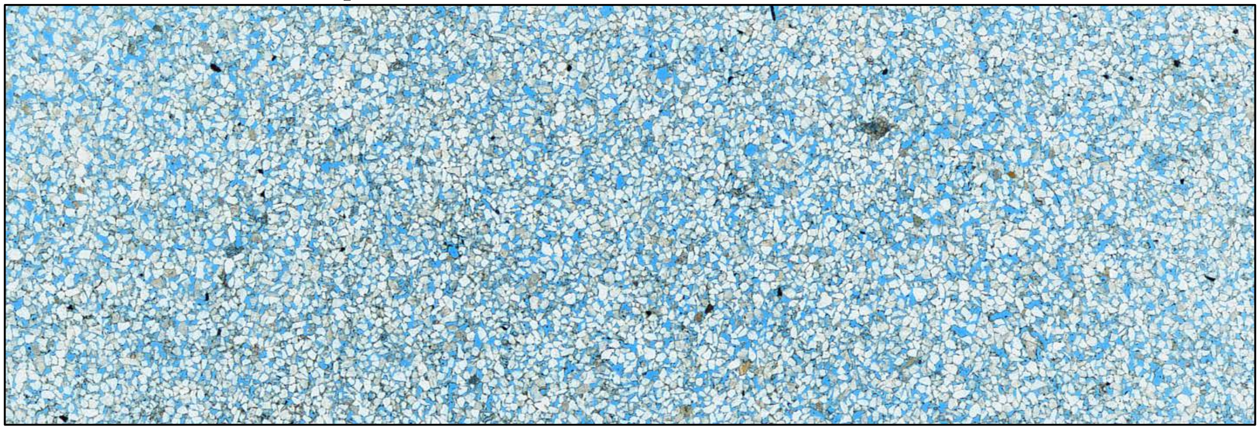

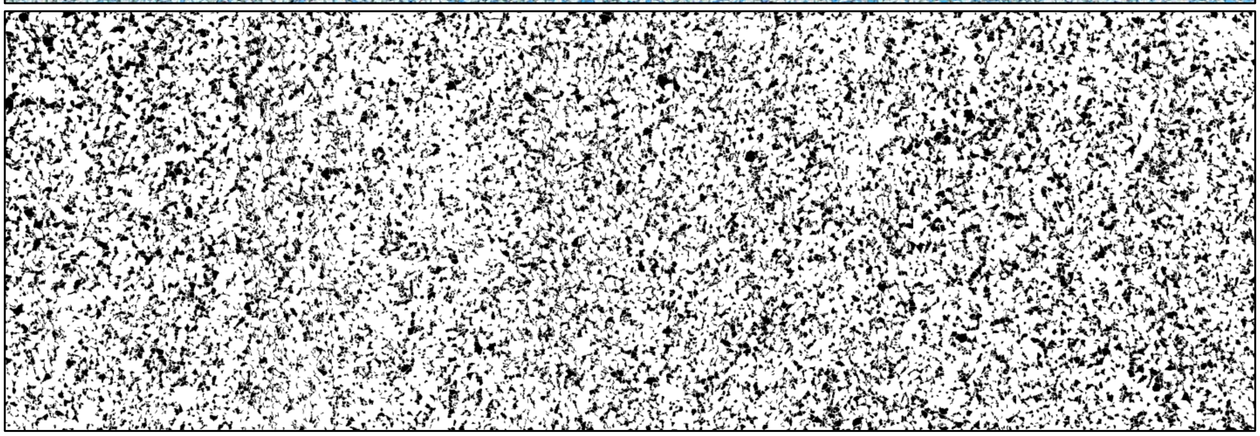

Pore Space, area%	Mean Pore Area, μm^2	Pore Area Range, μm^2	Mean Pore Perimeter, µm	Pore Perimeter Range, µm
23.4	3348	112–52,027	258	41–1279

This page intentionally left blank.

SAMPLE PHOTOGRAPH

PHYSICAL PROPERTIES

Porosity

Pycnometer Effective Porosity Average (range), vol%	Pycnometer Effective Porosity by MetaRock Laboratories, vol%	Thin-Section Point Count Porosity, % occurrence	Thin-Section Image Segmentation Pore Space, area%
N/A	N/A	NT	27.7

Density

Bulk Volume, cm^3	Skeletal Density, g/cm^3
N/A	N/A

Residual Fluid Saturations

Residual Oil Saturation, %	Residual Water Saturation, %
N/A	N/A

Permeability

Permeability to Water, mD	Permeability to Air, mD
N/A	N/A

PHOTOMICROGRAPHS

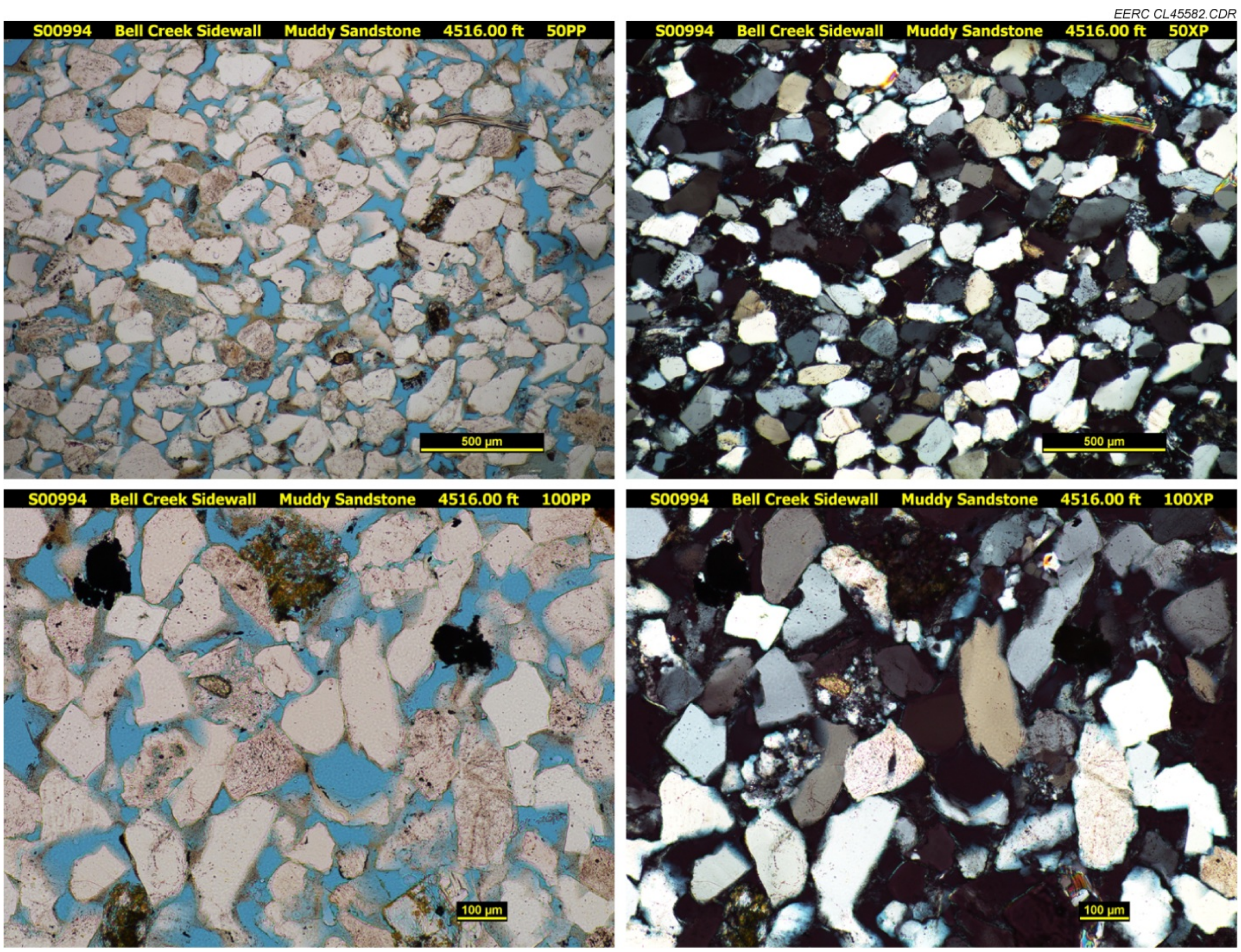

The sample collected at depth 4516.00 ft shows clean, fine-grained, moderately well sorted sandstone. Quartz grains are angular to subrounded, displaying monocrystalline and few polycrystalline grains. Porosity exists as intergranular and as the result of cement and (feldspar) grain dissolution. Muscovite occurs in higher concentration than in any previous samples. Feldspars, clays, metals, and rutile occur at trace levels. Some evidence of compaction is observed through muscovite crushing. No fractures, fossilization, and little quartz overgrowth are detected.

THIN-SECTION PORE ANALYSIS BY DIGITAL IMAGE SEGMENTATION

Depth: 4516.00 ft; W = 31.38 mm; H = 13.95 mm

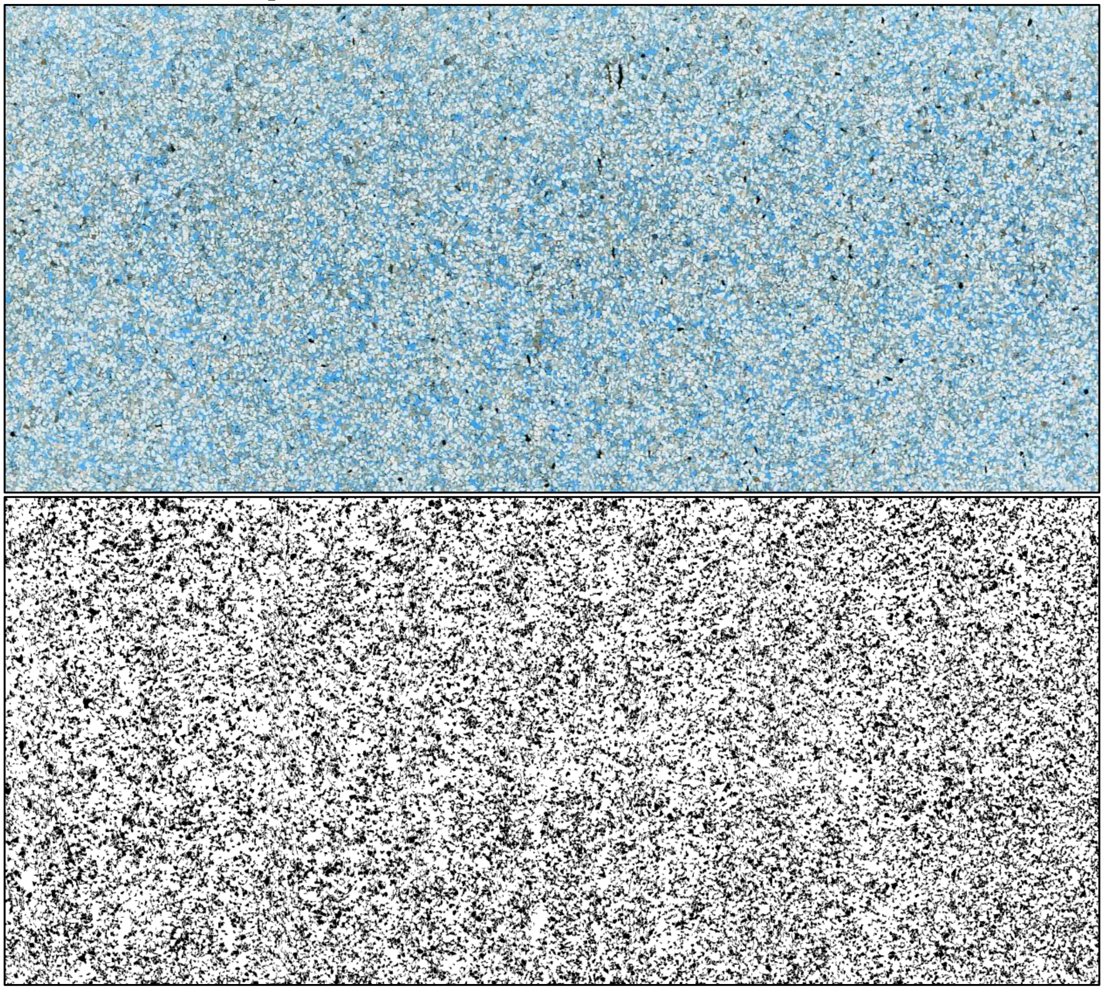

Pore Space, area%	Mean Pore Area, µm^2	Pore Area Range, µm^2	Mean Pore Perimeter, µm	Pore Perimeter Range, µm
27.7	2835	84–46,679	242	30–244

This page intentionally left blank.

SAMPLE PHOTOGRAPH

PHYSICAL PROPERTIES

Porosity

Pycnometer Effective Porosity Average (range), vol%	Pycnometer Effective Porosity by MetaRock Laboratories, vol%	Thin-Section Point Count Porosity, % occurrence	Thin-Section Image Segmentation Pore Space, area%
24.7 (16.2–31.2)	26.9	NT	17.8

Density

Bulk Volume, cm^3	Skeletal Density, g/cm^3
17.9	2.51

Residual Fluid Saturations

Residual Oil Saturation, %	Residual Water Saturation, %
21.5	58.4

Permeability

Permeability to Water, mD	Permeability to Air, mD
27	Pending

PHOTOMICROGRAPHS

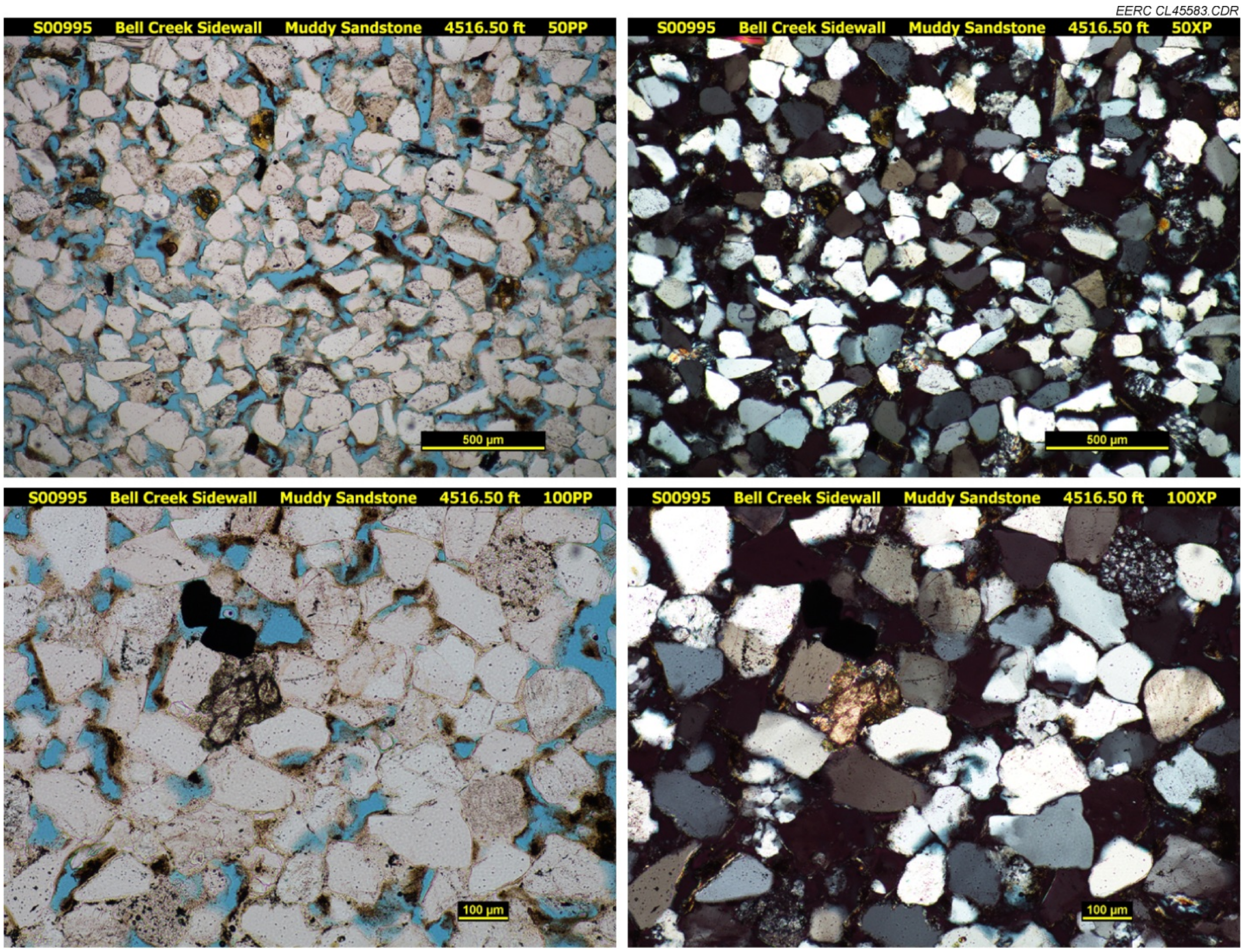

The sample collected at a depth of 4516.50 ft is clean, fine-grained, moderately well to well-sorted, grain-supported sandstone. Quartz grains are subangular to subrounded and include predominantly monocrystalline and occasional polycrystalline grains. Porosity aided by mineral dissolution is intergranular. Original porosity has been reduced by clay-lined pores and minor quartz overgrowth as well as compaction evidenced by sutured grain contacts and muscovite crushing and bending. Feldspars, clays, metals, and rutile occur at trace levels. No fractures or fossilization are observed.

THIN-SECTION PORE ANALYSIS BY DIGITAL IMAGE SEGMENTATION

Depth: 4516.50 ft; W = 21.50 mm; H = 13.18 mm

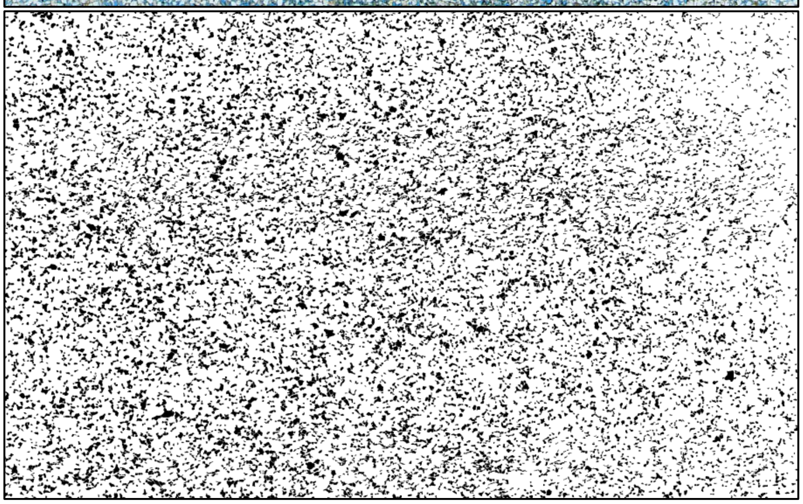

Pore Space, area%	Mean Pore Area, µm^2	Pore Area Range, µm^2	Mean Pore Perimeter, µm	Pore Perimeter Range, µm
17.8	3082	168–45,055	229	48–1108

This page intentionally left blank.

SAMPLE PHOTOGRAPH

PHYSICAL PROPERTIES

Porosity

Pycnometer Effective Porosity Average (range), vol%	Pycnometer Effective Porosity by MetaRock Laboratories, vol%	Thin-Section Point Count Porosity, % occurrence	Thin-Section Image Segmentation Pore Space, area%
27.9 (26.2–30.4)	24.9	NT	11.2

Density

Bulk Volume, cm^3	Skeletal Density, g/cm^3
28.4	2.68

Residual Fluid Saturations

Residual Oil Saturation, %	Residual Water Saturation, %
12.0	45.4

Permeability

Permeability to Water, mD	Permeability to Air, mD
79	Pending

PHOTOMICROGRAPHS

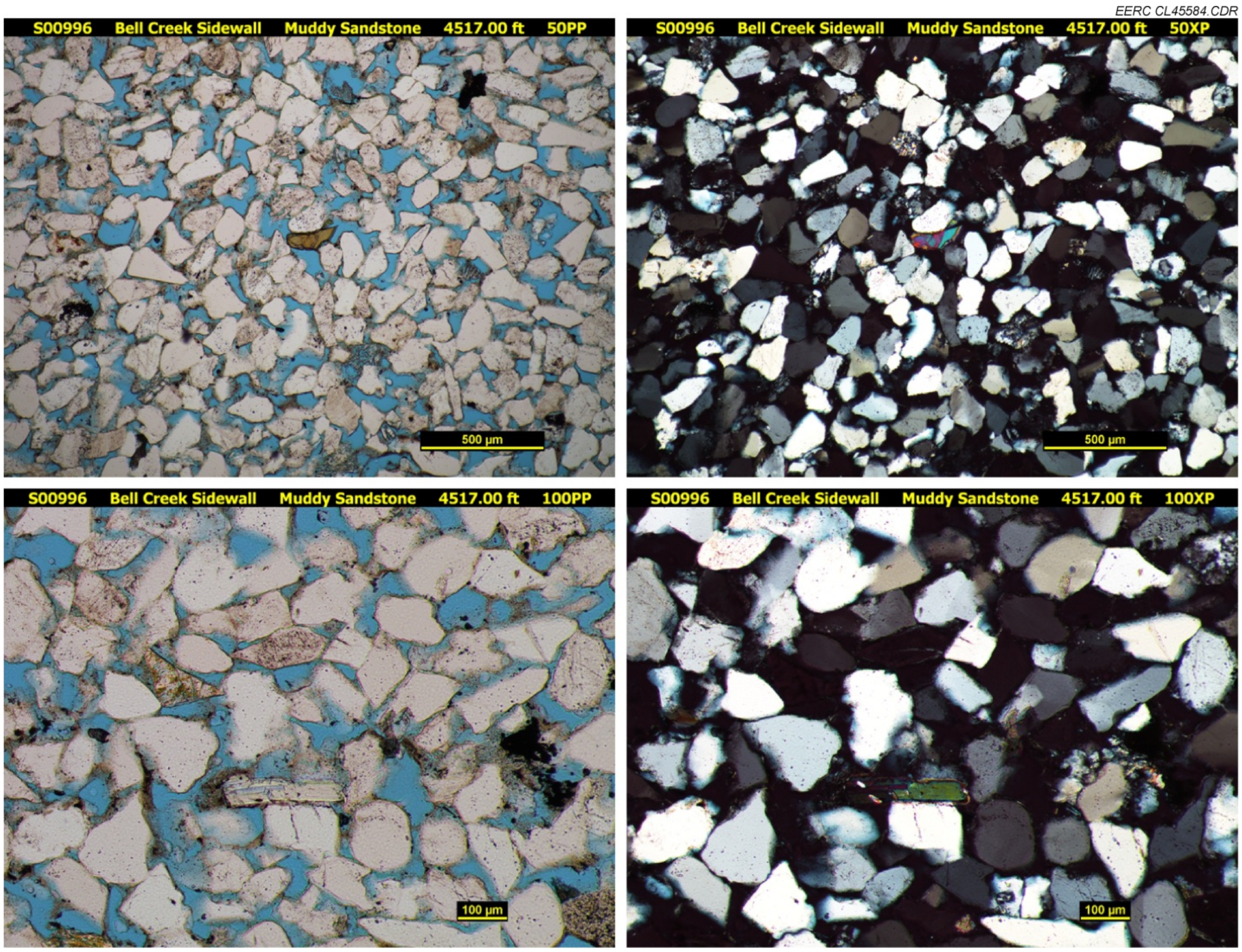

The sample collected at a depth of 4517.00 ft is very similar to the sample from the 4516.5-ft depth. It is clean, fine-grained, moderately well to well-sorted, grain-supported sandstone. Quartz grains are subangular to subrounded, displaying predominantly monocrystalline and occasional polycrystalline grains. Original intergranular porosity is altered by a small amount of compaction, quartz overgrowth, and residual clays lining some of the pore throats. Trace levels of muscovite, siderite, feldspars, clays, and metals are observed. No fractures or fossilization are detected.

THIN-SECTION PORE ANALYSIS BY DIGITAL IMAGE SEGMENTATION

Depth: 4517.00 ft; W = 14.76 mm; H = 13.54 mm

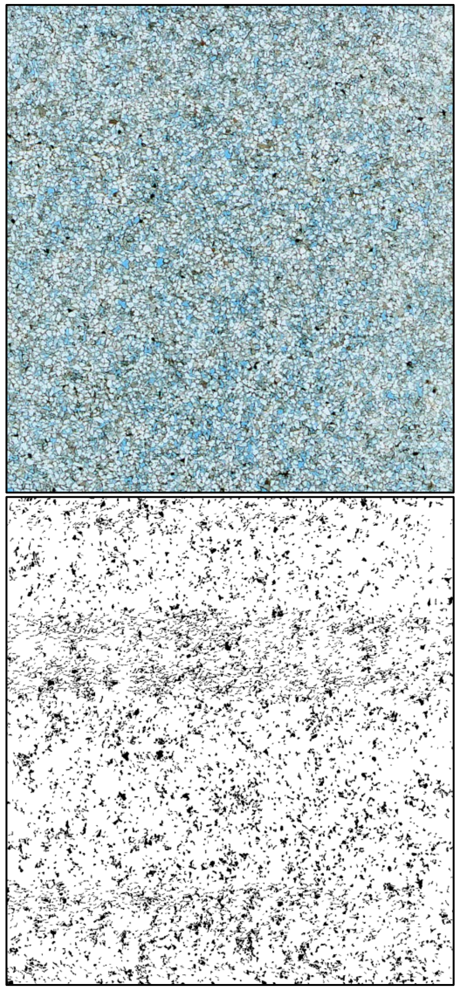

Pore Space, area%	Mean Pore Area, µm^2	Pore Area Range, µm^2	Mean Pore Perimeter, µm	Pore Perimeter Range, µm
11.2	2098	140–34,666	193	45–922

This page intentionally left blank.

SAMPLE PHOTOGRAPH

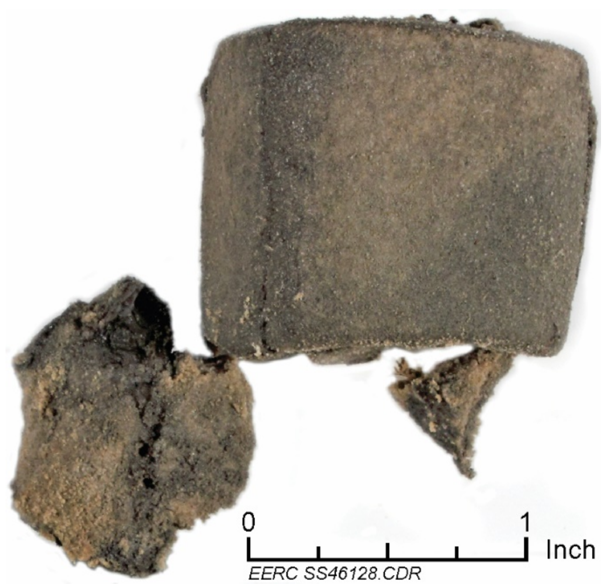

PHYSICAL PROPERTIES

Porosity

Pycnometer Effective Porosity Average (range), vol%	Pycnometer Effective Porosity by MetaRock Laboratories, vol%	Thin-Section Point Count Porosity, % occurrence	Thin-Section Image Segmentation Pore Space, area%
N/A	N/A	NT	10.9

Density

Bulk Volume, cm^3	Skeletal Density, g/cm^3
N/A	N/A

Residual Fluid Saturations

Residual Oil Saturation, %	Residual Water Saturation, %
N/A	N/A

Permeability

Permeability to Water, mD	Permeability to Air, mD
N/A	N/A

PHOTOMICROGRAPHS

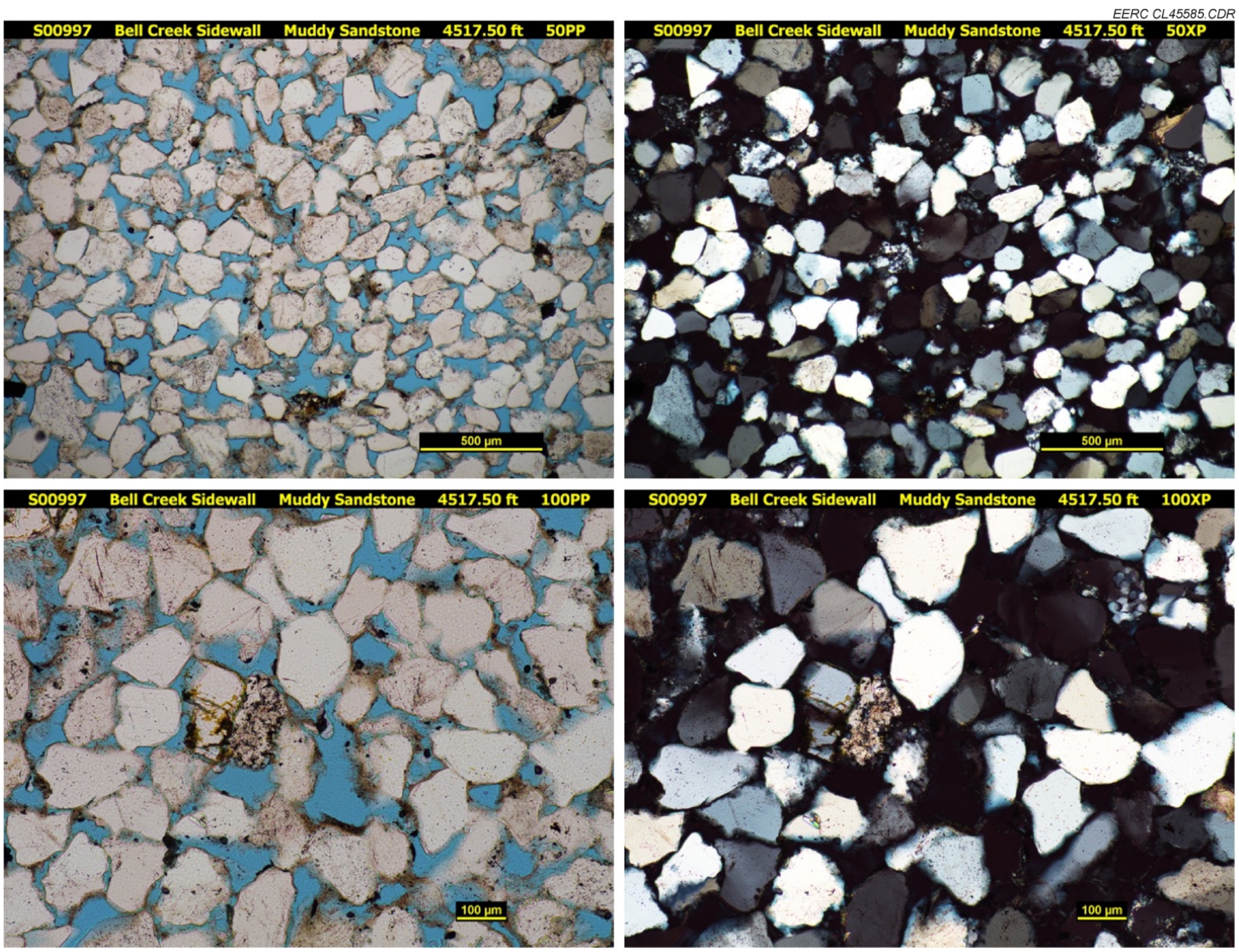

The sample collected at the 4517.50-ft depth is clean, fine-grained, moderately well to well-sorted, grain-supported sandstone. Quartz grains are subangular to subrounded, with predominantly monocrystalline and occasional polycrystalline grains. In some areas, the pores are lined by clay or are completely full of clay, while in other areas, very little clay is observed in the pores. Slight compaction and quartz overgrowths are observed. Trace levels of siderite, metals, and muscovite are detected. Limited facture-based porosity is observed. No fossils are observed.

THIN-SECTION PORE ANALYSIS BY DIGITAL IMAGE SEGMENTATION

Depth: 4517.50 ft; W = 20.13 mm; H = 11.46 mm

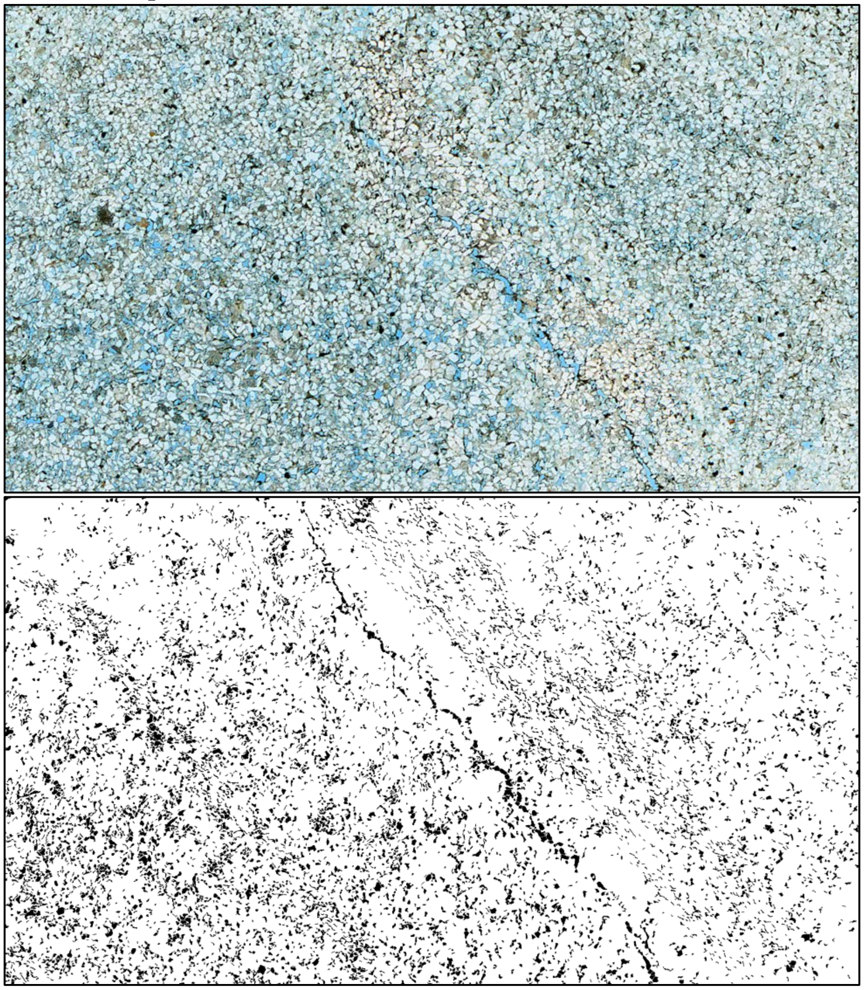

Pore Space, area%	Mean Pore Area, μm^2	Pore Area Range, μm^2	Mean Pore Perimeter, µm	Pore Perimeter Range, µm
10.9	1967	140–25,958	191	37–966

This page intentionally left blank.

SAMPLE PHOTOGRAPH

PHYSICAL PROPERTIES

Porosity

Pycnometer Effective Porosity Average (range), vol%	Pycnometer Effective Porosity by MetaRock Laboratories, vol%	Thin-Section Point Count Porosity, % occurrence	Thin-Section Image Segmentation Pore Space, area%
18.0 (13.9–20.8)	NT	NT	15.9

Density

Bulk Volume, cm^3	Skeletal Density, g/cm^3
30.0	2.60

Residual Fluid Saturations

Residual Oil Saturation, %	Residual Water Saturation, %
30.5	64.4

Permeability

Permeability to Water, mD	Permeability to Air, mD
30	Pending

EERC UND NORTH DAKOTA	Applied Geology Laboratory		
	Muddy Formation	Well Name: 05-06 OW	ID: S-00999
	API No.: 25075224310000	Lithology: Sandstone	Depth: 4518.50'

PHOTOMICROGRAPHS

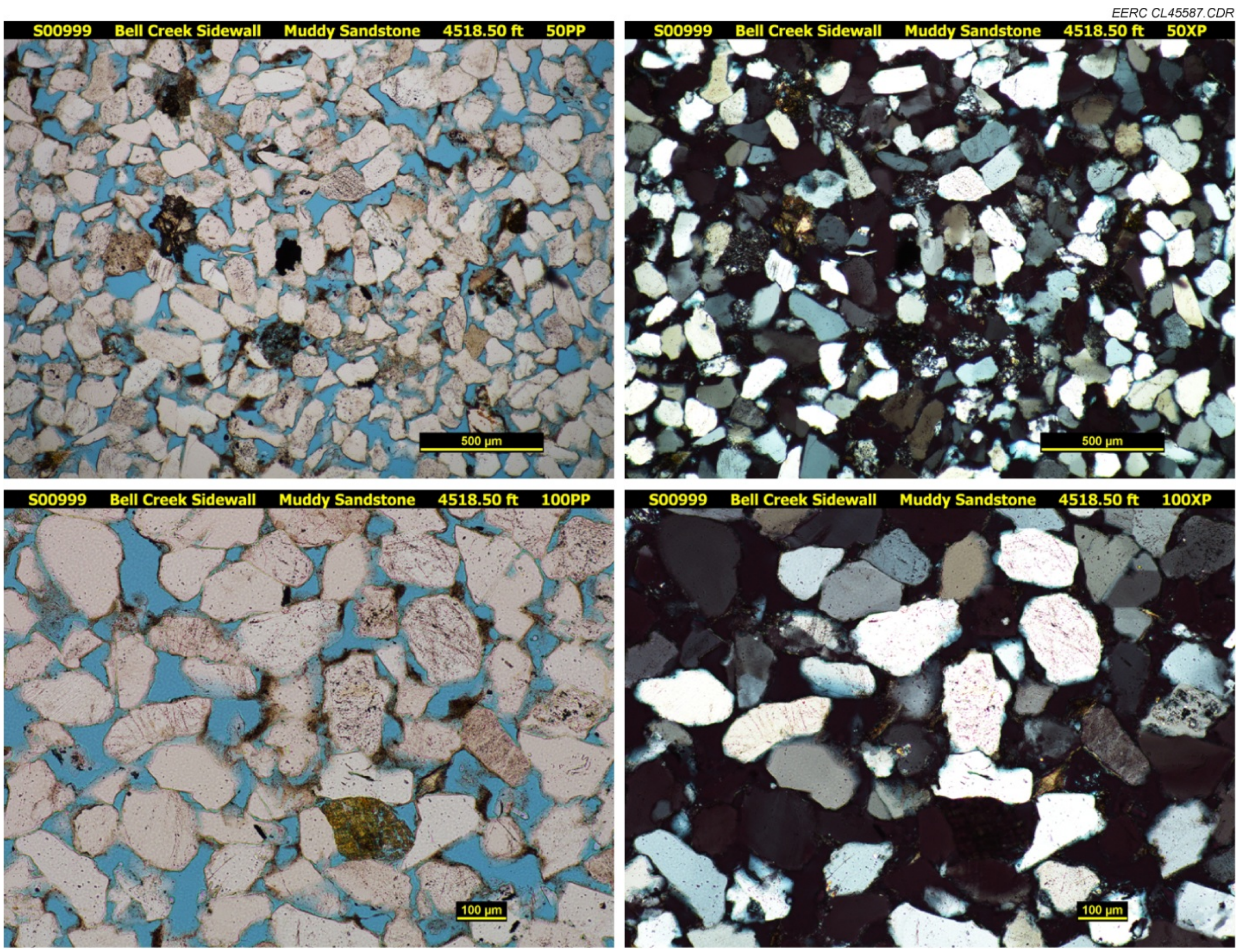

The sample collected at a 4518.50-ft depth is moderately well sorted, fine-grained, fairly clean sandstone. The quartz grains are subangular to subrounded and predominantly monocrystalline along with occasional polycrystalline grains. Pores are inconsistently lined with clays throughout the sample. In some localities, quartz grains have partially dissolved and silica has accumulated within some of the intergranular pores, greatly reducing original porosity. Mild syntaxial quartz overgrowth and grain compaction is observed. Trace levels of muscovite and metals are observed. No fractures or fossilization are detected.

	Applied Geology Laboratory		
EERC UND NORTH DAKOTA	Muddy Formation	Well Name: 05-06 OW	ID: S-00999
	API No.: 25075224310000	Lithology: Sandstone	Depth: 4518.50'

THIN-SECTION PORE ANALYSIS BY DIGITAL IMAGE SEGMENTATION

Depth: 4518.50 ft; W = 14.52 mm; H = 14.19 mm

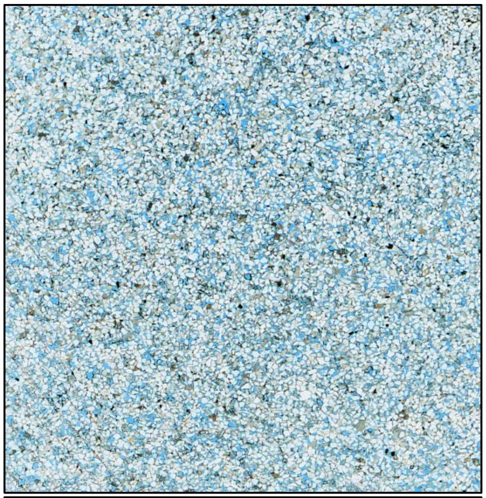

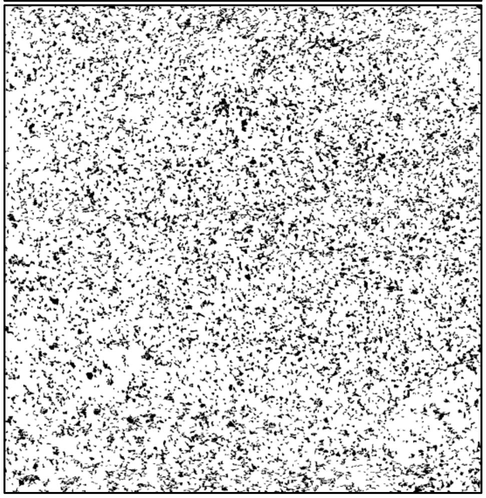

Pore Space, area%	Mean Pore Area, µm²	Pore Area Range, µm²	Mean Pore Perimeter, µm	Pore Perimeter Range, µm
15.9	2813	168–31,474	219	48–892

This page intentionally left blank.

SAMPLE PHOTOGRAPH

PHYSICAL PROPERTIES

Porosity

Pycnometer Effective Porosity Average (range), vol%	Pycnometer Effective Porosity by MetaRock Laboratories, vol%	Thin-Section Point Count Porosity, % occurrence	Thin-Section Image Segmentation Pore Space, area%
24.0 (21.8–25.6)	NT	NT	17.1

Density

Bulk Volume, cm^3	Skeletal Density, g/cm^3
30.3	2.69

Residual Fluid Saturations

Residual Oil Saturation, %	Residual Water Saturation, %
5.0	48.1

Permeability

Permeability to Water, mD	Permeability to Air, mD
5.0	Pending

PHOTOMICROGRAPHS

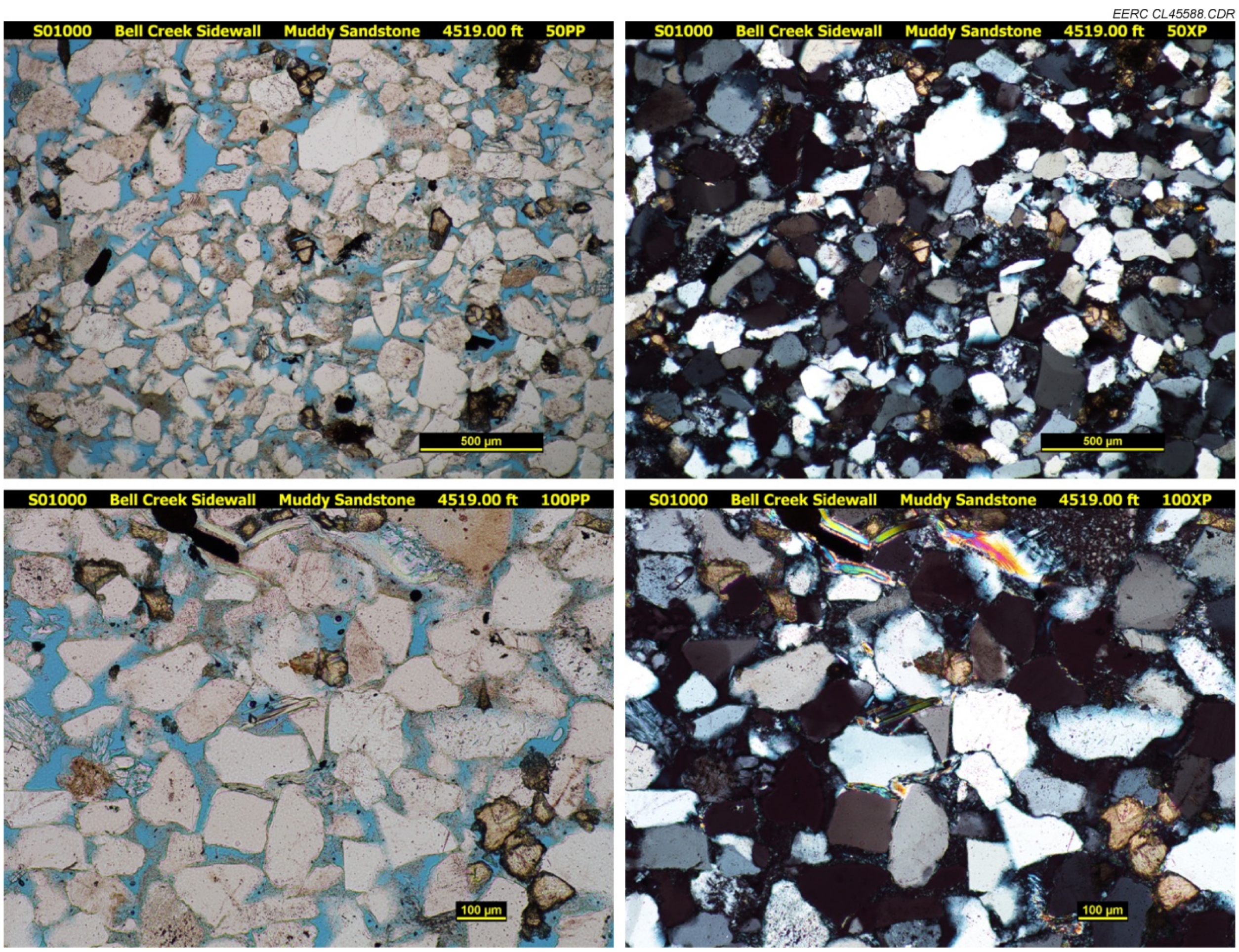

The sample collected at a 4519.00-ft depth is moderately well sorted, fine-grained, fairly clean sandstone. The quartz grains are subangular to subrounded, and predominantly monocrystalline along with occasional polycrystalline grains. Largely clay, along with some silica, cement has reduced original intergranular porosity. Some pores are nearly completely cemented by clays, others are partially filled, and some pores are thinly lined because of dissolution. Mild compaction is observed by quartz grain contacts and muscovite bending or breaking. Trace levels of metals, feldspars, and siderite are observed. No fractures or fossilization are detected.

THIN-SECTION PORE ANALYSIS BY DIGITAL IMAGE SEGMENTATION

Depth: 4519.00 ft; W = 24.79 mm; H = 16.29 mm

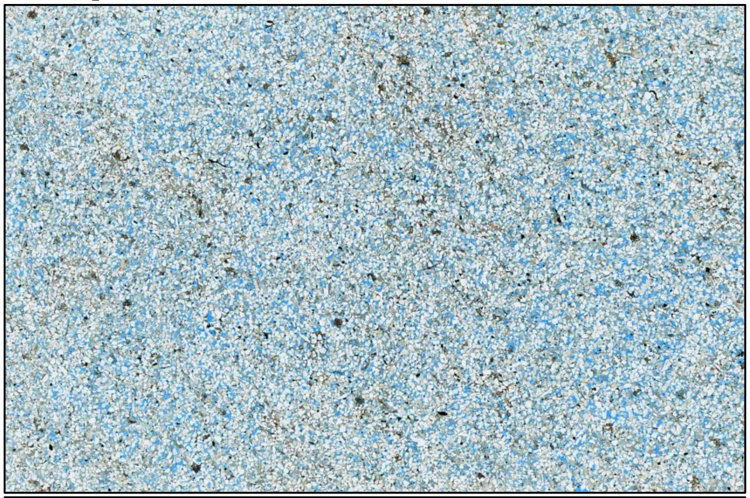

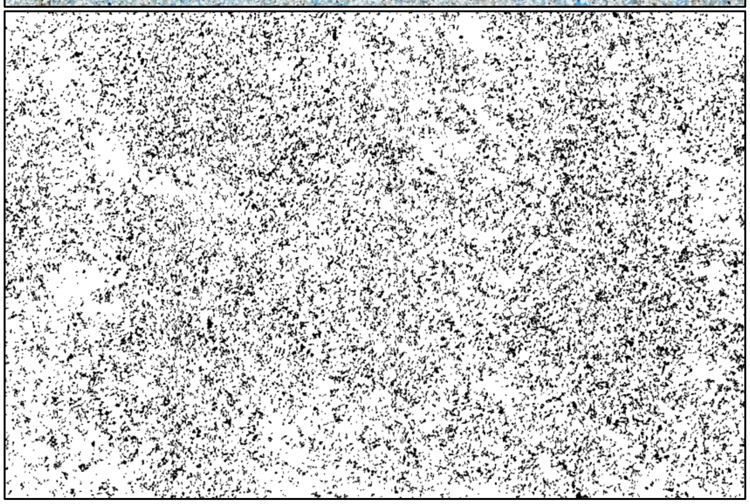

Pore Space, area%	Mean Pore Area, μm^2	Pore Area Range, μm^2	Mean Pore Perimeter, μm	Pore Perimeter Range, μm
17.1	2912	140–39,034	222	45–1005

This page intentionally left blank.

SAMPLE PHOTOGRAPH

PHYSICAL PROPERTIES

Porosity

Pycnometer Effective Porosity Average (range), vol%	Pycnometer Effective Porosity by MetaRock Laboratories, vol%	Thin-Section Point Count Porosity, % occurrence	Thin-Section Image Segmentation Pore Space, area%
N/A	N/A	NT	9.2

Density

Bulk Volume, cm^3	Skeletal Density, g/cm^3
N/A	N/A

Residual Fluid Saturations

Residual Oil Saturation, %	Residual Water Saturation, %
N/A	N/A

Permeability

Permeability to Water, mD	Permeability to Air, mD
N/A	N/A

	Applied Geology Laboratory		
	Muddy Formation	Well Name: 05-06 OW	ID: S-01001
	API No.: 25075224310000	Lithology: Sandstone	Depth: 4519.25'

PHOTOMICROGRAPHS

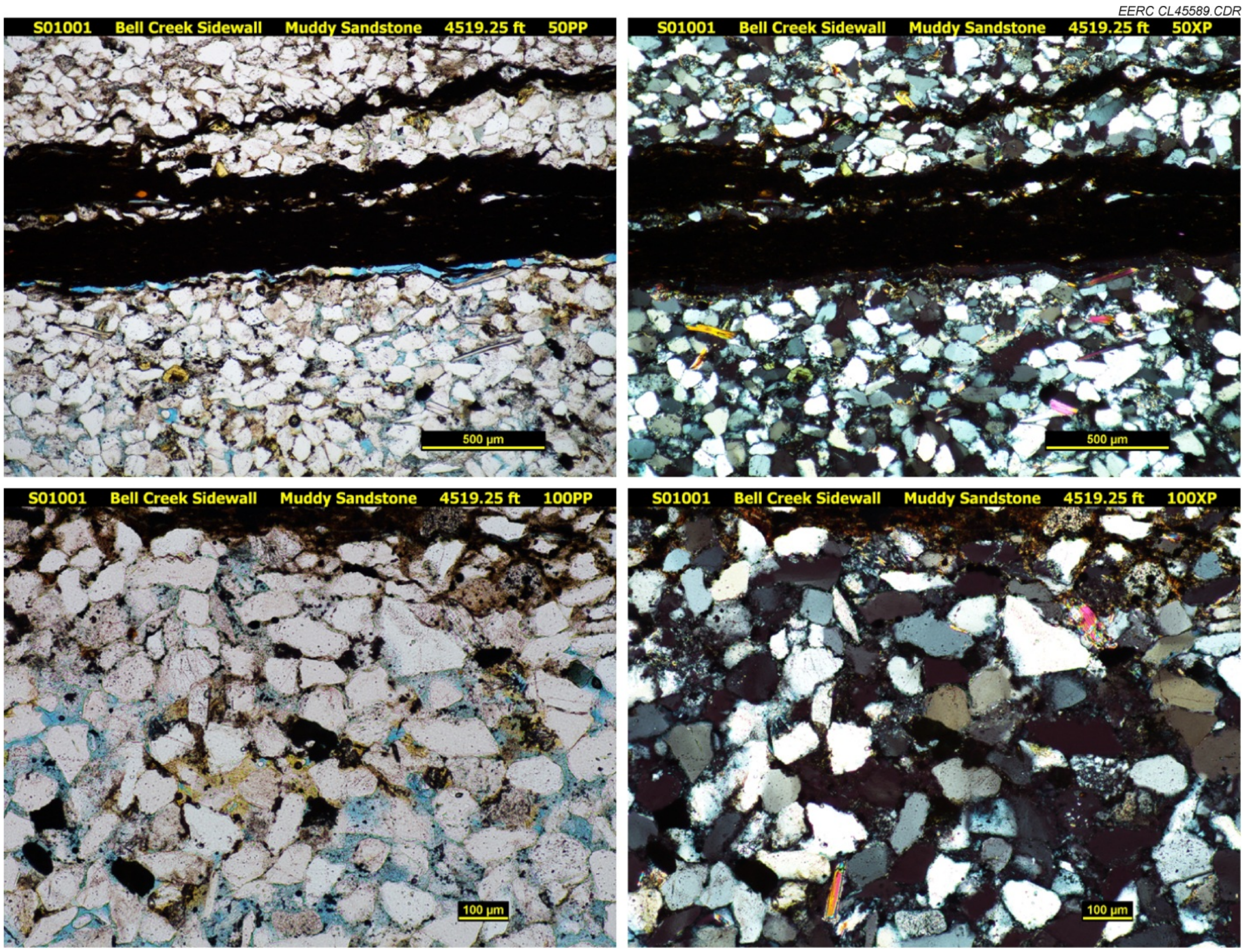

The sample collected at the 4519.25-ft depth is moderately well sorted, fine-grained, fairly clean sandstone with subangular to subrounded predominantly monocrystalline quartz grains and occasional polycrystalline grains. Original intergranular porosity has been reduced by partial inconsistent clay infill. Some pores are almost completely cemented by clays, others are partially filled, and some pores are thinly lined due to dissolution. Laminations of a mixture of clays and organics are commonly present. Mild compaction is observed by quartz grain contacts and muscovite bending or breaking. Additional minerals found in trace levels are siderite, feldspars, rutile, and metals. No fractures or fossilization are detected.

THIN-SECTION PORE ANALYSIS BY DIGITAL IMAGE SEGMENTATION

Depth: 4519.25 ft; W = 25.56 mm; H = 15.86 mm

Pore Space, area%	Mean Pore Area, μm^2	Pore Area Range, μm^2	Mean Pore Perimeter, µm	Pore Perimeter Range, µm
9.2*	1656	84–26,210	175	30–867

* The pore space consists of a) pores: 9.1 area% and b) fractures: 0.1 area%.

This page intentionally left blank.

SAMPLE PHOTOGRAPH

PHYSICAL PROPERTIES

Porosity

Pycnometer Effective Porosity Average (range), vol%	Pycnometer Effective Porosity by MetaRock Laboratories, vol%	Thin-Section Point Count Porosity, % occurrence	Thin-Section Image Segmentation Pore Space, area%
23.3 (20.2–24.9)	NT	NT	19.5

Density

Bulk Volume, cm^3	Skeletal Density, g/cm^3
32.3	2.67

Residual Fluid Saturations

Residual Oil Saturation, %	Residual Water Saturation, %
37.2	14.3

Permeability

Permeability to Water, mD	Permeability to Air, mD
2.8	Pending

EERC UND NORTH DAKOTA	Applied Geology Laboratory		
	Muddy Formation	Well Name: 05-06 OW	ID: S-01003
	API No.: 25075224310000	Lithology: Sandstone	Depth: 4520.00'

PHOTOMICROGRAPHS

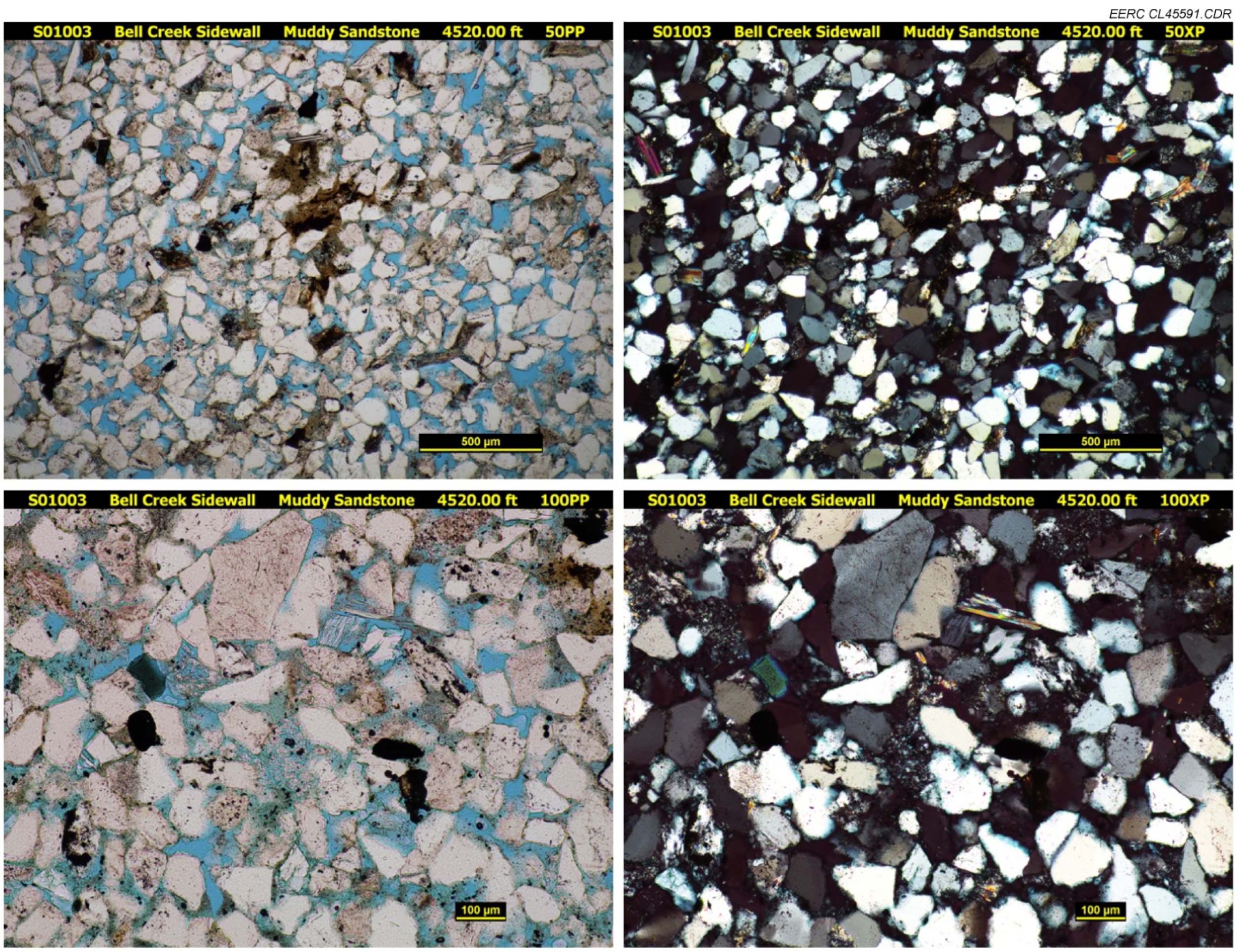

The sample collected at a 4520.00-ft depth is fine-grained, fairly clean, moderately well to well-sorted sandstone containing subangular to subrounded monocrystalline quartz grains and a minor occurrence of polycrystalline grains. Porosity is characterized as intergranular and is a result of cement and grain (feldspar) dissolution. Original porosity has been reduced by quartz contact relationships, slight quartz overgrowths, and compaction as observed by bent muscovite grains. Cementing agents are clays, silica, and carbonates. Muscovite, feldspars, rutile, metals, siderite, and organics are observed at trace levels. No fractures or fossilization are present.

THIN-SECTION PORE ANALYSIS BY DIGITAL IMAGE SEGMENTATION

Depth: 4520.00 ft; W = 22.69 mm; H = 16.00 mm

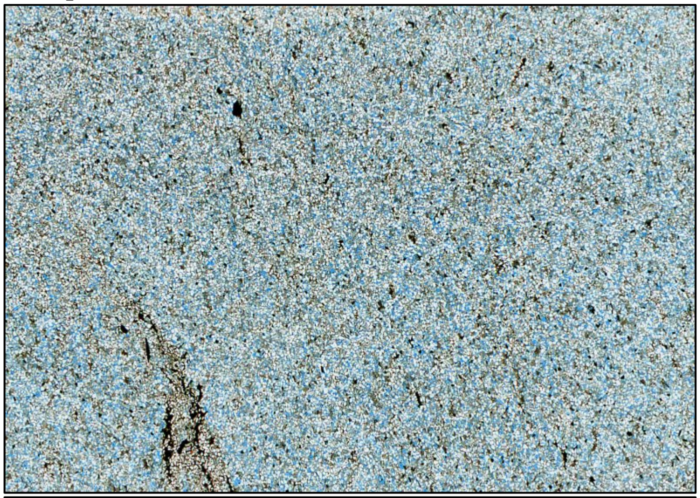

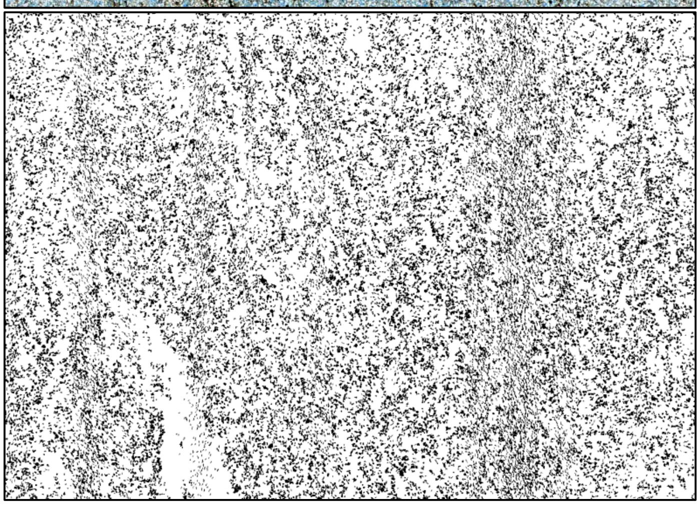

Pore Space, area%	Mean Pore Area, µm^2	Pore Area Range, µm^2	Mean Pore Perimeter, µm	Pore Perimeter Range, µm
19.5	2297	28–25,174	206	15–944

This page intentionally left blank.

SAMPLE PHOTOGRAPH

PHYSICAL PROPERTIES

Porosity

Pycnometer Effective Porosity Average (range), vol%	Pycnometer Effective Porosity by MetaRock Laboratories, vol%	Thin-Section Point Count Porosity, % occurrence	Thin-Section Image Segmentation Pore Space, area%
22.3 (17.9–25.5)	NT	NT	23.6

Density

Bulk Volume, cm^3	Skeletal Density, g/cm^3
25.4	2.58

Residual Fluid Saturations

Residual Oil Saturation, %	Residual Water Saturation, %
22.1	35.3

Permeability

Permeability to Water, mD	Permeability to Air, mD
83	Pending

PHOTOMICROGRAPHS

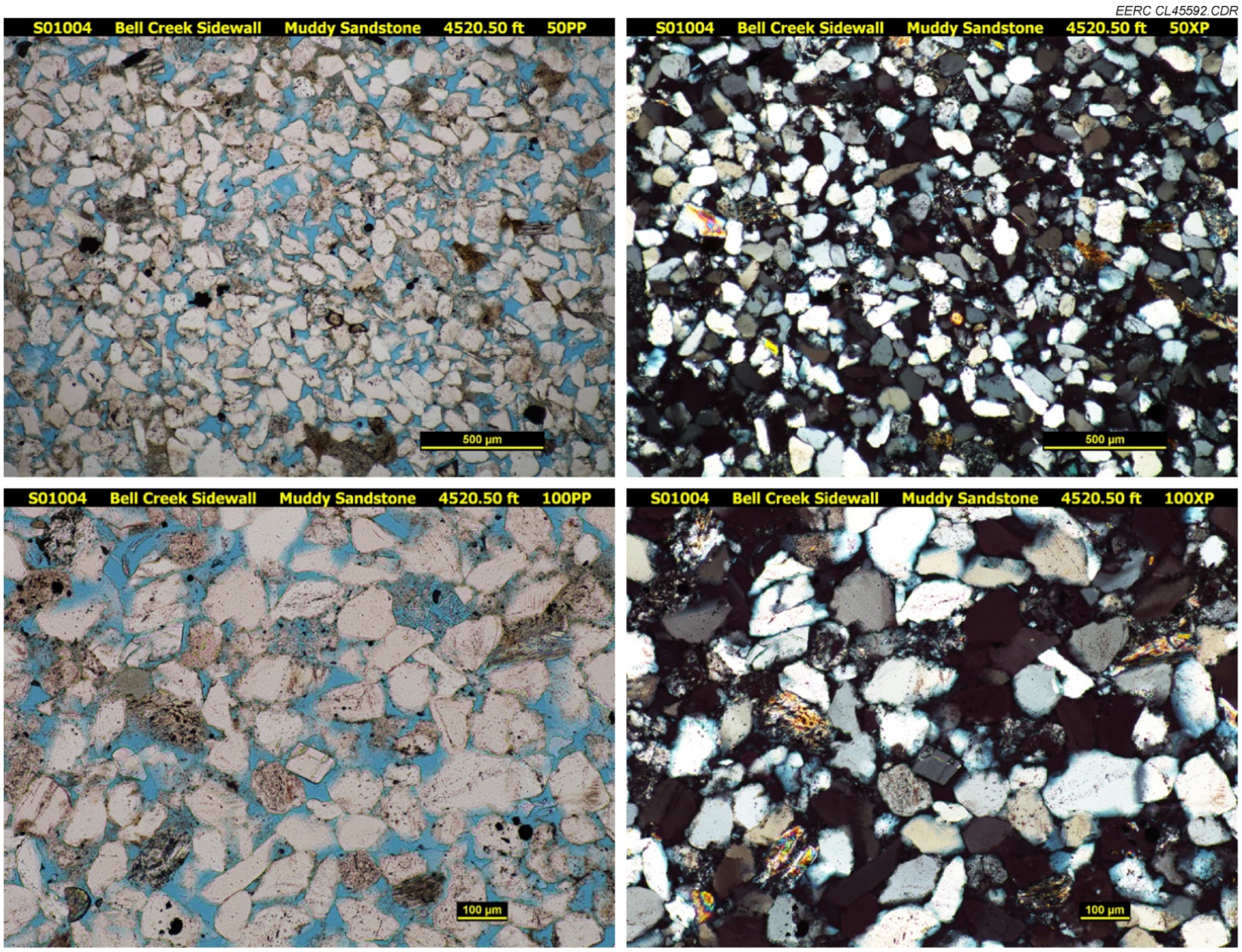

The sample collected at a 4520.50-ft depth is fine-grained, clean, moderately well to well-sorted sandstone containing subangular to subrounded monocrystalline quartz grains and a minor occurrence of polycrystalline grains. Porosity is characterized as intergranular and is a result of cement and grain (feldspar) dissolution. Compaction observed through muscovite bending, quartz contact relationships, and slight quartz overgrowths are limiting factors of original porosity. Cementing agents in small quantities are clays, silica, and carbonates. Muscovite, feldspars, rutile, metals, siderite, and organics are observed at trace levels. No fractures or fossilization are present.

THIN-SECTION PORE ANALYSIS BY DIGITAL IMAGE SEGMENTATION

Depth: 4520.50 ft; W = 28.14 mm; H = 13.47 mm

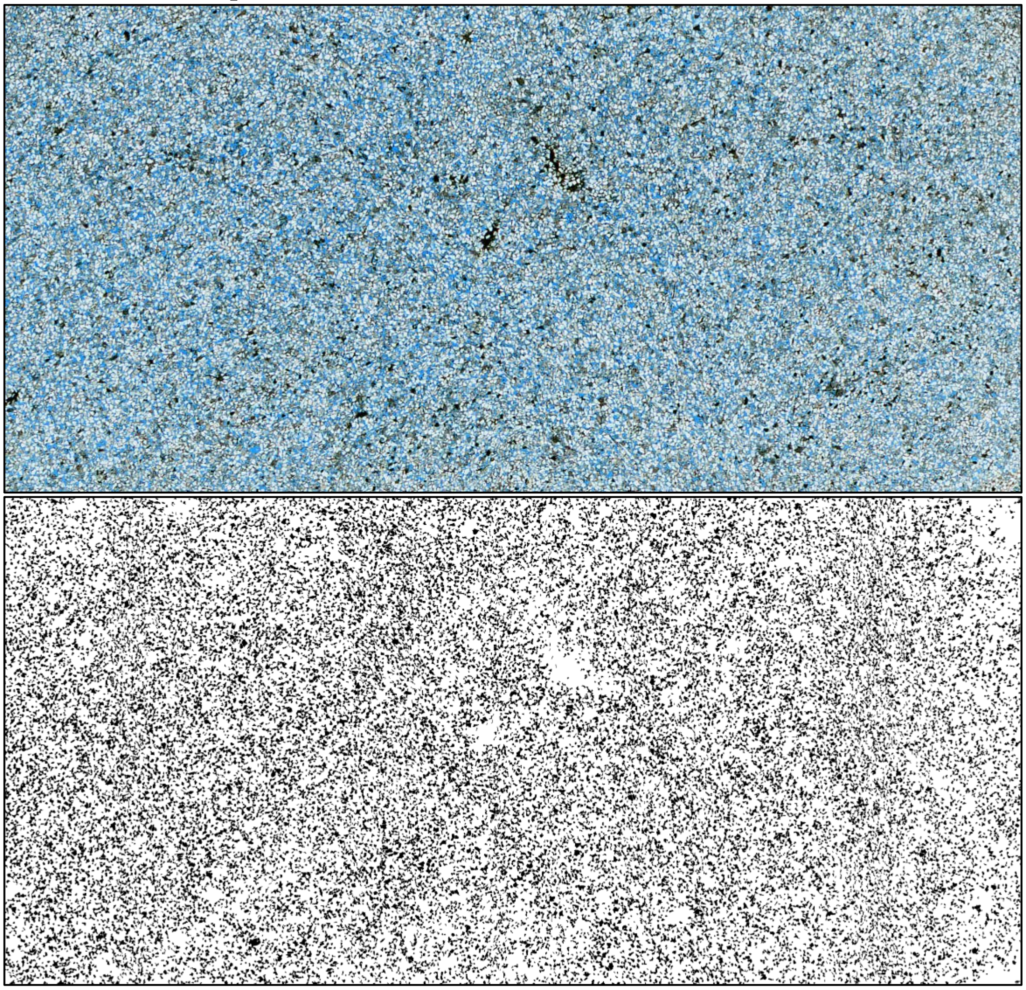

Pore Space, area%	Mean Pore Area, µm^2	Pore Area Range, µm^2	Mean Pore Perimeter, µm	Pore Perimeter Range, µm
23.6	2597	140–38,334	217	45–1039

This page intentionally left blank.

SAMPLE PHOTOGRAPH

PHYSICAL PROPERTIES

Porosity

Pycnometer Effective Porosity Average (range), vol%	Pycnometer Effective Porosity by MetaRock Laboratories, vol%	Thin-Section Point Count Porosity, % occurrence	Thin-Section Image Segmentation Pore Space, area%
26.5 (23.5–28.7)	NT	NT	N/A

Density

Bulk Volume, cm^3	Skeletal Density, g/cm^3
27.0	2.69

Residual Fluid Saturations

Residual Oil Saturation, %	Residual Water Saturation, %
11.5	12.5

Permeability

Permeability to Water, mD	Permeability to Air, mD
73.2	Pending

In order to retain the longest possible plug for other analyses, very little was removed during the facing process. Therefore, the sample did not provide enough material for thin-section preparation.

SAMPLE PHOTOGRAPH

PHYSICAL PROPERTIES

Porosity

Pycnometer Effective Porosity Average (range), vol%	Pycnometer Effective Porosity by MetaRock Laboratories, vol%	Thin-Section Point Count Porosity, % occurrence	Thin-Section Image Segmentation Pore Space, area%
26.7 (25.1–28.2)	NT	NT	31.8

Density

Bulk Volume, cm^3	Skeletal Density, g/cm^3
34.4	2.70

Residual Fluid Saturations

Residual Oil Saturation, %	Residual Water Saturation, %
13.5	14.1

Permeability

Permeability to Water, mD	Permeability to Air, mD
110	Pending

PHOTOMICROGRAPHS

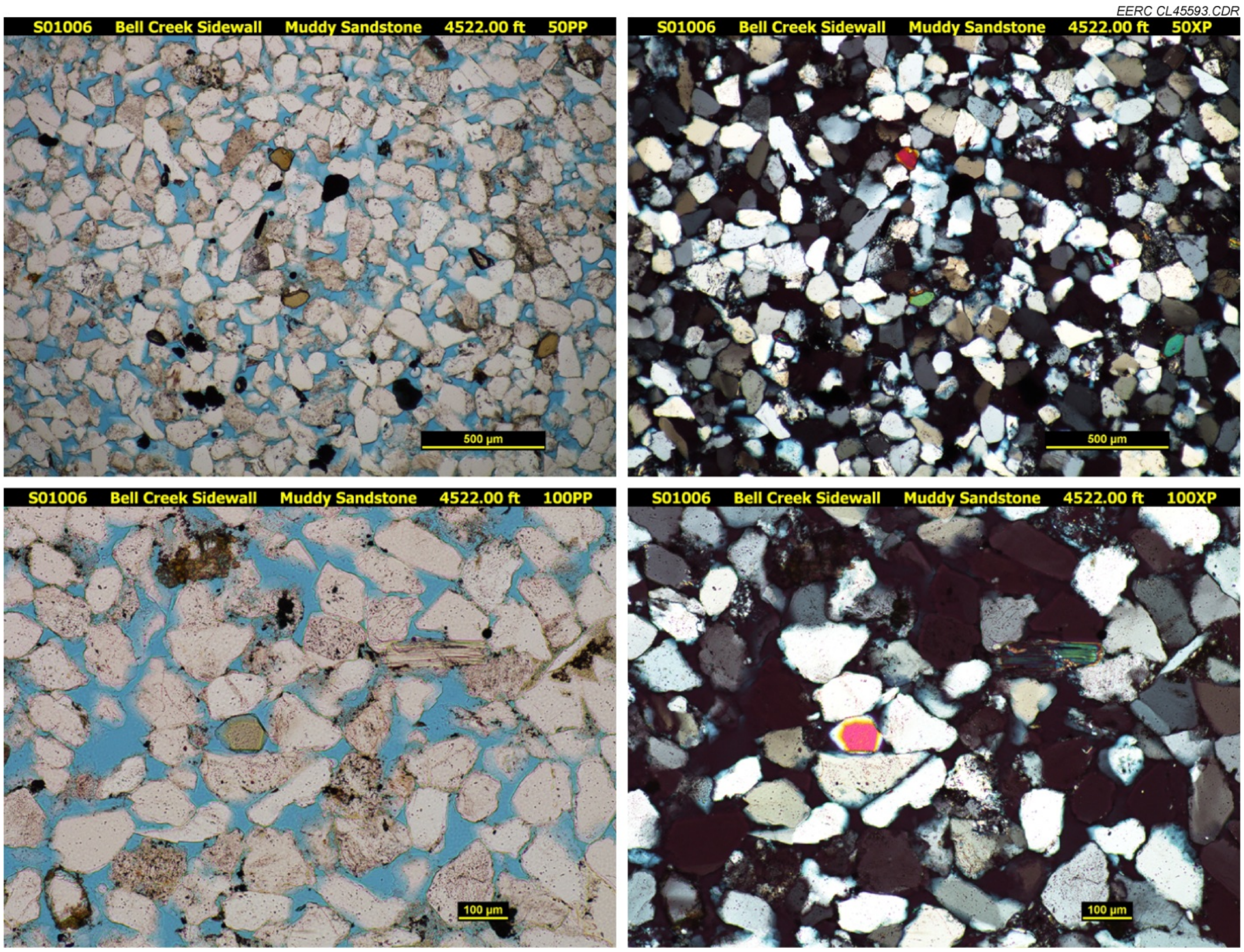

The sample collected at a 4522.00-ft depth is fine-grained, clean, moderately well to well-sorted sandstone containing subangular to subrounded, monocrystalline quartz grains and some rare polycrystalline grains. Porosity is characterized as intergranular and is a result of cement and grain (feldspar and quartz) dissolution. Slight quartz overgrowth and compaction are observed. Additional minerals observed in small amounts are muscovite, siderite, and metals.

THIN-SECTION PORE ANALYSIS BY DIGITAL IMAGE SEGMENTATION

Depth: 4522.00 ft; W = 23.31 mm; H = 16.62 mm

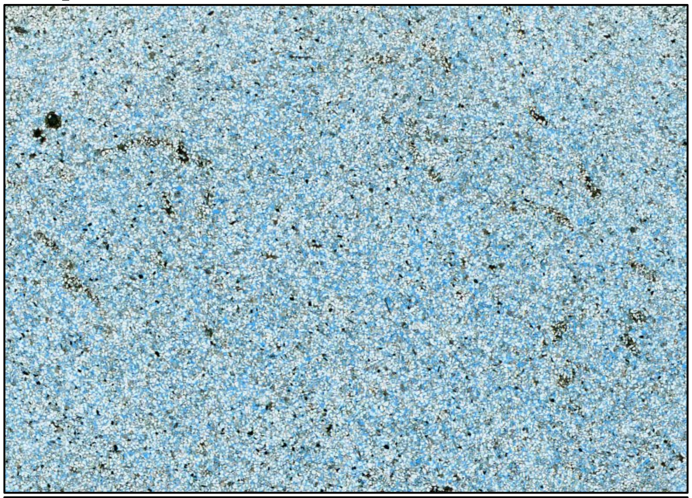

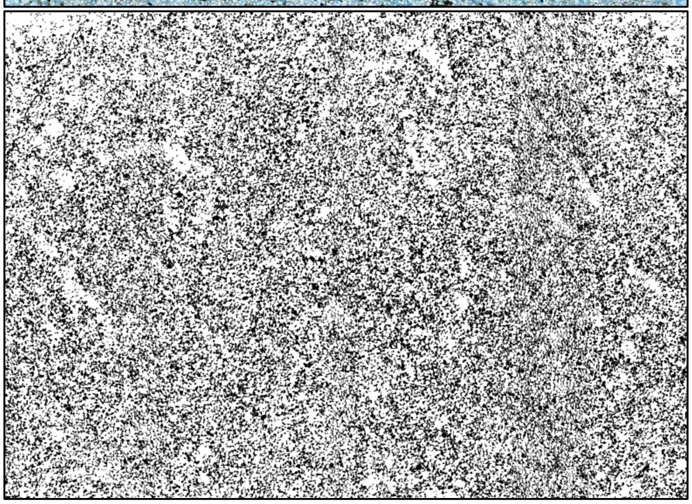

Pore Space, area%	Mean Pore Area, µm^2	Pore Area Range, µm^2	Mean Pore Perimeter, µm	Pore Perimeter Range, µm
31.8	3008	84–41,667	235	30–1180

This page intentionally left blank.

SAMPLE PHOTOGRAPH

PHYSICAL PROPERTIES

Porosity

Pycnometer Effective Porosity Average (range), vol%	Pycnometer Effective Porosity by MetaRock Laboratories, vol%	Thin-Section Point Count Porosity, % occurrence	Thin-Section Image Segmentation Pore Space, area%
25.7 (23.7–28.5)	NT	NT	27.6

Density

Bulk Volume, cm^3	Skeletal Density, g/cm^3
30.8	2.67

Residual Fluid Saturations

Residual Oil Saturation, %	Residual Water Saturation, %
13.2	29.3

Permeability

Permeability to Water, mD	Permeability to Air, mD
26	Pending

PHOTOMICROGRAPHS

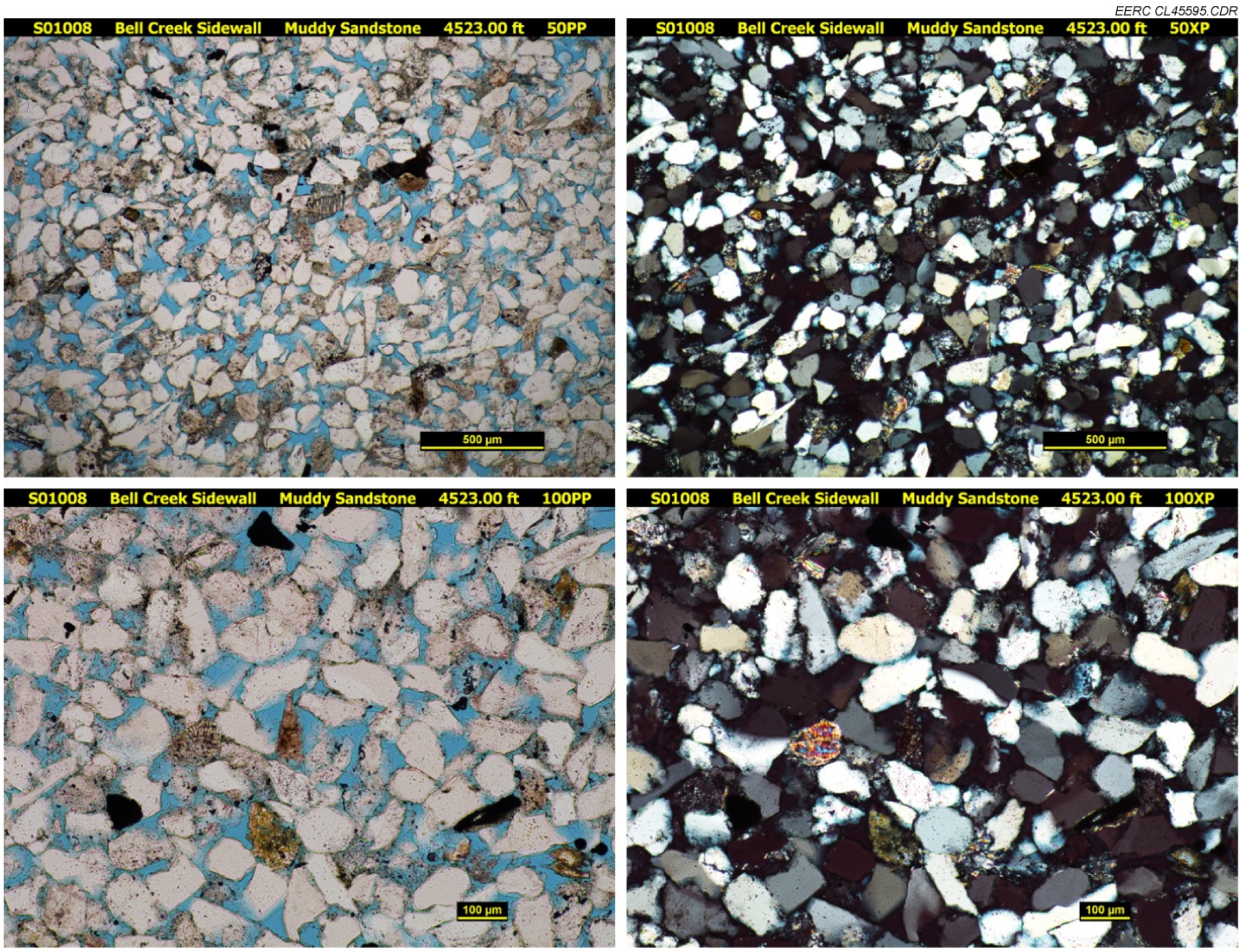

The sample collected at a 4523.00-ft depth is very fine to fine-grained, moderately well to well-sorted sandstone. Quartz grains are subangular to subrounded, displaying frequent monocrystalline and occasional polycrystalline grains. Both quartz and feldspar dissolution are observed, along with grain compaction and quartz overgrowth. Intergranular porosity is partially reduced by cement-coated grains and pore throats. Trace levels of muscovite, feldspars, rutile, and metals are witnessed. No fractures or fossilization are observed.

Applied Geology Laboratory		
Muddy Formation	Well Name: 05-06 OW	ID: S-01008
API No.: 25075224310000	Lithology: Sandstone	Depth: 4523.00'

THIN-SECTION PORE ANALYSIS BY DIGITAL IMAGE SEGMENTATION

Depth: 4523.00 ft; W = 24.22 mm; H = 14.04 mm

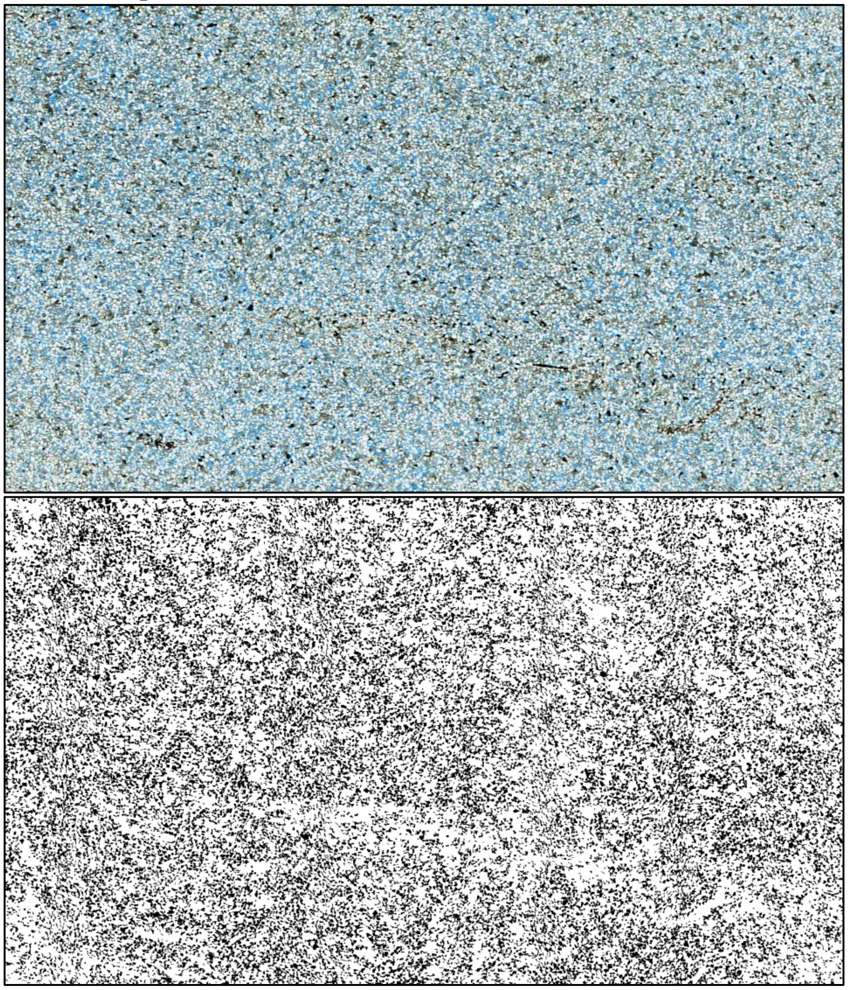

Pore Space, area%	Mean Pore Area, μm^2	Pore Area Range, μm^2	Mean Pore Perimeter, µm	Pore Perimeter Range, µm
27.6	2588	140–27,414	220	45–952

This page intentionally left blank.

Applied Geology Laboratory		
Muddy Formation	Well Name: 05-06 OW	ID: S-01009
API No.: 25075224310000	Lithology: Sandstone	Depth: 4523.25'

SAMPLE PHOTOGRAPH

PHYSICAL PROPERTIES

Porosity

Pycnometer Effective Porosity Average (range), vol%	Pycnometer Effective Porosity by MetaRock Laboratories, vol%	Thin-Section Point Count Porosity, % occurrence	Thin-Section Image Segmentation Pore Space, area%
23.1 (20.9–24.6)	NT	NT	16.2

Density

Bulk Volume, cm^3	Skeletal Density, g/cm^3
34.8	2.67

Residual Fluid Saturations

Residual Oil Saturation, %	Residual Water Saturation, %
11.1	33.6

Permeability

Permeability to Water, mD	Permeability to Air, mD
5.6	Pending

Applied Geology Laboratory		
Muddy Formation	Well Name: 05-06 OW	ID: S-01009
API No.: 25075224310000	Lithology: Sandstone	Depth: 4523.25'

PHOTOMICROGRAPHS

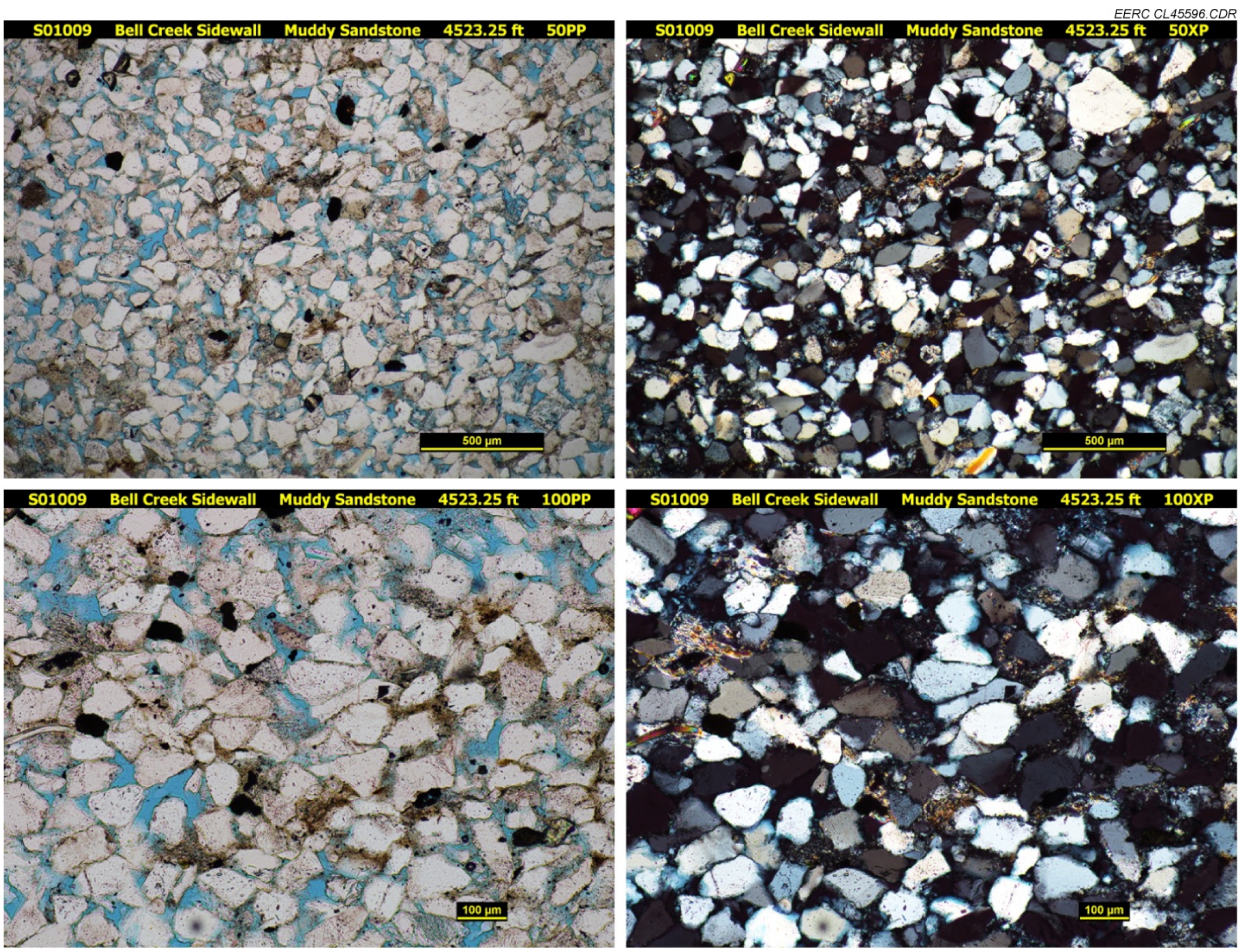

This sample collected at the 4523.25-ft depth is fine-grained, well-sorted sandstone. Quartz grains are predominantly subrounded, largely monocrystalline, and rarely polycrystalline. Original porosity is reduced by a combination of uneven cementation, composed mainly of clays, mild quartz overgrowths, and compaction of grains. Secondary porosity is produced by mineral (feldspar, clay, and siderite) dissolution. Slightly wavy thin laminations of clays, organics, and muscovite exist sporadically. Additional minerals present at trace levels are metals and rutile. No fractures or fossilization are observed.

THIN-SECTION PORE ANALYSIS BY DIGITAL IMAGE SEGMENTATION

Depth: 4523.25 ft; W = 26.03 mm; H = 15.52 mm

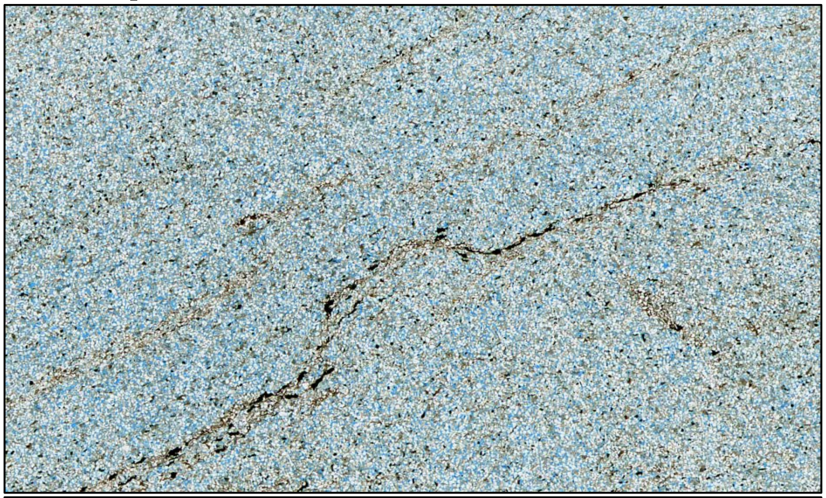

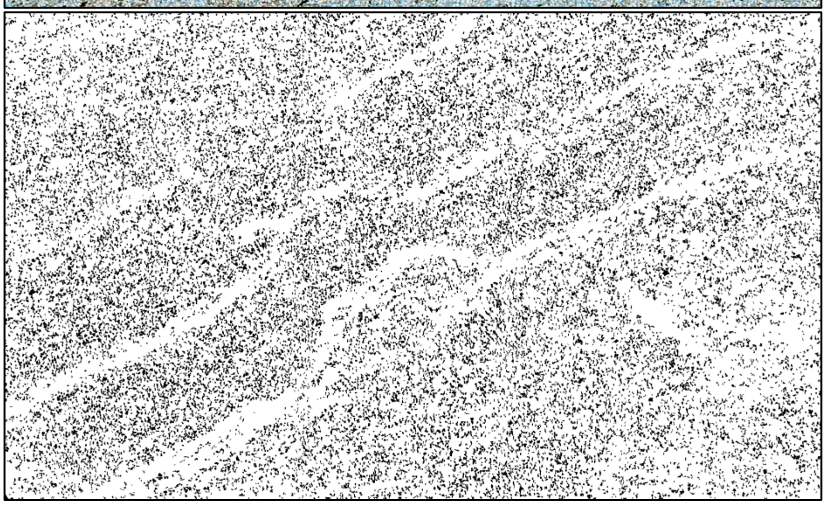

Pore Space, area%	Mean Pore Area, µm^2	Pore Area Range, µm^2	Mean Pore Perimeter, µm	Pore Perimeter Range, µm
16.2	2183	140–21,225	195	41–806

This page intentionally left blank.

	Applied Geology Laboratory		
	Muddy Formation	Well Name: 05-06 OW	ID: S-01010
	API No.: 25075224310000	Lithology: Sandstone	Depth: 4523.50'

SAMPLE PHOTOGRAPH

PHYSICAL PROPERTIES

Porosity

Pycnometer Effective Porosity Average (range), vol%	Pycnometer Effective Porosity by MetaRock Laboratories, vol%	Thin-Section Point Count Porosity, % occurrence	Thin-Section Image Segmentation Pore Space, area%
25.5 (24.0–27.0)	NT	NT	8.9

Density

Bulk Volume, cm^3	Skeletal Density, g/cm^3
30.8	2.67

Residual Fluid Saturations

Residual Oil Saturation, %	Residual Water Saturation, %
15.0	26.8

Permeability

Permeability to Water, mD	Permeability to Air, mD
22	Pending

Applied Geology Laboratory		
Muddy Formation	Well Name: 05-06 OW	ID: S-01010
API No.: 25075224310000	Lithology: Sandstone	Depth: 4523.50'

PHOTOMICROGRAPHS

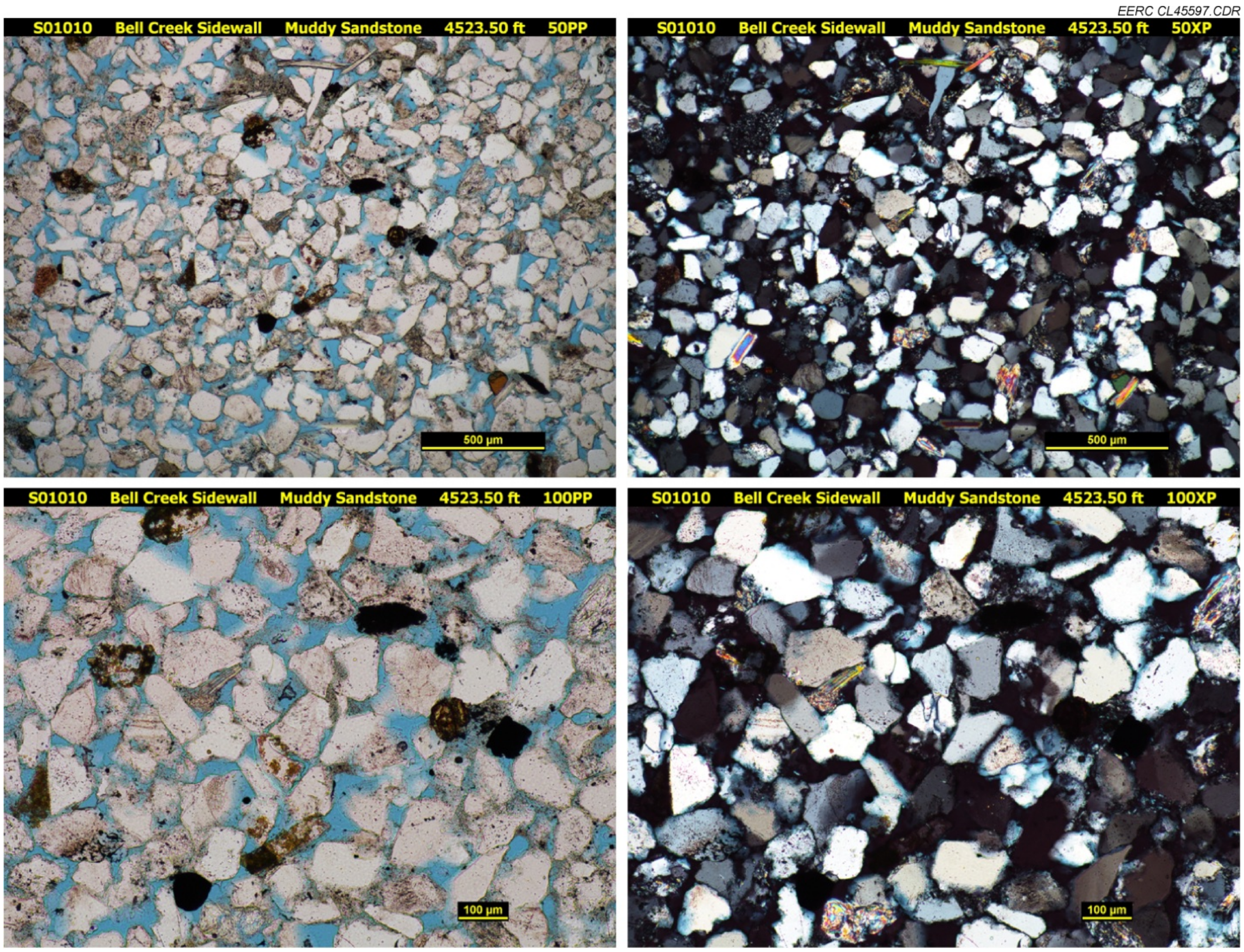

This sample collected at a 4523.50-ft depth is fine-grained, moderately well sorted, fairly clean sandstone. Quartz grains are subangular to subrounded, displaying commonly monocrystalline grains and occasional polycrystalline grains. Original porosity is intergranular. Observed cementation, quartz overgrowths, and compaction have reduced original porosity. Secondary porosity is produced by mineral/cement dissolution. A fracture is located within thin clay/organic laminations. Additional minerals found at trace levels are muscovite, feldspars, and metals. No fossils are observed.

THIN-SECTION PORE ANALYSIS BY DIGITAL IMAGE SEGMENTATION

Depth: 4523.50 ft; W = 11.39 mm; H = 7.88 mm

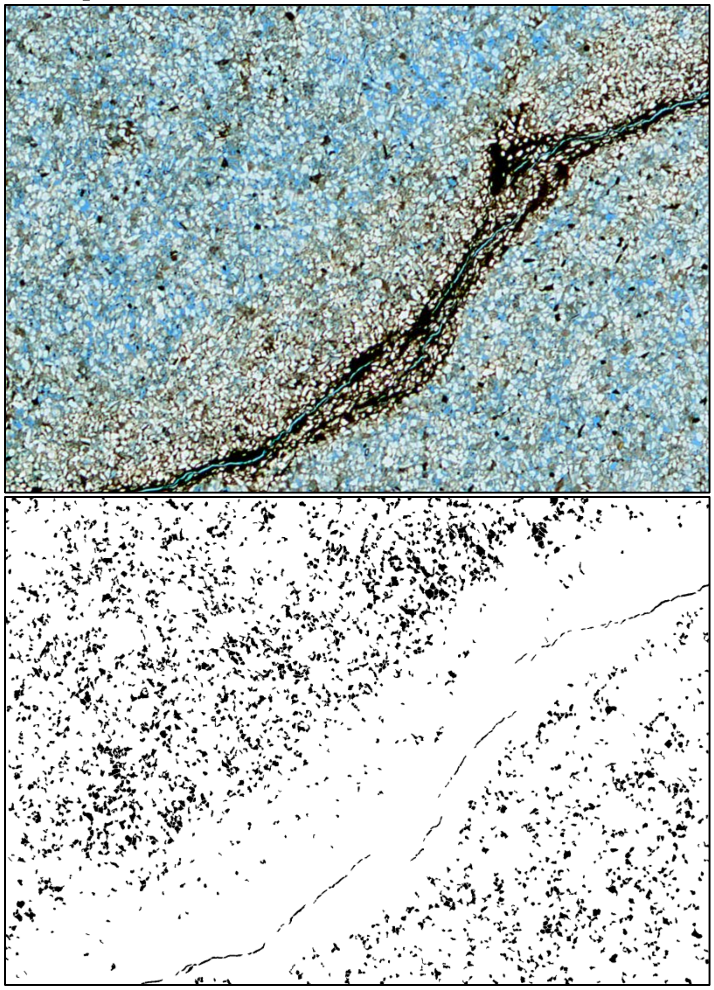

Pore Space, area%	Mean Pore Area, µm^2	Pore Area Range, µm^2	Mean Pore Perimeter, µm	Pore Perimeter Range, µm
8.9*	2294	252–18,761	195	51–857

* The pore space consists of a) pores: 8.7 area% and b) fractures: 0.2 area%.

This page intentionally left blank.

	Applied Geology Laboratory		
EERC / UND North Dakota	Muddy Formation	Well Name: 05-06 OW	ID: S-01011
	API No.: 25075224310000	Lithology: Sandstone	Depth: 4524.00'

SAMPLE PHOTOGRAPH

PHYSICAL PROPERTIES

Porosity

Pycnometer Effective Porosity Average (range), vol%	Pycnometer Effective Porosity by MetaRock Laboratories, vol%	Thin-Section Point Count Porosity, % occurrence	Thin-Section Image Segmentation Pore Space, area%
22.7 (19.4–25.0)	NT	NT	N/A

Density

Bulk Volume, cm^3	Skeletal Density, g/cm^3
27.0	2.58

Residual Fluid Saturations

Residual Oil Saturation, %	Residual Water Saturation, %
16.8	32.6

Permeability

Permeability to Water, mD	Permeability to Air, mD
19	Pending

PHOTOMICROGRAPHS

EERC CL45598.CDR

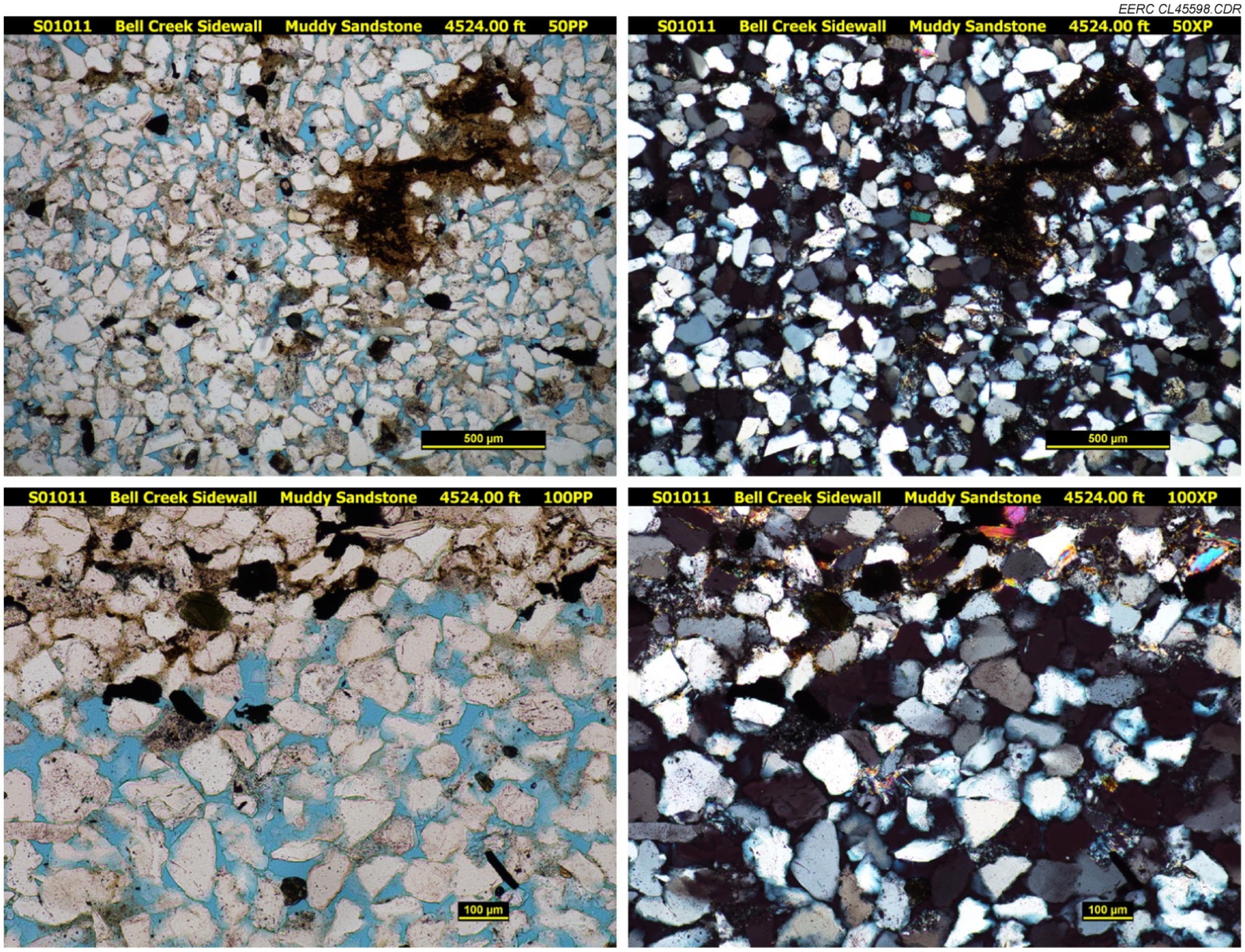

This sample collected at a 4524.00-ft depth is fine-grained, moderately well sorted, fairly clean, sandstone. Quartz grains are subangular to subrounded, with commonly monocrystalline grains and rare polycrystalline grains. Porosity is intergranular. Observed cementation, quartz overgrowths, and compaction have reduced original porosity. Secondary porosity is produced by mineral/cement dissolution. Remaining clay infill is zonally concentrated and within small laminations. Additional minerals found at trace levels are muscovite, feldspars, and metals. No fossils are observed.

	Applied Geology Laboratory		
	Muddy Formation	Well Name: 05-06 OW	ID: S-01012
	API No.: 25075224310000	Lithology: Sandstone	Depth: 4524.50'

SAMPLE PHOTOGRAPH

PHYSICAL PROPERTIES

Porosity

Pycnometer Effective Porosity Average (range), vol%	Pycnometer Effective Porosity by MetaRock Laboratories, vol%	Thin-Section Point Count Porosity, % occurrence	Thin-Section Image Segmentation Pore Space, area%
24.9 (22.7–26.6)	NT	NT	18.5

Density

Bulk Volume, cm^3	Skeletal Density, g/cm^3
31.6	2.67

Residual Fluid Saturations

Residual Oil Saturation, %	Residual Water Saturation, %
19.6	25.4

Permeability

Permeability to Water, mD	Permeability to Air, mD
23	Pending

	Applied Geology Laboratory		
	Muddy Formation	Well Name: 05-06 OW	ID: S-01012
	API No.: 25075224310000	Lithology: Sandstone	Depth: 4524.50'

PHOTOMICROGRAPHS

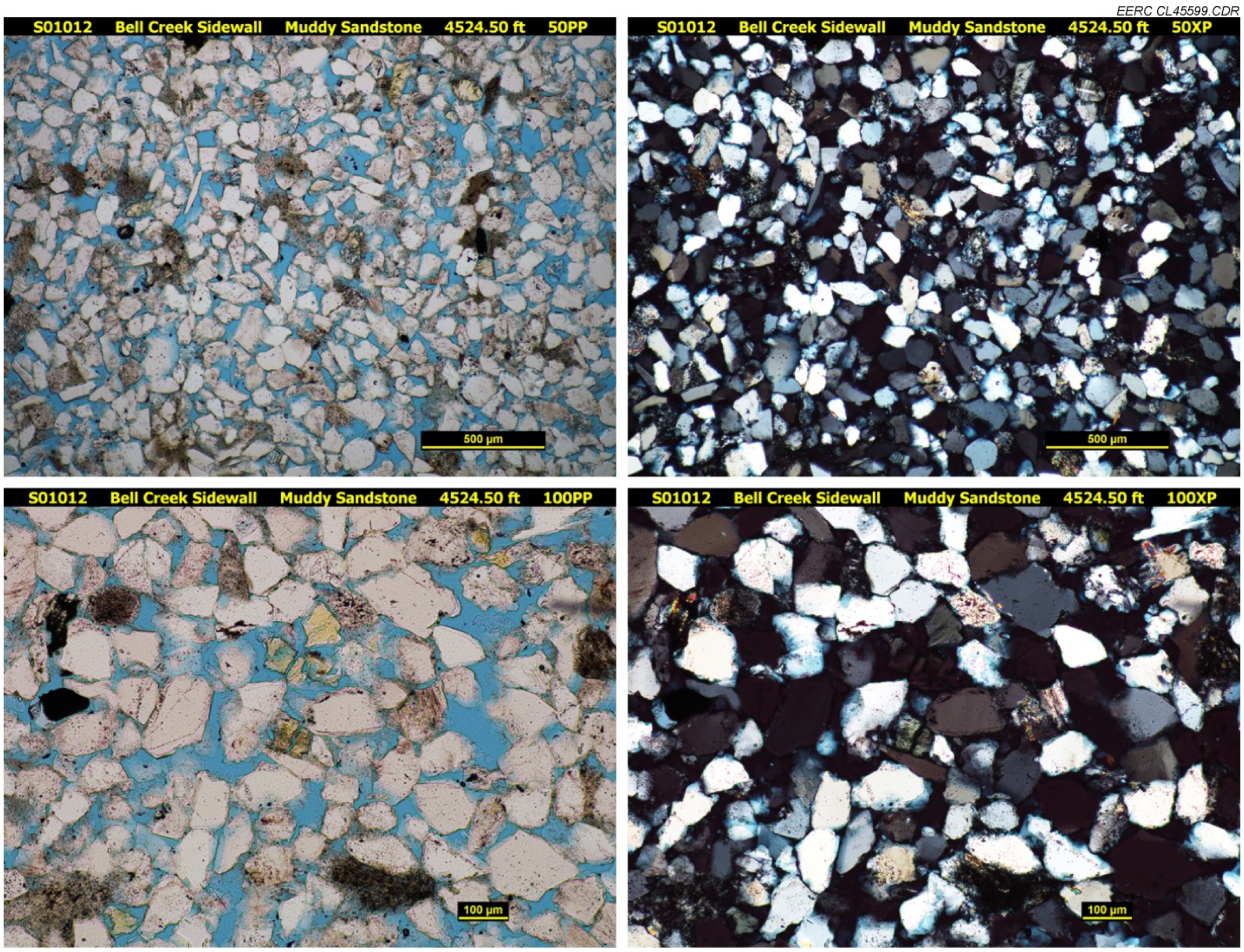

The sample collected at the 4524.50-ft depth is fine-grained, moderately well sorted, fairly clean sandstone. Quartz grains are angular to subangular, largely monocrystalline and rarely polycrystalline. Mild compaction, accumulation of cements, and quartz overgrowth have diminished original intergranular porosity. Secondary porosity has been created by feldspar and cement dissolution. Clays and organics are unevenly distributed; certain pores have been completely enclosed, others have been coated, and others appear unaltered. Trace levels of metals are observed. No fractures or fossils are observed.

THIN-SECTION PORE ANALYSIS BY DIGITAL IMAGE SEGMENTATION

Depth: 4524.50 ft; W = 27.71 mm; H = 13.76 mm

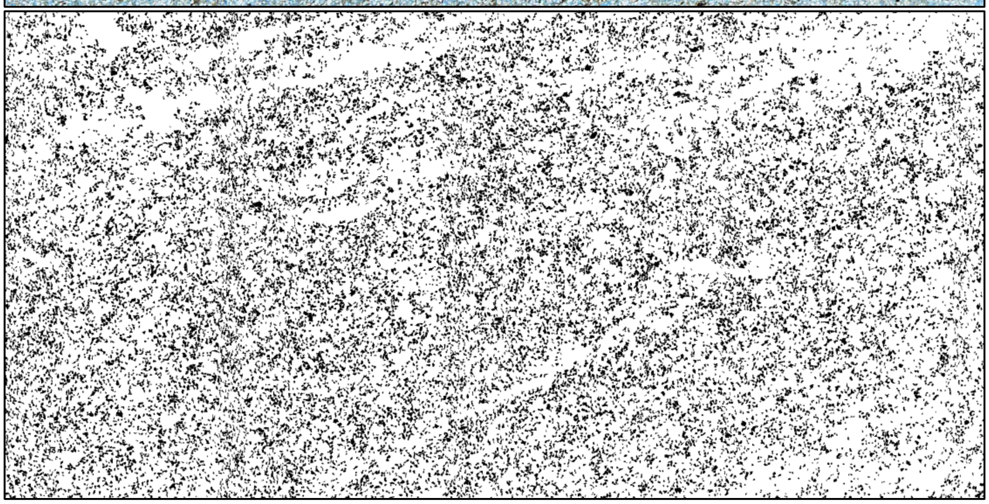

Pore Space, area%	Mean Pore Area, μm^2	Pore Area Range, μm^2	Mean Pore Perimeter, μm	Pore Perimeter Range, μm
18.5	2543	140–26,826	209	45–770

This page intentionally left blank.

Applied Geology Laboratory		
Muddy Formation	Well Name: 05-06 OW	ID: S-01013
API No.: 25075224310000	Lithology: Sandstone	Depth: 4525.00'

SAMPLE PHOTOGRAPH

PHYSICAL PROPERTIES

Porosity

Pycnometer Effective Porosity Average (range), vol%	Pycnometer Effective Porosity by MetaRock Laboratories, vol%	Thin-Section Point Count Porosity, % occurrence	Thin-Section Image Segmentation Pore Space, area%
18.3 (15.2–20.2)	NT	NT	29.5

Density

Bulk Volume, cm^3	Skeletal Density, g/cm^3
34.2	2.66

Residual Fluid Saturations

Residual Oil Saturation, %	Residual Water Saturation, %
9.8	33.4

Permeability

Permeability to Water, mD	Permeability to Air, mD
5.5	Pending

PHOTOMICROGRAPHS

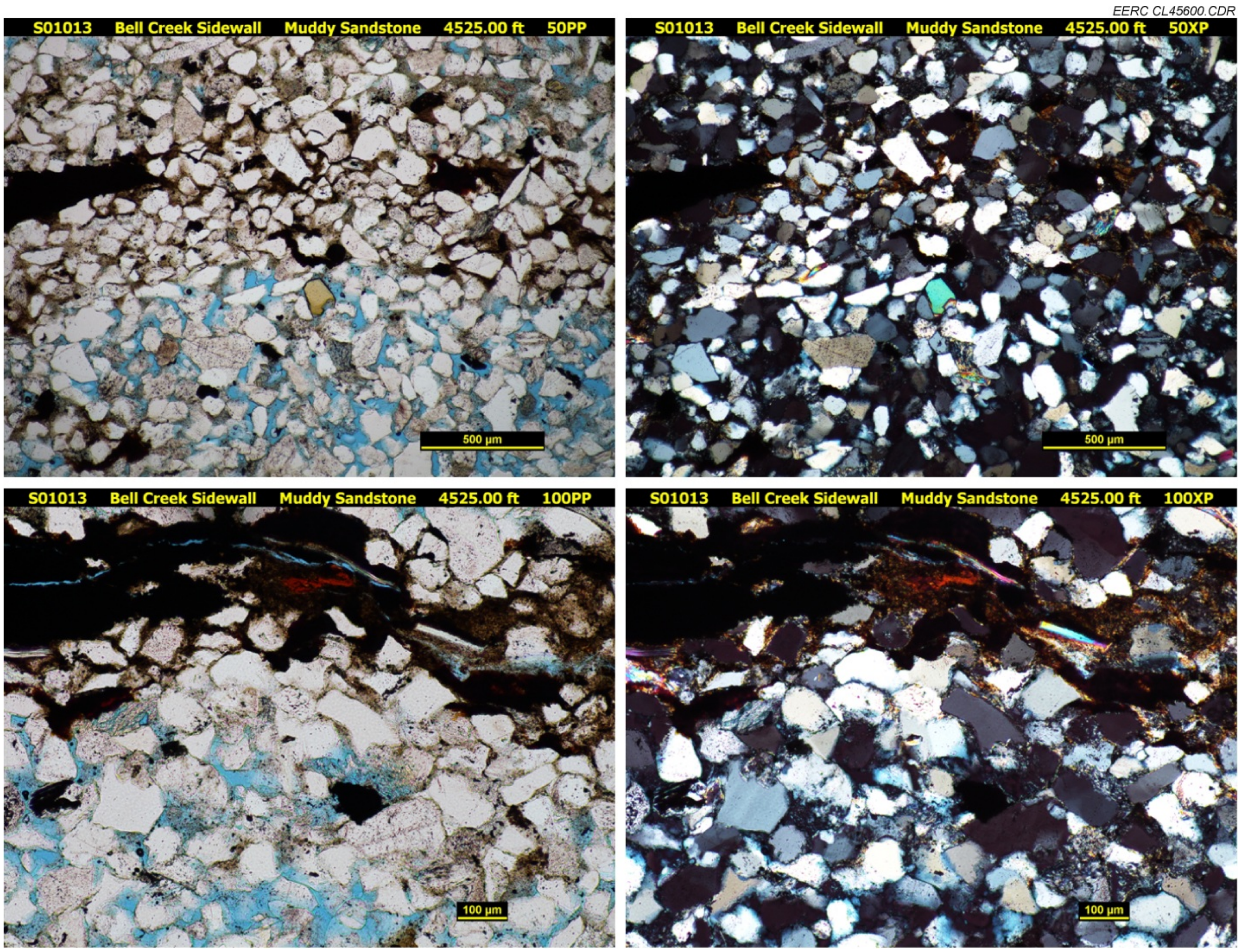

The sample collected at the 4525.00-ft depth is fine- to medium-grained, moderately sorted sandstone. Quartz grains are angular to subangular, displaying mostly monocrystalline grains with some polycrystalline grains. Observed cementation, quartz overgrowths, and compaction have reduced original porosity. Secondary porosity is produced by mineral/cement dissolution. A fracture is located within thin clay/organic laminations. Additional minerals found at trace levels are muscovite, feldspars, and metals. No fossils are observed.

THIN-SECTION PORE ANALYSIS BY DIGITAL IMAGE SEGMENTATION

Depth: 4525.00 ft; W = 19.99 mm; H = 18.34 mm

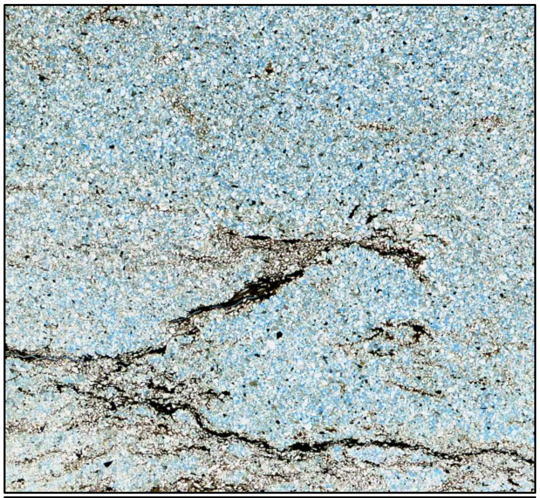

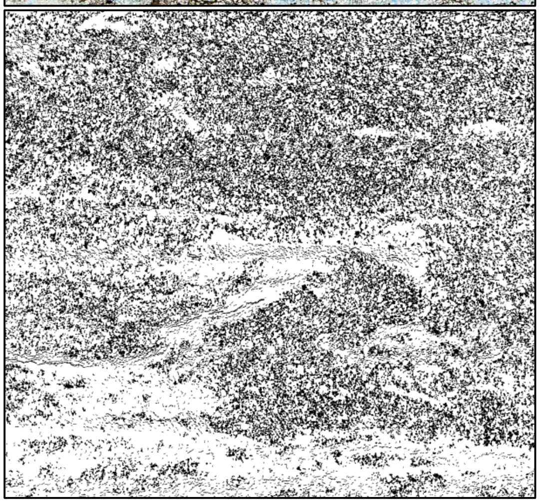

Pore Space, area%	Mean Pore Area, µm^2	Pore Area Range, µm^2	Mean Pore Perimeter, µm	Pore Perimeter Range, µm
29.5	2797	84–37,914	226	30–1239

This page intentionally left blank.

SAMPLE PHOTOGRAPH

PHYSICAL PROPERTIES

Porosity

Pycnometer Effective Porosity Average (range), vol%	Pycnometer Effective Porosity by MetaRock Laboratories, vol%	Thin-Section Point Count Porosity, % occurrence	Thin-Section Image Segmentation Pore Space, area%
24.5 (21.8–26.6)	NT	NT	16.8

Density

Bulk Volume, cm^3	Skeletal Density, g/cm^3
34.8	2.61

Residual Fluid Saturations

Residual Oil Saturation, %	Residual Water Saturation, %
15.9	34.1

Permeability

Permeability to Water, mD	Permeability to Air, mD
74	Pending

PHOTOMICROGRAPHS

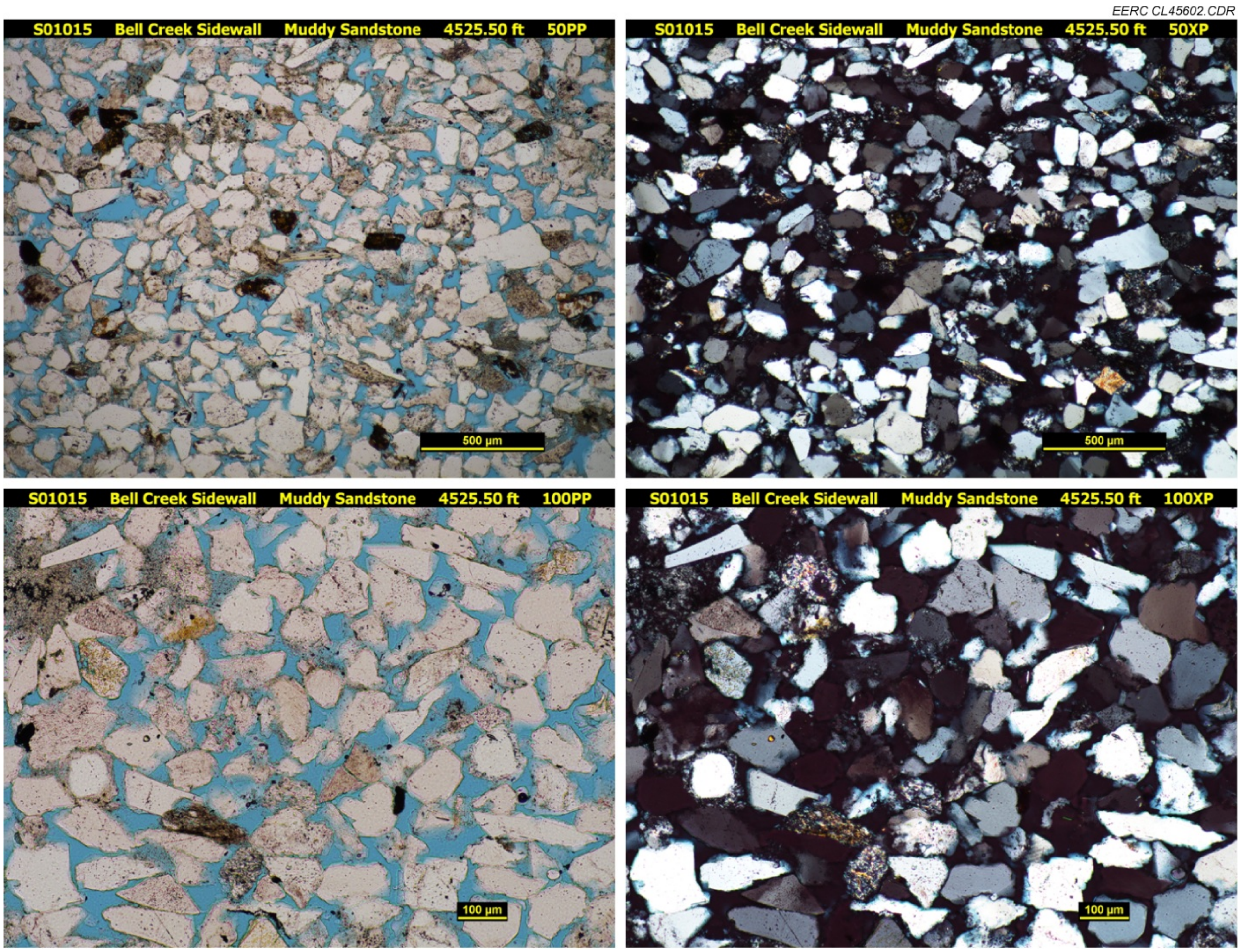

The sample collected at a 4525.50-ft depth is moderately well sorted, fine-grained sandstone. Quartz grains are subangular, frequently monocrystalline grains with sporadic polycrystalline grains. Original intergranular porosity is diminished by compaction, small quartz overgrowths, and uneven clay filling. Trace levels of feldspars, siderite, muscovite, and metals are observed. No fractures or fossils are seen.

THIN-SECTION PORE ANALYSIS BY DIGITAL IMAGE SEGMENTATION

Depth: 4525.50 ft; W = 22.74 mm; H = 14.62 mm

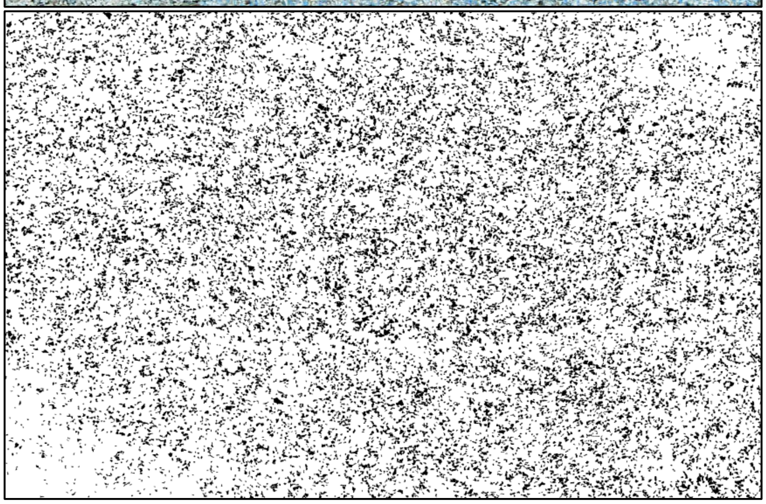

Pore Space, area%	Mean Pore Area, µm^2	Pore Area Range, µm^2	Mean Pore Perimeter, µm	Pore Perimeter Range, µm
16.8	2656	140–28,842	213	45–852

This page intentionally left blank.

SAMPLE PHOTOGRAPH

PHYSICAL PROPERTIES

Porosity

Pycnometer Effective Porosity Average (range), vol%	Pycnometer Effective Porosity by MetaRock Laboratories, vol%	Thin-Section Point Count Porosity, % occurrence	Thin-Section Image Segmentation Pore Space, area%
27.0 (25.3–28.8)	NT	NT	14.2

Density

Bulk Volume, cm^3	Skeletal Density, g/cm^3
38.3	2.66

Residual Fluid Saturations

Residual Oil Saturation, %	Residual Water Saturation, %
13.3	33.0

Permeability

Permeability to Water, mD	Permeability to Air, mD
28	Pending

PHOTOMICROGRAPHS

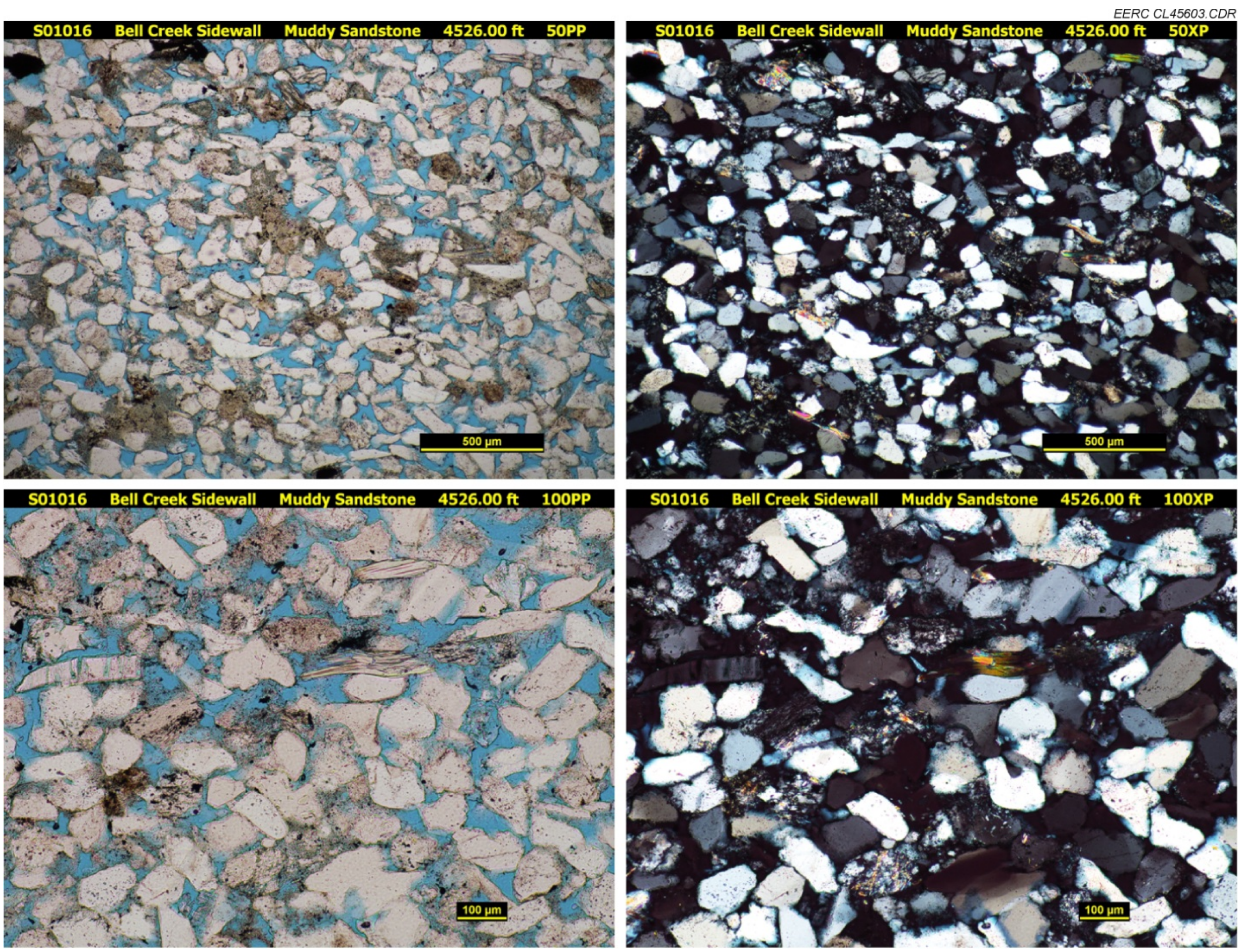

The sample collected at the 4526.00-ft depth is moderately well sorted, fine-grained sandstone. Quartz grains are characterized as subangular, largely monocrystalline grains with occasional polycrystalline grains. Original intergranular porosity is diminished by compaction, small quartz overgrowths, and uneven clay filling. Trace levels of feldspars, siderite, muscovite, and metals are observed. No fractures or fossils are seen.

THIN-SECTION PORE ANALYSIS BY DIGITAL IMAGE SEGMENTATION

Depth: 4526.00 ft; W = 21.54 mm; H = 14.00 mm

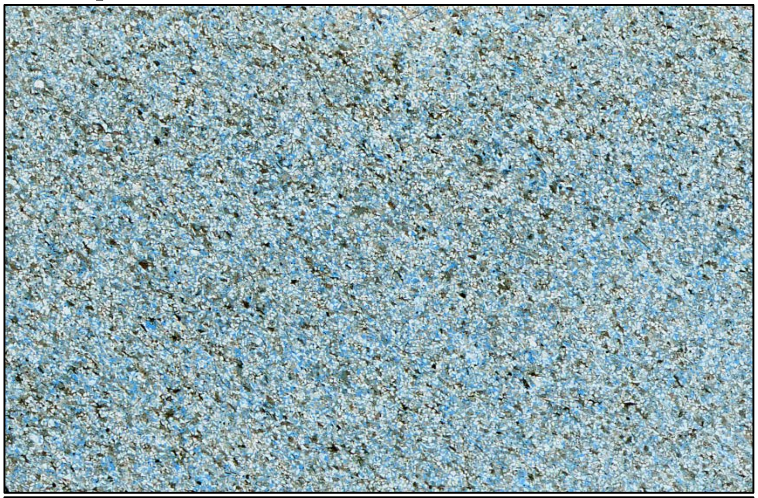

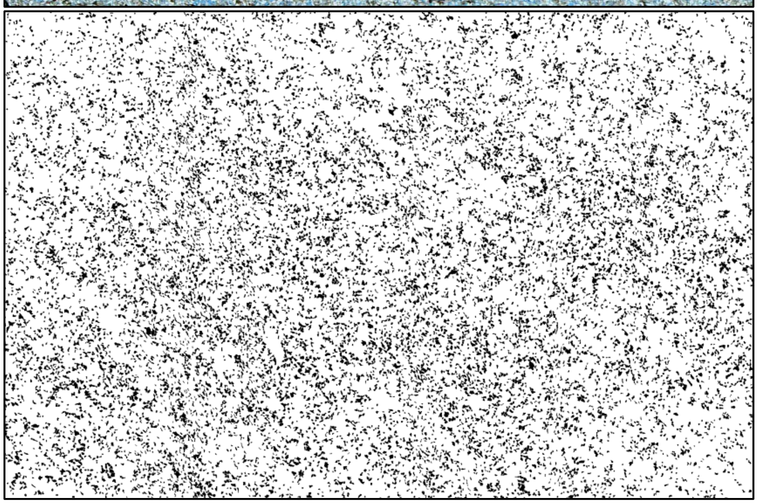

Pore Space, area%	Mean Pore Area, µm²	Pore Area Range, µm²	Mean Pore Perimeter, µm	Pore Perimeter Range, µm
14.2	2441	196–23,942	204	51–873

This page intentionally left blank.

	Applied Geology Laboratory		
EERC / UND University of North Dakota	Muddy Formation	Well Name: 05-06 OW	ID: S-01017
	API No.: 25075224310000	Lithology: Sandstone	Depth: 4526.50'

SAMPLE PHOTOGRAPH

PHYSICAL PROPERTIES

Porosity

Pycnometer Effective Porosity Average (range), vol%	Pycnometer Effective Porosity by MetaRock Laboratories, vol%	Thin-Section Point Count Porosity, % occurrence	Thin-Section Image Segmentation Pore Space, area%
23.7 (21.4–25.7)	NT	NT	20.5

Density

Bulk Volume, cm^3	Skeletal Density, g/cm^3
36.3	2.59

Residual Fluid Saturations

Residual Oil Saturation, %	Residual Water Saturation, %
17.5	29.1

Permeability

Permeability to Water, mD	Permeability to Air, mD
12	Pending

PHOTOMICROGRAPHS

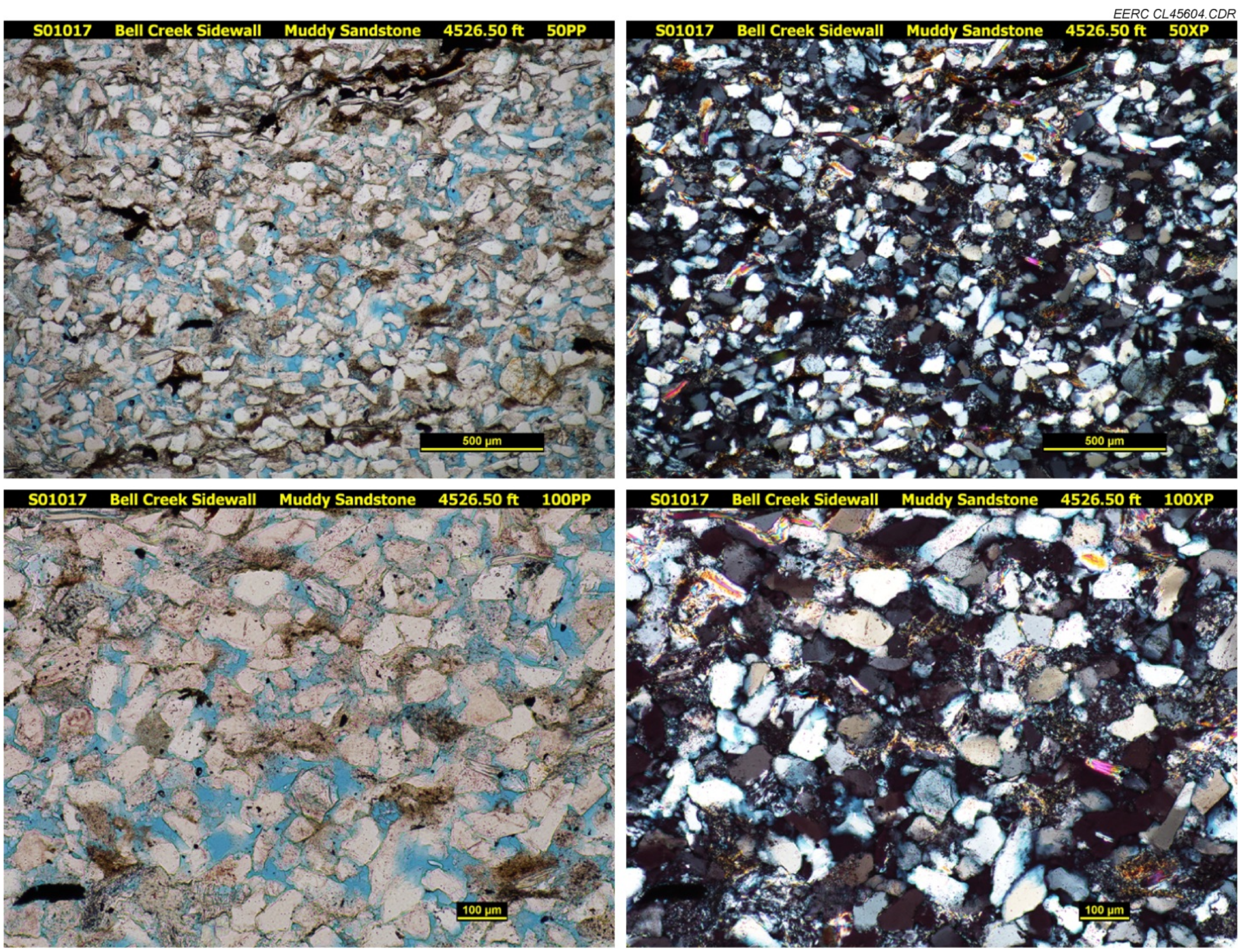

The sample collected at the 4526.50-ft depth is fine- to medium-grained, moderately sorted sandstone. Quartz grains are subangular, largely monocrystalline grains with occasional polycrystalline grains. Observed cementation, quartz overgrowths, and compaction have reduced original intergranular porosity. Secondary porosity is produced by mineral/cement dissolution. Trace levels of feldspars, siderite, muscovite, and metals are observed. No fractures or fossils are seen.

THIN-SECTION PORE ANALYSIS BY DIGITAL IMAGE SEGMENTATION

Depth: 4526.5 ft; W = 16.62 mm; H = 15.62 mm

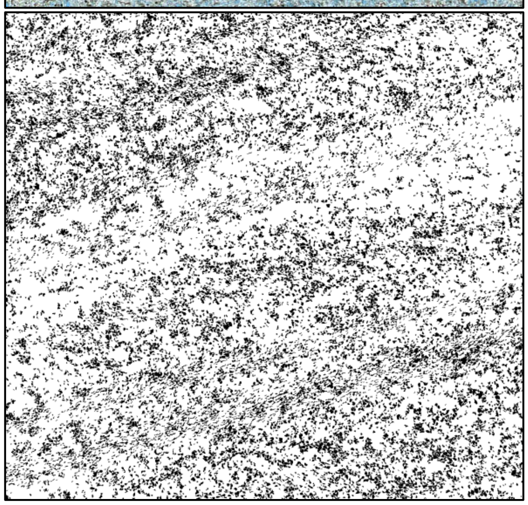

Pore Space, area%	Mean Pore Area, µm^2	Pore Area Range, µm^2	Mean Pore Perimeter, µm	Pore Perimeter Range, µm
20.5	2347	56–31,698	210	26–1225

This page intentionally left blank.

Applied Geology Laboratory		
Muddy Formation	Well Name: 05-06 OW	ID: S-01018
API No.: 25075224310000	Lithology: Sandstone	Depth: 4527.00'

SAMPLE PHOTOGRAPH

PHYSICAL PROPERTIES

Porosity

Pycnometer Effective Porosity Average (range), vol%	Pycnometer Effective Porosity by MetaRock Laboratories, vol%	Thin-Section Point Count Porosity, % occurrence	Thin-Section Image Segmentation Pore Space, area%
N/A	N/A	NT	10.2

Density

Bulk Volume, cm^3	Skeletal Density, g/cm^3
N/A	N/A

Residual Fluid Saturations

Residual Oil Saturation, %	Residual Water Saturation, %
N/A	N/A

Permeability

Permeability to Water, mD	Permeability to Air, mD
N/A	N/A

PHOTOMICROGRAPHS

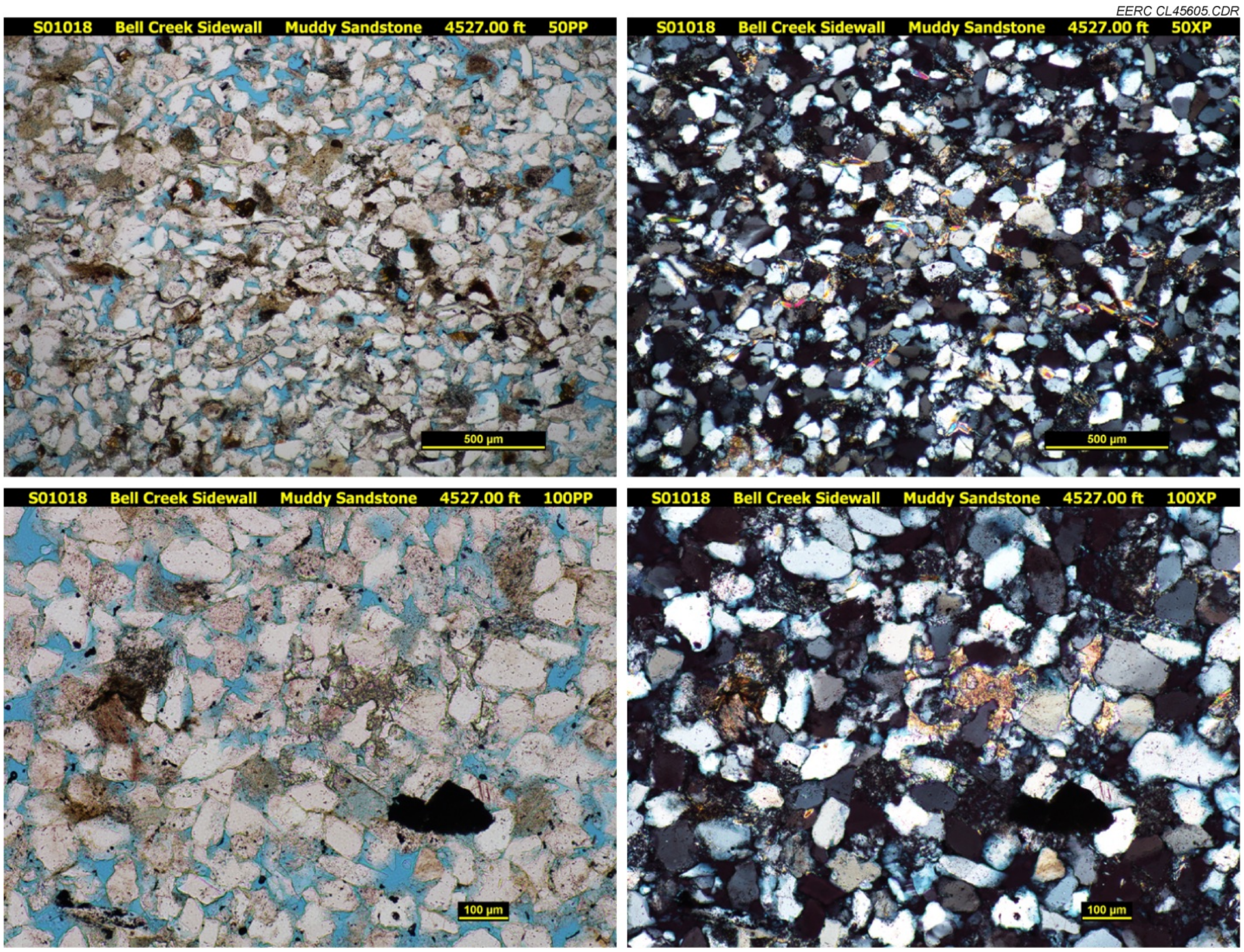

The sample collected at a 4527.00-ft depth is fine-grained, moderately well sorted sandstone. Quartz grains are angular to subangular, predominately monocrystalline grains with rare polycrystalline grains. Porosity is intergranular and is a result of cement (clay, carbonate, and silica based) and mineral (largely feldspars) dissolution. Compaction, quartz overgrowth, and higher amounts of muscovite are observed. Additional components found at trace levels are siderite, metals, and organics. No fractures or fossils are seen.

THIN-SECTION PORE ANALYSIS BY DIGITAL IMAGE SEGMENTATION

Depth: 4527.00 ft; W = 21.16 mm; H = 16.10 mm

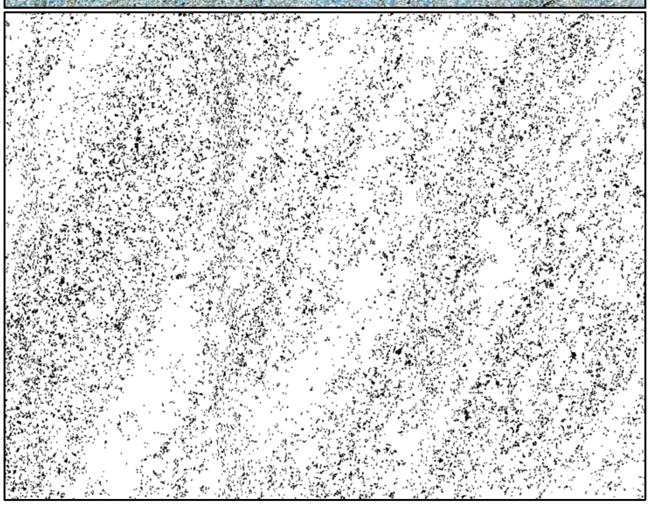

Pore Space, area%	Mean Pore Area, µm^2	Pore Area Range, µm^2	Mean Pore Perimeter, µm	Pore Perimeter Range, µm
10.2	1964	140–25,902	184	45–813

This page intentionally left blank.

SAMPLE PHOTOGRAPH

PHYSICAL PROPERTIES

Porosity

Pycnometer Effective Porosity Average (range), vol%	Pycnometer Effective Porosity by MetaRock Laboratories, vol%	Thin-Section Point Count Porosity, % occurrence	Thin-Section Image Segmentation Pore Space, area%
13.5 (10.3–15.9)	13.5	NT	8.0

Density

Bulk Volume, cm^3	Skeletal Density, g/cm^3
30.0	2.63

Residual Fluid Saturations

Residual Oil Saturation, %	Residual Water Saturation, %
14.2	31.9

Permeability

Permeability to Water, mD	Permeability to Air, mD
0.70	Pending

PHOTOMICROGRAPHS

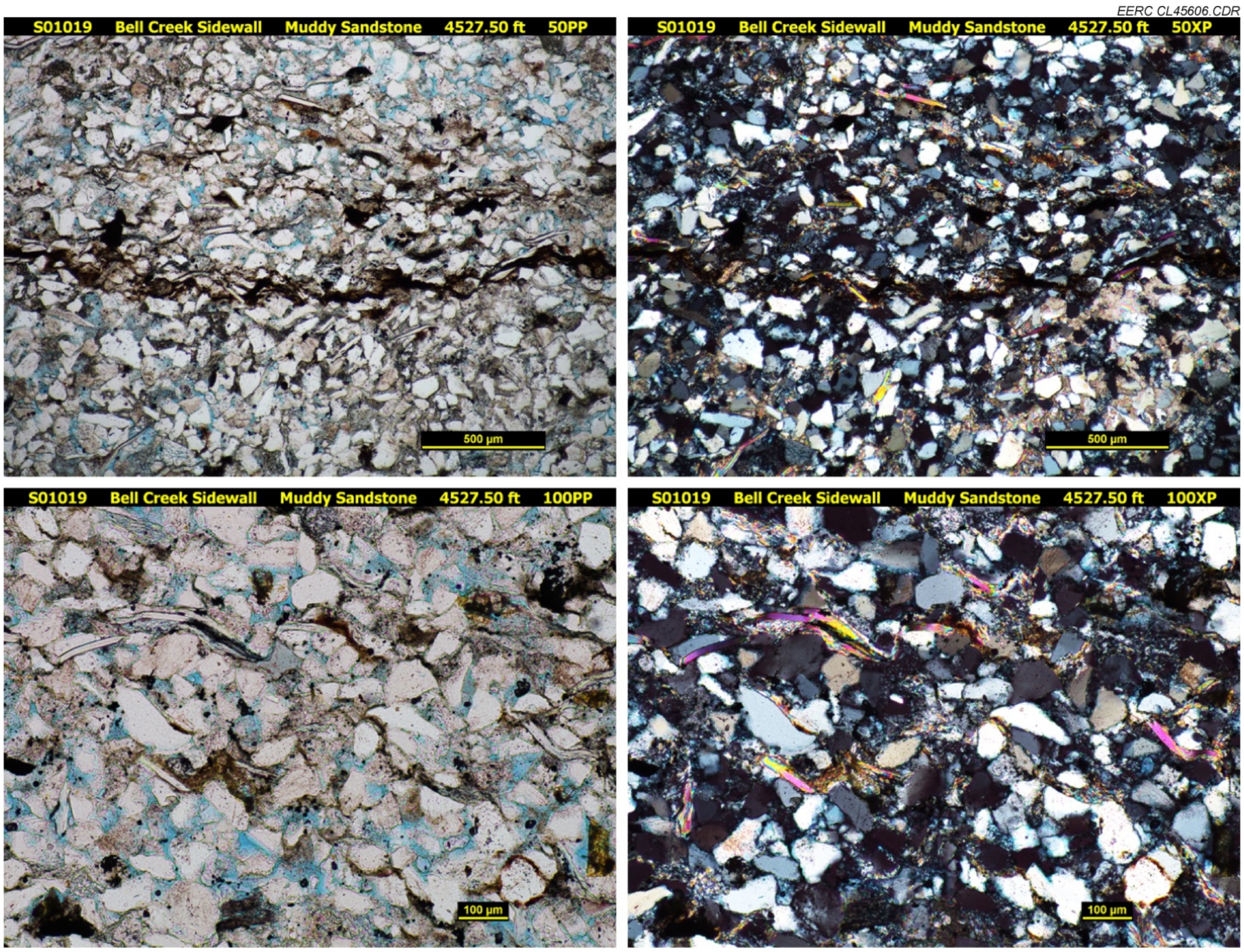

The sample collected at the 4527.50-ft depth is fine-grained, moderately sorted sandstone. Weak bedding planes are observed and the sample is grain-supported and well cemented throughout most of the sample. Quartz grains are angular to subangular, frequently monocrystalline grains with a fair amount of polycrystalline grains. Much of the intergranular porosity has been reduced by carbonate-, clay-, and silica-based cements. Mild compaction is evidenced by the warping and breaking of muscovite grains (found in higher concentration). A small extent of additional porosity-reducing characteristics, such as quartz overgrowth and mineral dissolution, are observed. No fractures or fossils are noted.

THIN-SECTION PORE ANALYSIS BY DIGITAL IMAGE SEGMENTATION

Depth: 4527.50 ft; W = 27.04 mm; H = 16.00 mm

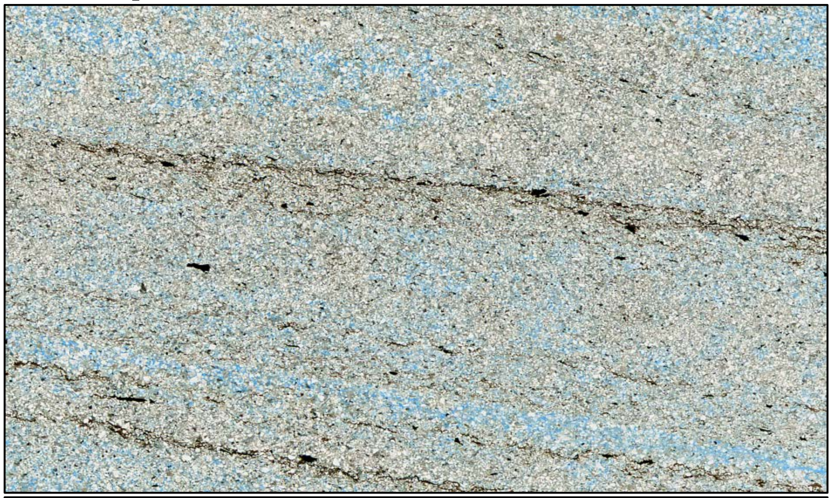

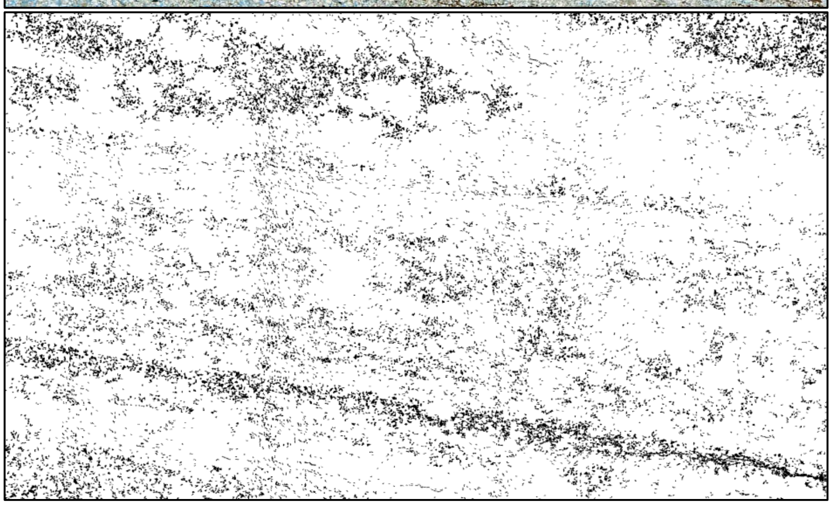

Pore Space, area%	Mean Pore Area, μm^2	Pore Area Range, μm^2	Mean Pore Perimeter, μm	Pore Perimeter Range, μm
8.0	1810	140–29,178	178	45–992

This page intentionally left blank.

SAMPLE PHOTOGRAPH

PHYSICAL PROPERTIES

Porosity

Pycnometer Effective Porosity Average (range), vol%	Pycnometer Effective Porosity by MetaRock Laboratories, vol%	Thin-Section Point Count Porosity, % occurrence	Thin-Section Image Segmentation Pore Space, area%
15.9 (14.7–16.7)	14.9	NT	11.4*

* Pore space across entire slide. The slide consists of a porous side and a tight side, with the pore space measured as 13.7 and 0.04 area%, respectively, for sections of each side analyzed individually.

Density

Bulk Volume, cm^3	Skeletal Density, g/cm^3
41.2	2.65

Residual Fluid Saturations

Residual Oil Saturation, %	Residual Water Saturation, %
18.5	30.6

Permeability

Permeability to Water, mD	Permeability to Air, mD
87	Pending

PHOTOMICROGRAPHS

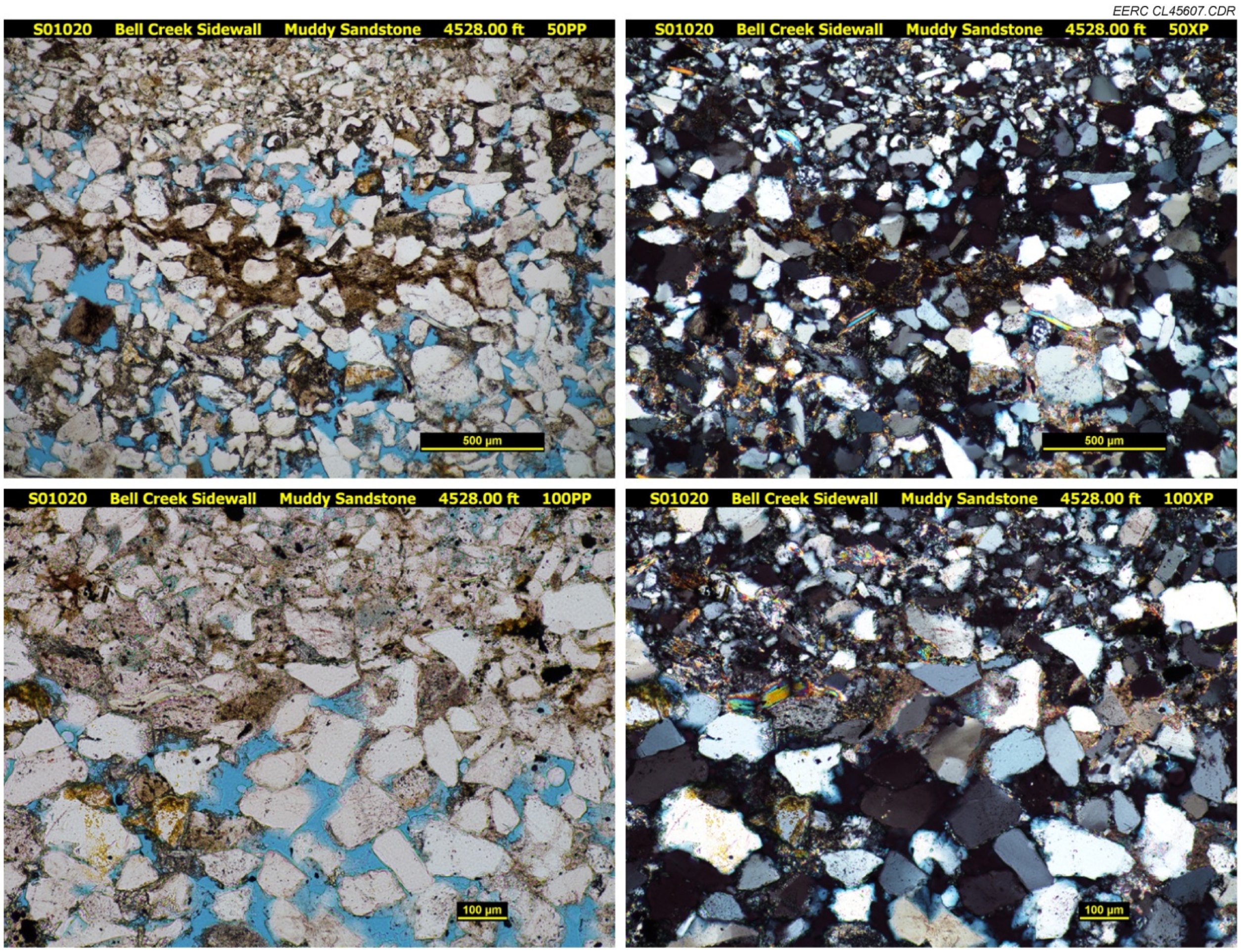

The sample collected at a 4528.00-ft depth displays a contact boundary. The first lithofacie is consistent with the previous sample (S-01019, 4527.50 ft). It is fine-grained, moderately sorted, cemented sandstone. Quartz grains are angular to subangular, predominately monocrystalline grains with sporadic polycrystalline grains. Much of the intergranular porosity has been reduced by carbonate-, clay-, and silica-based cements. Across the boundary, quartz grains (angular to subangular) double in size and the presence of silica-, clay-, and carbonate-based cements are substantially less; thus, there is substantially more intergranular porosity. Each lithofacie is mineralogically similar: quartz-dominated with silica, carbonate, and clay cements along with traces of muscovite, metals, and feldspars. No fossils or fractures are observed in either.

THIN-SECTION PORE ANALYSIS BY DIGITAL IMAGE SEGMENTATION

Across the Whole Slide

Depth: 4528.00 ft; W = 23.26 mm; H = 15.62 mm

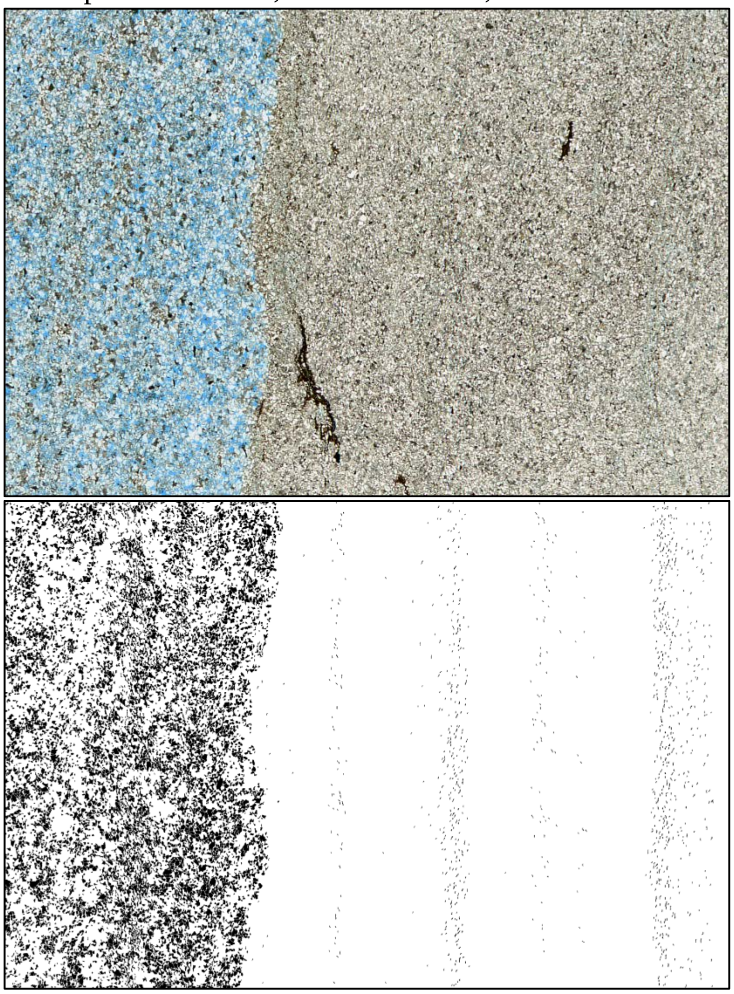

Pore Space, area%	Mean Pore Area, μm^2	Pore Area Range, μm^2	Mean Pore Perimeter, µm	Pore Perimeter Range, µm
11.4	2849	168–21,533	223	48–904

Portion of Porous Side of Slide

Depth: 4528.00 ft; W = 11.70 mm; H = 11.23 mm

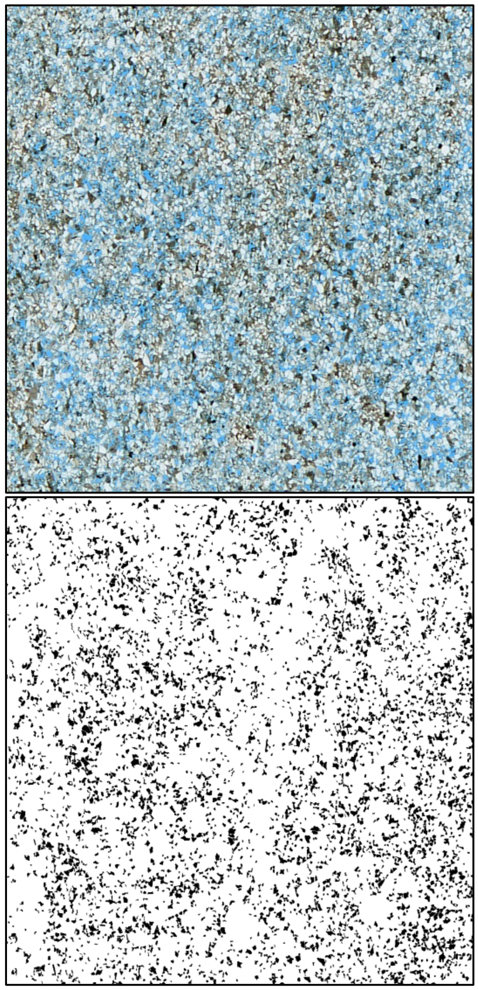

Pore Space, area%	Mean Pore Area, µm^2	Pore Area Range, µm^2	Mean Pore Perimeter, µm	Pore Perimeter Range, µm
13.7	3233	140–49,591	239	45–1304

Portion of Tight Side of Slide

Depth: 4528.00 ft; W = 17.24 mm; H = 11.56 mm

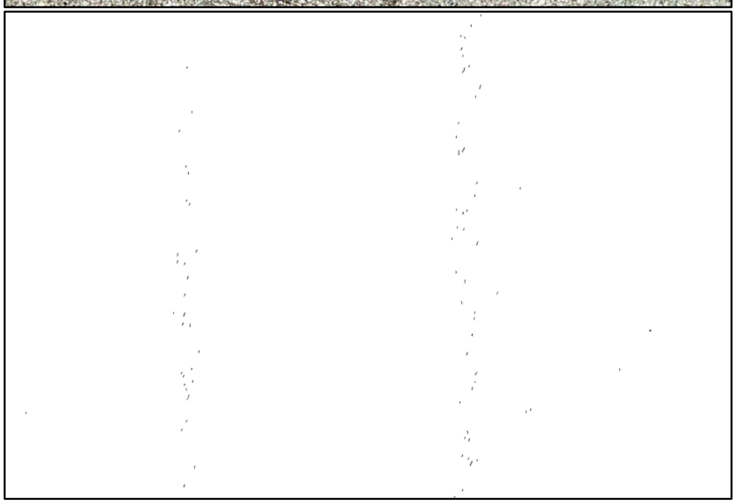

Pore Space, area%	Mean Pore Area, µm^2	Pore Area Range, µm^2	Mean Pore Perimeter, µm	Pore Perimeter Range, µm
0.04	749	420–1708	14	104–295

This page intentionally left blank.

EERC / UND University of North Dakota	**Applied Geology Laboratory**		
	Muddy Formation	Well Name: 05-06 OW	ID: S-01021
	API No.: 25075224310000	Lithology: Sandstone	Depth: 4528.50'

SAMPLE PHOTOGRAPH

PHYSICAL PROPERTIES

Porosity

Pycnometer Effective Porosity Average (range), vol%	Pycnometer Effective Porosity by MetaRock Laboratories, vol%	Thin-Section Point Count Porosity, % occurrence	Thin-Section Image Segmentation Pore Space, area%
N/A	N/A	NT	0.02

Density

Bulk Volume, cm^3	Skeletal Density, g/cm^3
N/A	N/A

Residual Fluid Saturations

Residual Oil Saturation, %	Residual Water Saturation, %
N/A	N/A

Permeability

Permeability to Water, mD	Permeability to Air, mD
N/A	N/A

PHOTOMICROGRAPHS

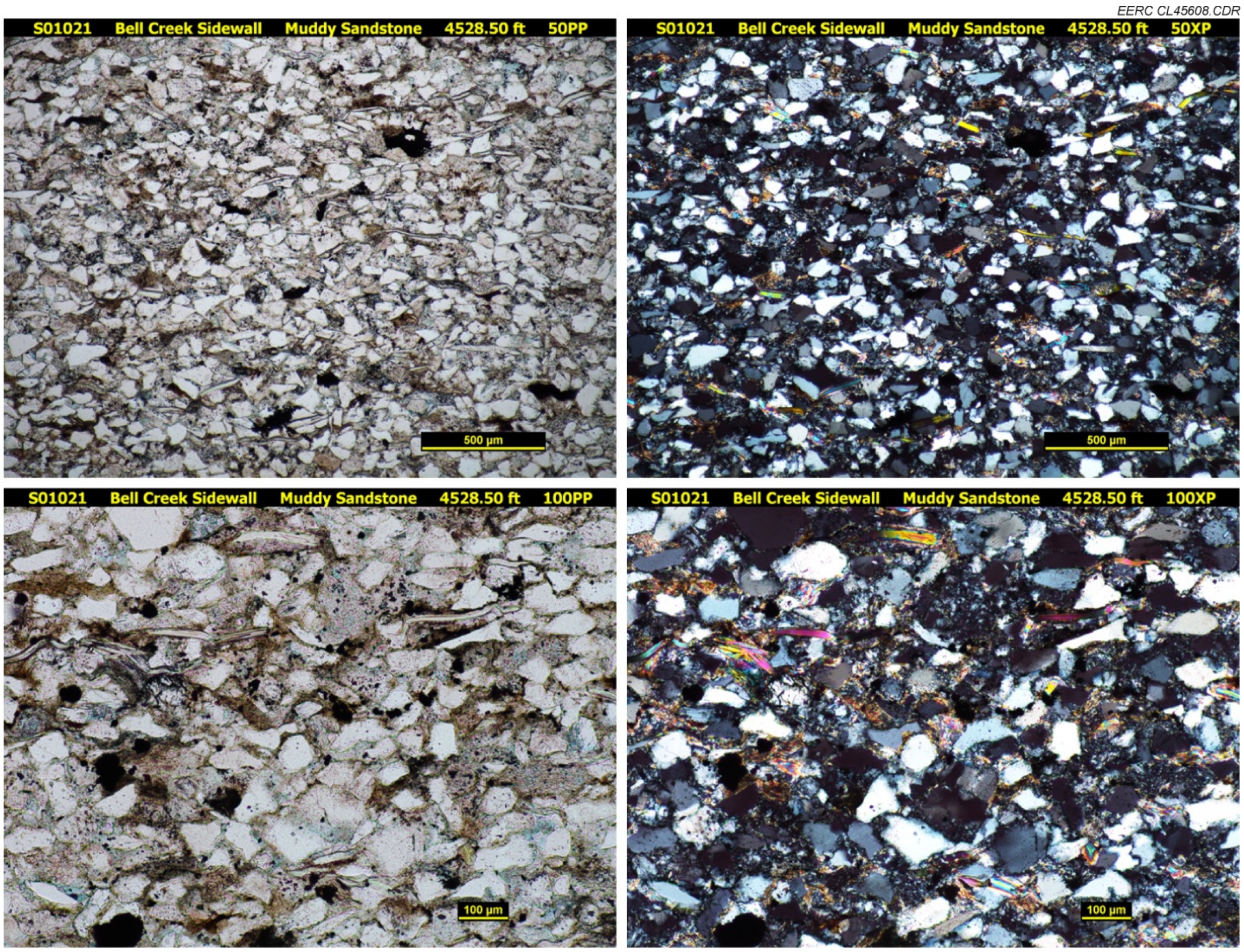

The sample collected at a 4528.50-ft depth represents tight, fine-grained sandstone. Quartz grains are moderately well sorted, angular to subangular, with occasional monocrystalline and some polycrystalline grains. Carbonate, silica, and clay cementation is significant, allowing for no observed porosity. Very mild compaction is evidenced by the bending of muscovite grains (found in higher concentration). Higher globular concentrations of metals (likely pyrite) exist throughout the sample. No fractures or fossils are noted.

THIN-SECTION PORE ANALYSIS BY DIGITAL IMAGE SEGMENTATION

Depth: 4528.50 ft; W = 23.22 mm; H = 14.76 mm

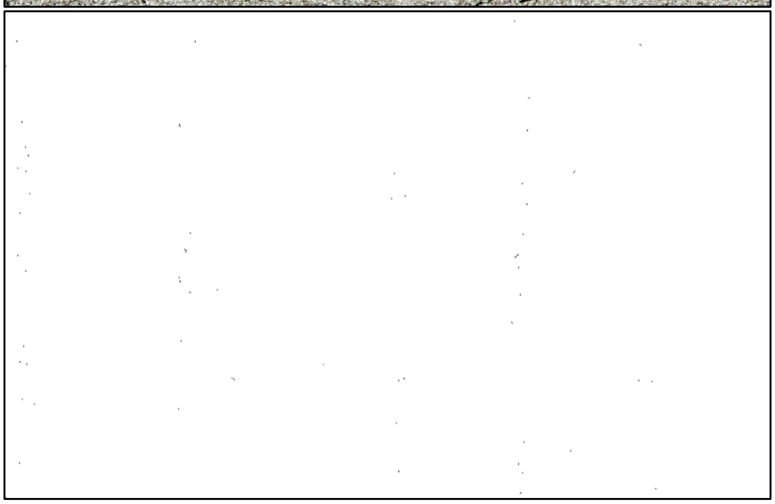

Pore Space, area%	Mean Pore Area, µm^2	Pore Area Range, µm^2	Mean Pore Perimeter, µm	Pore Perimeter Range, µm
0.02	811	364–1792	128	75–241

This page intentionally left blank.

	Applied Geology Laboratory		
	Muddy Formation	Well Name: 05-06 OW	ID: S-01022
	API No.: 25075224310000	Lithology: Sandstone	Depth: 4529.50'

SAMPLE PHOTOGRAPH

PHYSICAL PROPERTIES

Porosity

Pycnometer Effective Porosity Average (range), vol%	Pycnometer Effective Porosity by MetaRock Laboratories, vol%	Thin-Section Point Count Porosity, % occurrence	Thin-Section Image Segmentation Pore Space, area%
22.1 (19.5–24.3)	NT	NT	13.6

Density

Bulk Volume, cm^3	Skeletal Density, g/cm^3
36.0	2.53

Residual Fluid Saturations

Residual Oil Saturation, %	Residual Water Saturation, %
18.9	35.2

Permeability

Permeability to Water, mD	Permeability to Air, mD
41	Pending

PHOTOMICROGRAPHS

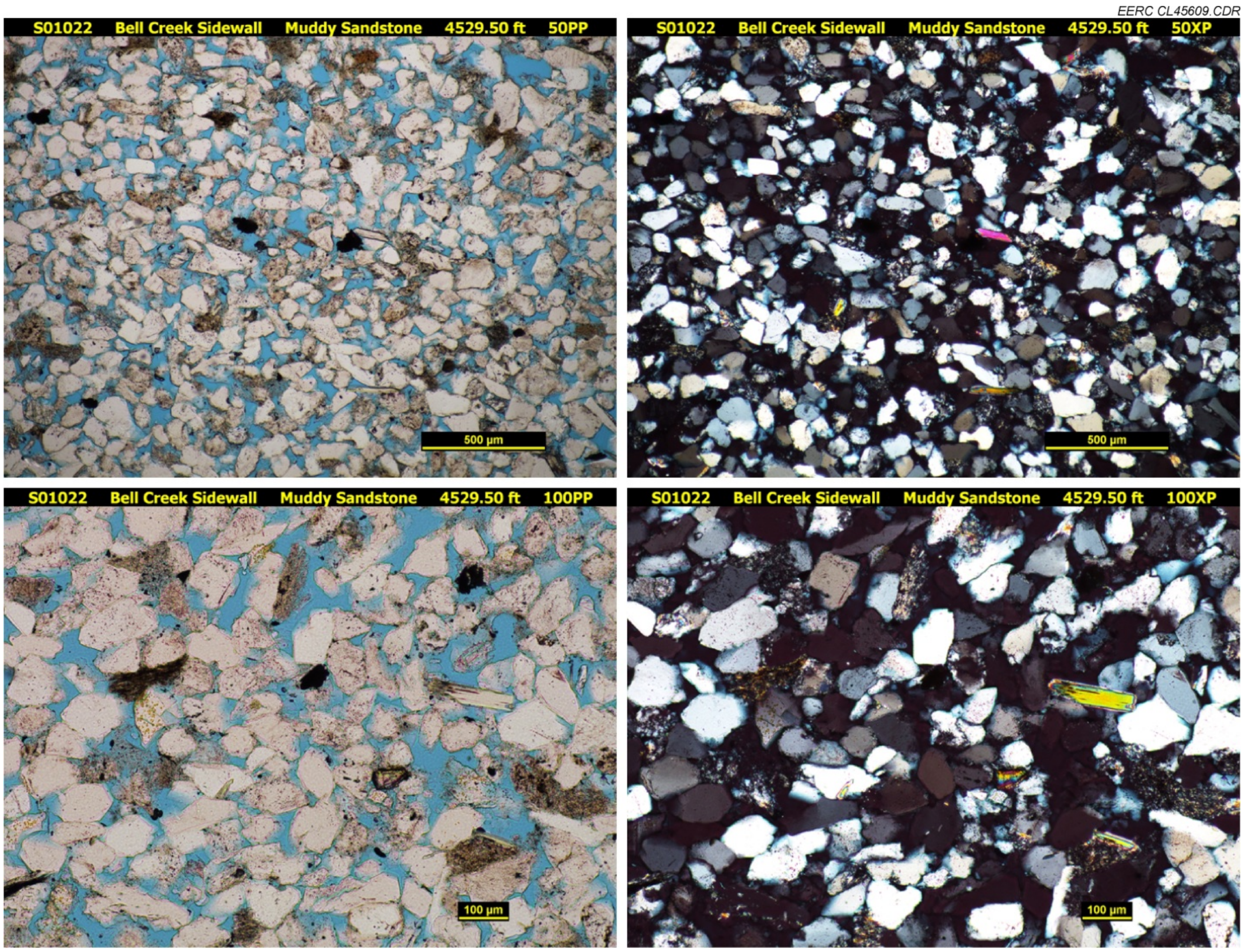

The sample collected at a 4529.50-ft depth is fairly clean, fine-grained, moderately well to well-sorted, grain-supported sandstone. Quartz grains are subangular to subrounded, predominantly monocrystalline and occasionally polycrystalline grains. Original intergranular porosity is altered by small amounts of compaction, quartz overgrowth, and residual clays lining a few of the pore throats. Trace levels of muscovite, siderite, feldspars, clays, and metals are observed. No fractures or fossilization are detected.

THIN-SECTION PORE ANALYSIS BY DIGITAL IMAGE SEGMENTATION

Depth: 4529.50 ft; W = 23.22 mm; H = 16.29 mm

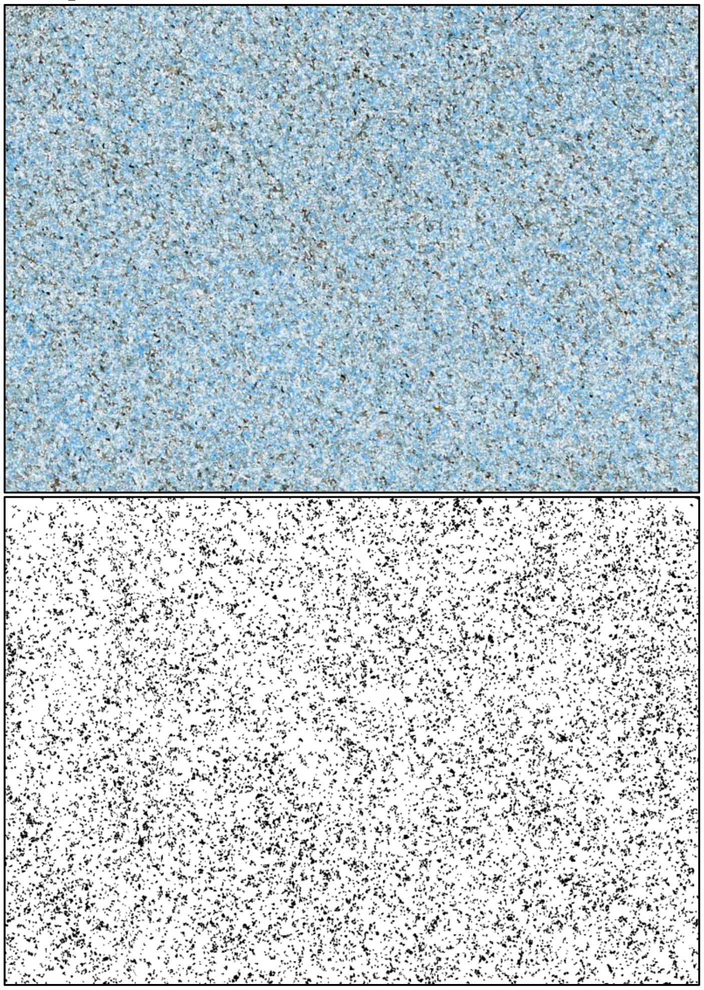

Pore Space, area%	Mean Pore Area, µm^2	Pore Area Range, µm^2	Mean Pore Perimeter, µm	Pore Perimeter Range, µm
13.6	2666	140–24,950	211	45–818

This page intentionally left blank.

SAMPLE PHOTOGRAPH

PHYSICAL PROPERTIES

Porosity

Pycnometer Effective Porosity Average (range), vol%	Pycnometer Effective Porosity by MetaRock Laboratories, vol%	Thin-Section Point Count Porosity, % occurrence	Thin-Section Image Segmentation Pore Space, area%
25.0 (21.7–27.6)	24.6	NT	19.5

Density

Bulk Volume, cm^3	Skeletal Density, g/cm^3
29.5	2.58

Residual Fluid Saturations

Residual Oil Saturation, %	Residual Water Saturation, %
16.3	42.0

Permeability

Permeability to Water, mD	Permeability to Air, mD
310	Pending

PHOTOMICROGRAPHS

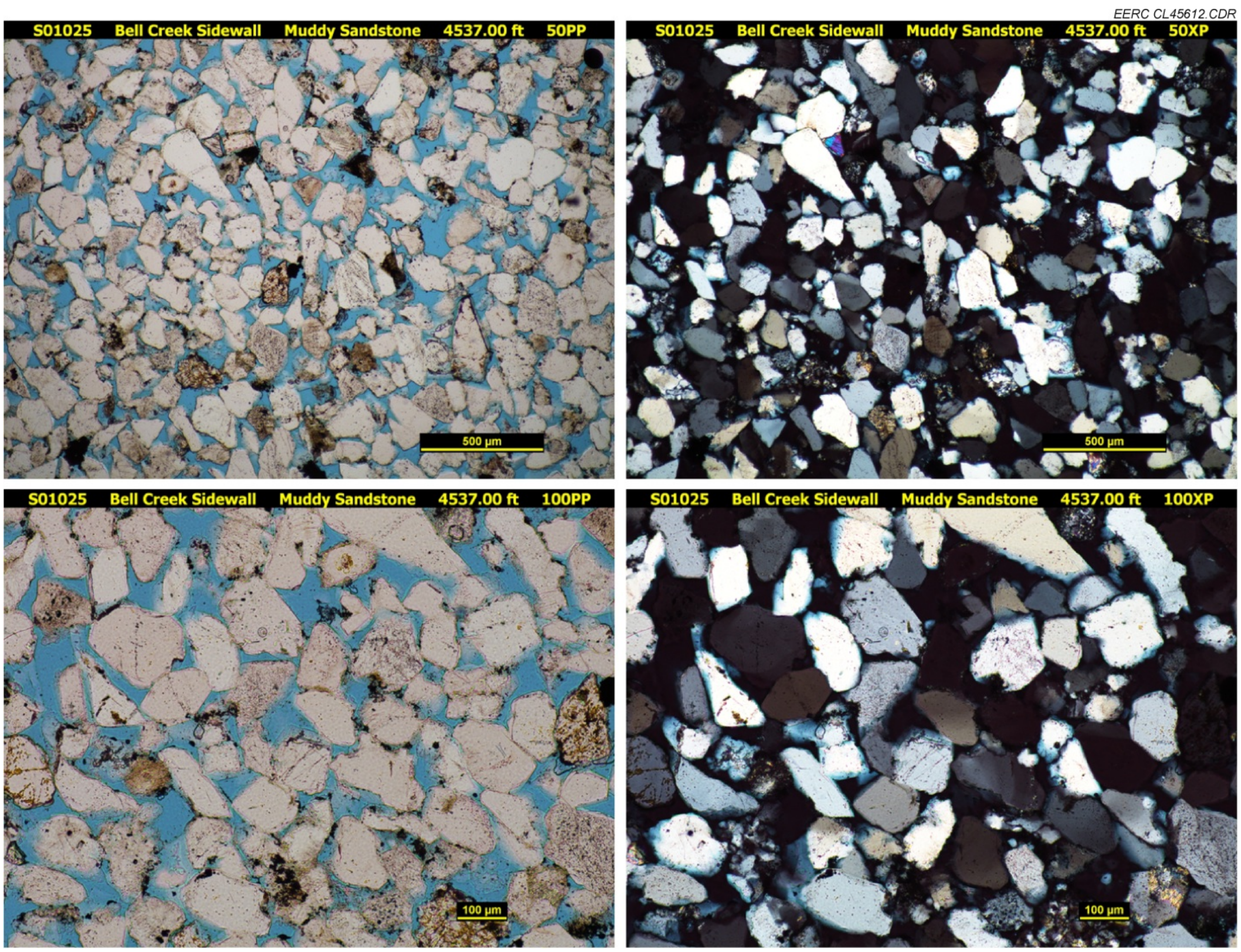

The sample collected at the 4537.00-ft depth represents clean, fine-grained, moderately well sorted sandstone. Quartz grains are angular to subrounded, mostly monocrystalline with few polycrystalline grains. Porosity is intergranular and is a result of cement (clay) and mineral (feldspars) dissolution. Few areas of clay-based cement still exist, mostly as pore linings. Minor amounts of muscovite, metals, rutile, and globby organics are present. No occurrences of fossils or fractures are observed.

THIN-SECTION PORE ANALYSIS BY DIGITAL IMAGE SEGMENTATION

Depth: 4537.00 ft; W = 15.33 mm; H = 14.33 mm

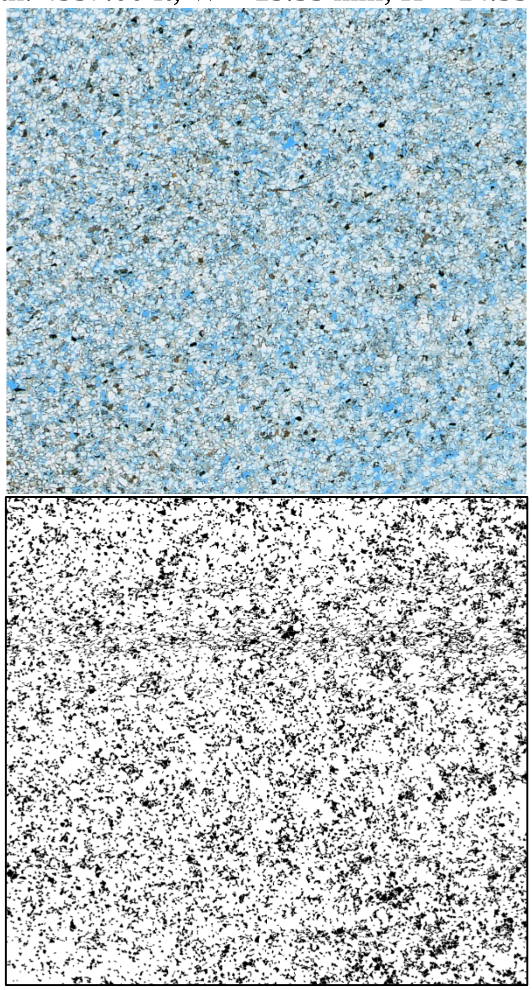

Pore Space, area%	Mean Pore Area, µm^2	Pore Area Range, µm^2	Mean Pore Perimeter, µm	Pore Perimeter Range, µm
19.5	2869	168–33,322	231	48–1169

This page intentionally left blank.

	Applied Geology Laboratory		
EERC UND North Dakota	Muddy Formation	Well Name: 05-06 OW	ID: S-01027
	API No.: 25075224310000	Lithology: Sandstone	Depth: 4538.00'

SAMPLE PHOTOGRAPH

PHYSICAL PROPERTIES

Porosity

Pycnometer Effective Porosity Average (range), vol%	Pycnometer Effective Porosity by MetaRock Laboratories, vol%	Thin-Section Point Count Porosity, % occurrence	Thin-Section Image Segmentation Pore Space, area%
26.4 (24.7–27.6)	NT	NT	22.8

Density

Bulk Volume, cm^3	Skeletal Density, g/cm^3
35.7	2.66

Residual Fluid Saturations

Residual Oil Saturation, %	Residual Water Saturation, %
12.6	43.4

Permeability

Permeability to Water, mD	Permeability to Air, mD
450	Pending

PHOTOMICROGRAPHS

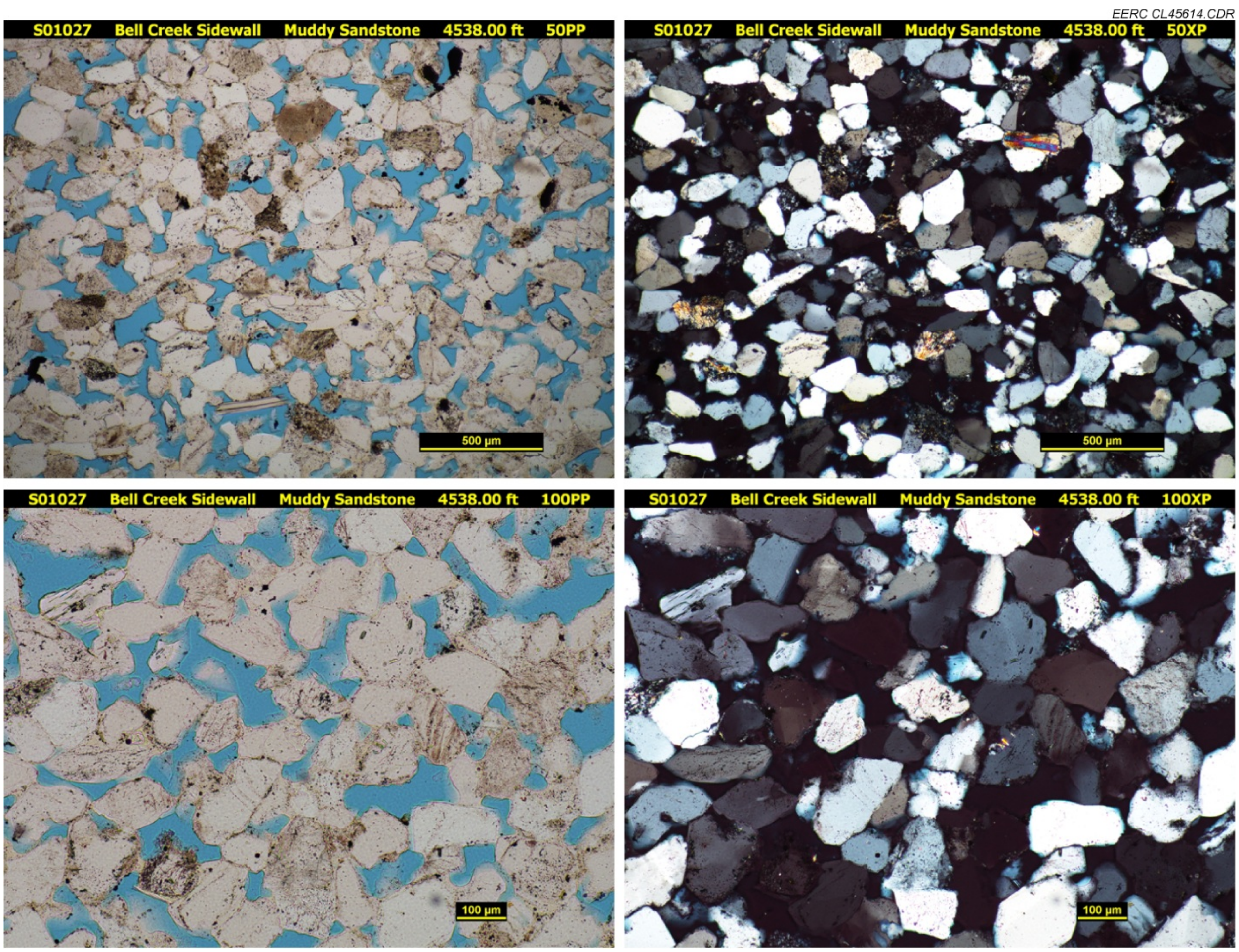

The sample collected at the 4538.00-ft depth is clean, fine-grained, moderately well sorted sandstone. Quartz grains are angular to subrounded, with predominantly monocrystalline and few polycrystalline grains. Porosity is intergranular and the result of cement and grain dissolution. Feldspars, clays, and muscovite occur at trace levels. No fractures or fossilization, and little quartz overgrowth, are detected.

THIN-SECTION PORE ANALYSIS BY DIGITAL IMAGE SEGMENTATION

Depth: 4538.00 ft; W = 30.56 mm; H = 12.23 mm

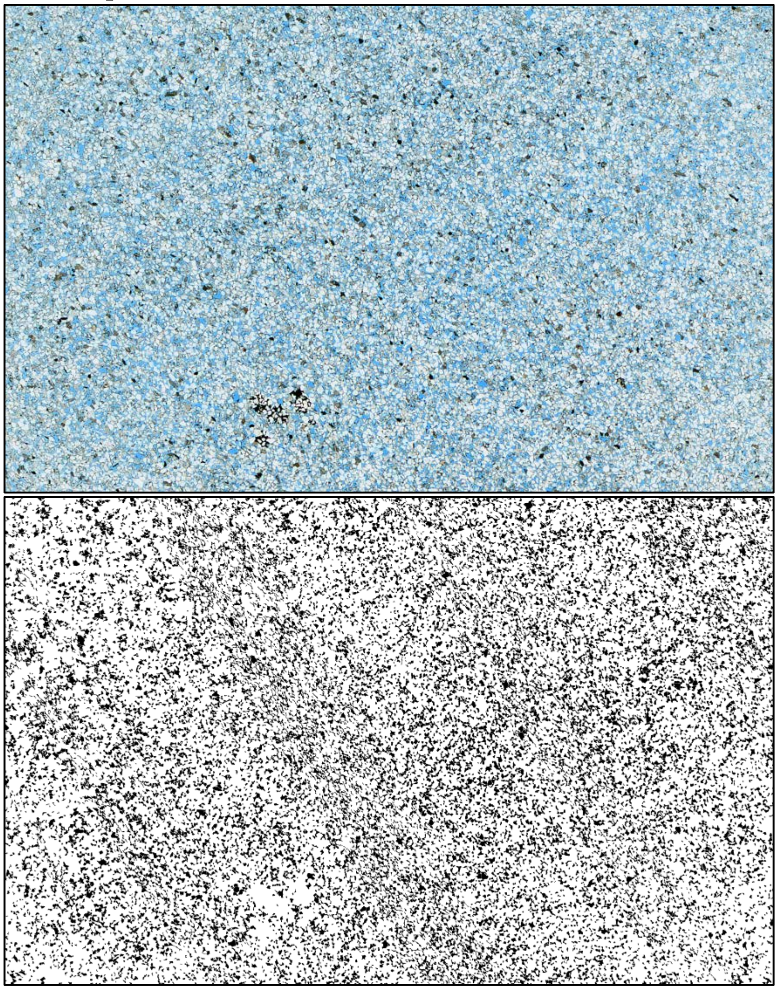

Pore Space, area%	Mean Pore Area, µm²	Pore Area Range, µm²	Mean Pore Perimeter, µm	Pore Perimeter Range, µm
22.8	3190	112–48,247	241	30–1397

This page intentionally left blank.

Applied Geology Laboratory		
Muddy Formation	Well Name: 05-06 OW	ID: S-01028
API No.: 25075224310000	Lithology: Sandstone	Depth: 4538.50'

SAMPLE PHOTOGRAPH

PHYSICAL PROPERTIES

Porosity

Pycnometer Effective Porosity Average (range), vol%	Pycnometer Effective Porosity by MetaRock Laboratories, vol%	Thin-Section Point Count Porosity, % occurrence	Thin-Section Image Segmentation Pore Space, area%
N/A	N/A	NT	25.3

Density

Bulk Volume, cm^3	Skeletal Density, g/cm^3
N/A	N/A

Residual Fluid Saturations

Residual Oil Saturation, %	Residual Water Saturation, %
N/A	N/A

Permeability

Permeability to Water, mD	Permeability to Air, mD
N/A	N/A

PHOTOMICROGRAPHS

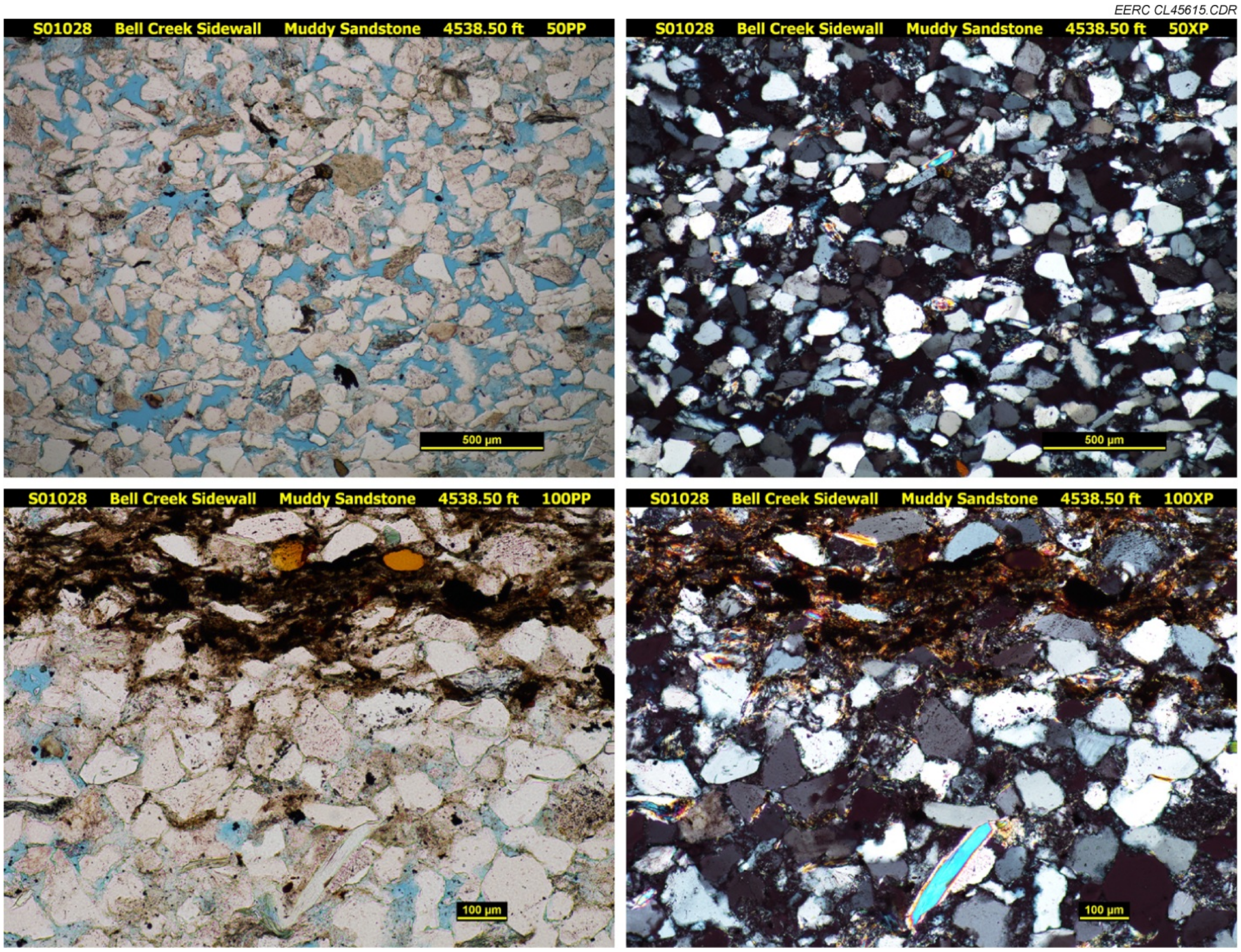

The sample collected at a 4538.50-ft depth is fine-grained sandstone with subangular to subrounded, predominantly monocrystalline quartz grains. Zonally grains are encompassed by combinations of wavy clay laminations and cement composed of clay and carbonate. Some fractures are present within clay laminations. Outside the areas of concentrated cements and laminations, intergranular porosity is well preserved and exhibits few-to-no clay pore linings. Trace amounts of feldspar, muscovite, and metals are observed. No fossilization is noted.

THIN-SECTION PORE ANALYSIS BY DIGITAL IMAGE SEGMENTATION

Depth: 4538.50 ft; W = 17.70 mm; H = 9.67 mm

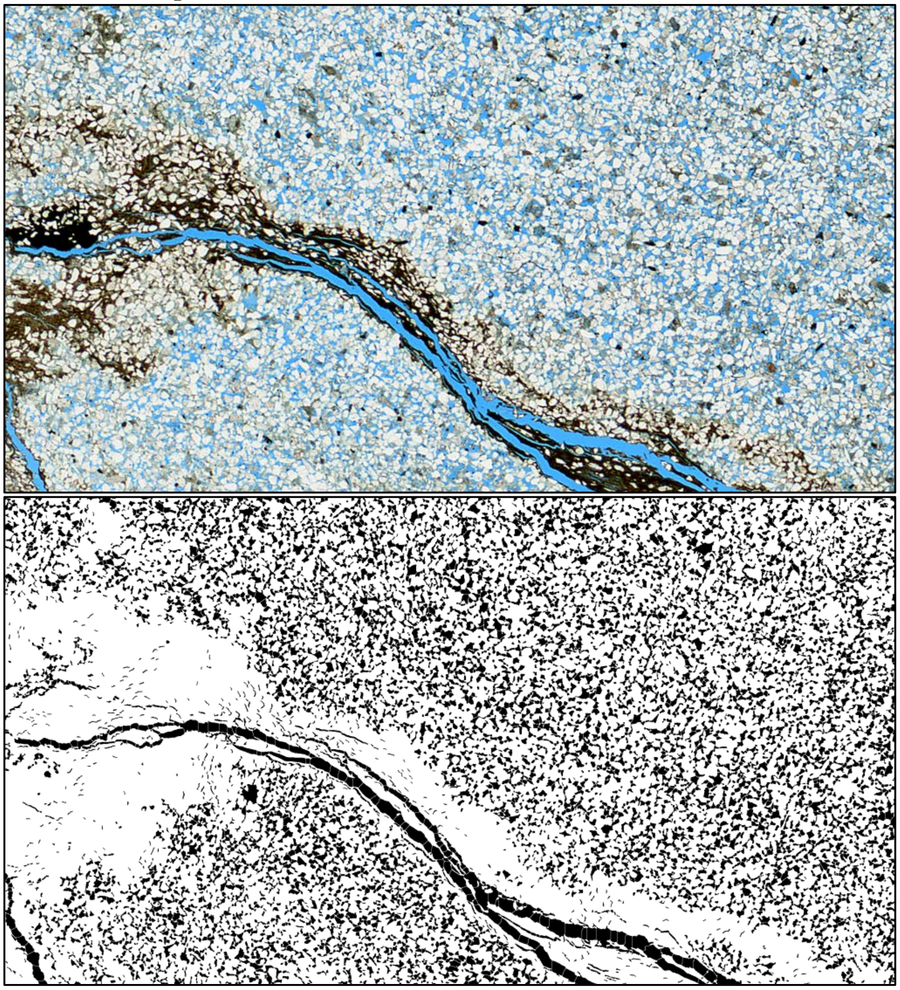

Pore Space, area%	Mean Pore Area, μm^2	Pore Area Range, μm^2	Mean Pore Perimeter, μm	Pore Perimeter Range, μm
25.3*	3668	140–90,138	251	45–2001

* The pore space consists of a) pores: 22.3 area% and b) fractures: 3.0 area%. Some of the observed fractures are likely the result of the sampling process.